1-1-2014

Rap1 Relocalization Contributes to the Chromatin-Mediated Gene Expression Profile and Pace of Cell Senescence

Jesse Platt
University of Pennsylvania, jessep2@gmail.com

Rap1 Relocalization Contributes to the Chromatin-Mediated Gene Expression Profile and Pace of Cell Senescence

Abstract
Cellular senescence is accompanied by dramatic changes in chromatin structure and gene expression. Using S. cerevisiae mutants lacking telomerase (tlc1Δ) to model senescence, we find that with critical telomere shortening the telomere binding protein Rap1 relocalizes to the upstream promoter regions of hundreds of new target genes. The set of new Rap1 targets at senescence (NRTS) are preferentially activated at senescence, and experimental manipulations of Rap1 levels indicate that it contributes directly to NRTS activation, potentially in conjunction with enzymes involved in H2B ubiquitylation (Bre1/Lge1). A notable subset of NRTS includes the core histone-encoding genes; we find that Rap1 contributes to their repression and that histone protein levels decline at senescence. Rap1 and histones also display a target site-specific antagonism that leads to diminished nucleosome occupancy at the promoters of upregulated NRTS. This antagonism apparently impacts the rate of senescence because under-expression of Rap1 or over-expression of the core histones delays senescence. Rap1 relocalization is not a simple consequence of lost telomere binding sites, but rather depends on the Mec1 checkpoint kinase. Rap1 relocalization is thus a novel mechanism connecting DNA damage responses (DDRs) at telomeres to global changes in chromatin and gene expression while driving the pace of senescence.

Degree Type
Dissertation

Degree Name
Doctor of Philosophy (PhD)

Graduate Group
Cell & Molecular Biology

First Advisor
F. Bradley Johnson

Keywords
cellular senescence, chromatin, Rap1, telomere

Subject Categories
Biology | Family, Life Course, and Society

RAP1 RELOCALIZATION CONTRIBUTES TO THE CHROMATIN-MEDIATED GENE EXPRESSION PROFILE AND PACE OF CELL SENESCENCE

Jesse Platt

A DISSERTATION

in

Cell and Molecular Biology

Presented to the Faculties of the University of Pennsylvania

in

Partial Fulfillment of the Requirements for the

Degree of Doctor of Philosophy

2014

Supervisor of Dissertation

_____

F. Bradley Johnson, MD PhD

Associate Professor of Pathology and Laboratory Medicine

Graduate Group Chairperson

_____

Daniel S. Kessler PhD, Associate Professor of Cell and Developmental Biology

Dissertation Committee

Eric Brown, PhD (Chair)
Associate Professor
of Cancer Biology

Shelly Berger, PhD
Daniel S. Och University Professor of
of Cell and Developmental Biology

Roger Greenberg, MD PhD
Associate Professor
of Cancer Biology

Paul Lieberman, PhD
Hilary Koprowski, M.D., Endowed Professor
McNeil Professor of Molecular Medicine & Translational Research

RAP1 RELOCALIZATION CONTRIBUTES TO THE CHROMATIN-MEDIATED GENE EXPRESSION PROFILE AND PACE OF CELL SENESCENCE

Dedication page

To my parents and my family

ACKNOWLEDGMENT

My PhD was a formative experience and I would like to thank many people for their help and support. First and foremost, I would like to thank my parents and family for their support during my PhD. As always, they were there for me during the toughest times. In addition, I need to thank my amazing girlfriend, Yu-San Huoh, who was a wonderful sounding board and helped me get though some of the toughest times (including a thesis printing fiasco). I don't think I can thank enough my outstanding advisor, Dr. F. Brad Johnson, who has helped me develop into the scientist I am today. It was an honor and a pleasure to get a chance to work with Brad, who continually blew me away with his smarts, patience, and ingenuity. Brad was always there for me answering my questions (at any hour of the day), helping me design better experiments, and constructively pointing out my weaknesses in the most kind and helpful ways. Though I still have much to learn, Brad has helped me take steps forward to become a more mature scientist. Working in the Johnson lab was some of the most fun I've had in a long time (and I hope to get some time to go back when I return to medical school). I also would like to thank the Johnson lab (in particular Alejandro Chavez) and my supportive committee.

ABSTRACT

RAP1 RELOCALIZATION CONTRIBUTES TO THE CHROMATIN-MEDIATED GENE EXPRESSION PROFILE AND PACE OF CELL SENESCENCE

Jesse Platt

F. Brad Johnson

Cellular senescence is accompanied by dramatic changes in chromatin structure and gene expression. Using *S. cerevisiae* mutants lacking telomerase (*tlc1Δ*) to model senescence, we find that with critical telomere shortening the telomere binding protein Rap1 relocalizes to the upstream promoter regions of hundreds of new target genes. The set of new Rap1 targets at senescence (NRTS) are preferentially activated at senescence, and experimental manipulations of Rap1 levels indicate that it contributes directly to NRTS activation, potentially in conjunction with enzymes involved in H2B ubiquitylation (Bre1/Lge1). A notable subset of NRTS includes the core histone-encoding genes; we find that Rap1 contributes to their repression and that histone protein levels decline at senescence. Rap1 and histones also display a target site-specific antagonism that leads to diminished nucleosome occupancy at the promoters of upregulated NRTS. This antagonism apparently impacts the rate of senescence because under-expression of Rap1 or over-expression of the core histones delays senescence. Rap1 relocalization

is not a simple consequence of lost telomere binding sites, but rather depends on the Mec1 checkpoint kinase. Rap1 relocalization is thus a novel mechanism connecting DNA damage responses (DDRs) at telomeres to global changes in chromatin and gene expression while driving the pace of senescence.

TABLE OF CONTENTS

LIST OF TABLES

LIST OF ILLUSTRATIONS

INTRODUCTION

Telomere structure and function

History and Background

Telomeres are nucleo-protein complexes at the ends of chromosomes that have many specialized functions. The word *telomere* was coined in 1941 by Hermann Müller and comes from the Greek words *telos* (τέλος) meaning 'end' and *meros* (μέρος) meaning 'part.' Independently, Hermann Müller and Barbara McClintock performed key experiments which predicted the existence of a telomere – that is, a specialized structure at the ends of chromosomes (McClintock 1941; Muller 1941). By studying the effects of X-rays on *Drosophila* and maize chromosomes, Müller and McClintock discovered that the chromosome ends were unlike the rest of the genome and when damaged do not behave like other double strand DNA breaks. These findings suggested that telomeres have unique properties that prevent fusions and breakages and were likely specialized structures.

Since these early experiments we have learned an enormous amount about telomere structure and function and their relationship to disease. In fact this large body of work ultimately resulted in the 2006 Albert Lasker Basic Medical Research Award and the 2009 Nobel Prize in Physiology or Medicine being awarded to

Elizabeth Blackburn, Carol Greider, and Jack Szostak. The field has blossomed and is now appreciated to have many far reaching affects on cellular and human physiology – including the DNA damage response, cellular stress response, senescence, metabolism, cancer, and potentially even human aging. It is an exciting time to be part of this field; many discoveries are being translated into therapeutics that might eventually improve human health.

Telomere Structure and Maintenance

Telomeres are evolutionarily conserved guanine-rich repeating structures that cap chromosome ends and prevent DNA damage response factors from recognizing them as double strand breaks. The telomere repeat is not perfectly conserved throughout evolution and varies from repeating arrays including *Tetrahymena* TTGGGG and mammalian TTAGGG to irregular repeating structures in *S. cerevisiae* $T(G)_{1\text{-}3}$ (Fajkus et al. 2005). Telomeres end in a 3' guanine-rich single stranded DNA overhand that is not only evolutionarily conserved (they are found in ciliates, yeast and humans), but also it is maintained in a regulated process (Wellinger et al. 1996; McElligott and Wellinger 1997; Jacob et al. 2003). Some data suggests that this 3' overhand folds back on the chromosome and forms a displacement loop (D-loop) that has been called a telomere-loop or t-loop (Griffith et al. 1999; Muñoz-Jordán et al. 2001; Stansel et al. 2001). Telomere repeats are

bound by a protein complex that is *somewhat* evolutionarily conserved, which in mammals is called sheltrin (Palm and de Lange 2008). In humans, sheltrin is composed of TRF2, TRF1, hRAP1, TPP1, POT1, and TIN2, and each member of the complex plays a unique role in telomere homeostasis (Palm and de Lange 2008; Sfeir and de Lange 2012).

In part because of the mechanism of DNA replication and the resulting 'end replication problem' that was independently described by James Watson and Alexy Olovnikov, telomeres shorten with every cell division and ultimately become dysfunctional (Olovnikov 1973; Harley et al. 1990). The end replication problem does not completely explain the rate of telomere attrition and other mechanisms have been implicated to affect telomere shortening: including ROS, exonucleolytic processing and degradation, and errors in replication (Harley et al. 1990; Zglinicki 2002; Dionne and Wellinger 1996). Telomerase, a reverse transcriptase that is composed of a protein component and an RNA template for *de novo* telomere addition, can maintain telomere length by adding new telomere repeats to the ends of chromosomes (Greider and Blackburn 1985).

Senescence

Senescence, which is derived from the Latin word *senescere* that means 'to grow old,' is defined in cellular biology as a permanent state of cell cycle arrest.

Senescence was first discovered in 1961 by Hayflick and Moorhead, who showed that primary human cells go through a finite number of population doublings and then entered phase III, which has since been renamed senescence or the 'Hayflick limit' (Hayflick and Moorhead 1961). These findings directly contradicted Alexis Carrel's work on cultured embryonic chicken hearts, which suggested that primary cells did not senescence in culture and were instead immortal (Carrel 1912). The potential importance of senescence was immediately appreciated and it was suggested that it might regulate both carcinogenesis and aging (Campisi 2012; Campisi and d'Adda di Fagagna 2007). Because the ability of primary cells to senescence is one of their defining features that distinguish them from immortal cancer cells, senescence was thought to be an anti-cancer mechanism. On the other hand, senescence results in a loss of growth potential and provides a potential explanation why tissues break down over time and fail to regenerate with age.

Mammalian cell senescence is an active response to stresses that put cells at risk for neoplastic transformation, including DNA damage, oncogenic signals, dramatic chromatin changes, and critically shortened or dysfunctional telomeres (Campisi and d'Adda di Fagagna 2007). Accordingly, cell senescence limits carcinogenesis in a cell autonomous fashion (Campisi 2001; Dimri 2005; Wright and Shay 2001). Recent evidence indicates that it may also have negative consequences, including contributing to carcinogenesis in a non-cell autonomous manner as well as contributing to age-related degenerative pathology in both cell autonomous and

non-cell autonomous fashions (Baker et al. 2011; Molofsky et al. 2006; Krishnamurthy et al. 2006).

Senescence is initiated and maintained by activating either or both of the p53/p21 and $p16^{INK4a}$/pRB tumor suppressor pathways (Campisi 2012; Adams 2009; Collins and Sedivy 2003). These pathways are quite complicated and involve many upstream regulators and downstream effectors and even regulate each other (Chau and Wang 2003; Takeuchi et al. 2010; Zhang et al. 2006; Yamakoshi et al. 2009). Though most studies suggest that either the p53/p21 or p16INK4a/pRB pathway is necessary to maintain senescence, there are some reports of cellular senescence that are independent of both pathways (Olsen et al. 2002).

Senescent cells are characterized by persistent cell cycle arrest mediated by DNA damage checkpoint factors, and they also display profound changes in gene expression, chromatin organization, metabolism, and secretory behavior (senescence associated secretory phenotype, i.e. SASP) (Zwerschke et al. 2003; Shelton et al. 1999; Zhang 2003; Herbig et al. 2004; Howard 1996; Narita et al. 2003). An understanding of the mechanisms underlying these changes promises to enhance our treatments of cancer and age associated diseases. However, the molecular mechanisms underlying these changes are not well understood.

Senescence-associated gene expression changes

Senescence is associated with extreme changes in gene expression, including the up-regulation of cell cycle inhibitors (for example p21 and p16) and the down-regulation of cell cycle activators (including c-FOS, histones, cyclin A, cyclin B, and proliferating cell nuclear antigen (PCNA)) (Pang and Chen 1994; Seshadri and Campisi 1990; Stein et al. 1991; Zhang 2003; Yoon et al. 2004; Shelton et al. 1999). Both p53 and RB are transcription factors that directly regulate some of the gene expression changes at senescence (for example p53 activates p21 and GADD45 at senescence) (Espinosa et al. 2003; Jackson and Pereira-Smith 2006). Recent work also suggests that active SUMOylation (the covalent conjugation of SUMO1 or SUMO2/3) might represses histone and tRNA expression at senescence (Neyret-Kahn et al. 2013).

In addition, microRNAs have been implicated to regulate some portion of the gene expression changes at senescence (Fajkus et al. 2005; Lafferty-Whyte et al. 2009). Many microRNAs are differentially expressed at senescence including miR-34a and miR-22, which directly regulate the expression of p53/p21, E2F, Cdk6, Sirt6, Sp1 (Tazawa et al. 2007; Sun et al. 2008; Xu et al. 2011; Dhahbi et al. 2011). Overall, though some transcriptional changes are well characterized, it is still not known which factors regulate the majority of gene expression changes at senescence. One possibility is that there are 'master regulators' that control the majority of differentially expressed genes at senescence.

Senescence-associated chromatin changes

Senescence is also associated with dramatic changes in chromatin, including the loss of histone proteins, the loss of lamin B1, and the formation of heterochromatic foci (SAHF) (Griffith et al. 1999; Shah et al. 2013; Muñoz-Jordán et al. 2001; Sadaie et al. 2013; Stansel et al. 2001; Narita et al. 2003; 2006; O'Sullivan et al. 2010; Freund et al. 2012; Shimi et al. 2011; Benetti et al. 2007). As expected, many of these changes are also associated with changes in genes expression, in fact RNA polymerase II and active transcription is preferentially excluded from SAHFs (Palm and de Lange 2008; Narita et al. 2003; Shah et al. 2013; Zhang et al. 2007; Funayama et al. 2006). Interestingly, though chromatin grossly reorganizes into the SAHFs as observed via immuno-fluorescence, recent work from Narita and colleagues suggest that the occupancy of heterochromatic marks (including H3K9me3) does not change at senescence when viewed at higher resolution (i.e. with ChIP-seq) (Chandra et al. 2012). These findings suggest that SAHFs are blocks of pre-existing heterochromatin that have been brought together at senescence. However, when the Berger group reanalyzed these data they found important changes in H3K27me3 at senescence (including trends of “mesas” and “canyons”; Shah et al. 2013). In summary, many chromatin changes are occurring at senescence. Though still hotly debated, these include changes in the occupancy of various epigenetic marks and potentially gross chromatin confirmation.

In addition to epigenetic marks, both histone transcripts and proteins are downregulated at senescence (Seshadri et al.1990; Pang et al. 1994; O'Sullivan et al. 2010). Histone losses are associated with reduced expression of the stem loop–binding protein (*SLBP*) and histone chaperones *ASF1* and *CAF1*, however the precise mechanism of how histones are downregulated at senescence is not fully understood. Mammalian histone expression is a highly regulated process that that depends on the transcriptional regulatator *NPAT* (nuclear protein, ataxia–telangiectasia locus) and *FLASH* [FADD (Fas-associated death domain)-like IL-1β (interleukin 1β)-converting enzyme associated huge protein] and several complicated post-transcriptional processing steps prior to translation (Ewen 2000; Barcaroli et al. 2006). Each of these steps might be affected at senescence and potentially account for the loss of histone transcripts and proteins. It is important to note that histones are also lost with aging in other organisms – including replicatively aged yeast mother cells – which suggests that histone loss might be an evolutionarily conserved process that controls aging (Feser et al. 2010).

Yeast System to Model Senescence

In the budding yeast *S. cerevisiae* telomere length is maintained by constitutive expression of the telomerase enzyme, and thus yeast cells do not naturally senesce as a consequence of gradual telomere shortening. Nonetheless,

cell senescence can be modeled in yeast by genetic inactivation of telomerase, leading eventually to critical telomere shortening and mitotic arrest (Olovnikov 1973; Lundblad and Szostak 1989; Harley et al. 1990; Singer and Gottschling 1994). Remarkably, these cells display several features similar to mammalian cells that have senesced due to telomere shortening. For example both involve DNA damage responses, dependent on PI3-kinase-type kinases, which lead to cell cycle arrest (Harley et al. 1990; IJpma and Greider 2003; Zglinicki 2002; Herbig et al. 2004). Both also have dramatic gene expression changes that include activation of stress responses, inhibition of glycolysis, and downregulation of histone transcripts (Nautiyal et al. 2002; O'Sullivan et al. 2010; Zwerschke et al. 2003; Pang and Chen 1994; Seshadri and Campisi 1990; Shelton et al. 1999; Zhang 2003). And in both murine and yeast telomerase-deficient cells critical telomere shortening causes loss of heterochromatic histone marks and of subtelomeric gene silencing (Benetti et al. 2007; Kozak et al. 2010; Nautiyal et al. 2002), and the telomere ends become susceptible to end-to-end fusion events (Hackett et al. 2001; Blasco et al. 1997; Lee et al. 1998). Furthermore, similar factors modulate the pace of senescence in both systems. For example in mammals telomere-driven senescence is promoted by ATM, ATR and EXO1, and is delayed by the WRN and BLM helicases, and the orthologous yeast proteins Tel1, Mec1, Exo1, and Sgs1 function similarly (Campisi 2012; IJpma and Greider 2003; Campisi and d'Adda di Fagagna 2007; Herbig et al. 2004; Du et al. 2004; Hagelstrom et al. 2010; Faragher et al. 1993; Schaetzlein et al.

2007; Ritchie et al. 1999; Abdallah et al. 2009; Maringele and Lydall 2004; Johnson et al. 2001). Thus, yeast telomerase mutants provide a valuable model for understanding several features of cell senescence driven by telomere dysfunction.

Despite the similarities between senescence in primary human fibroblasts and yeast that lack telomerase, there are some key differences between the two systems. For example, although the cells stop dividing at senescence and enter a permanent state of cell cycle arrest in yeast and human cells, the precise cell cycle arrest is different. Whereas senescent primary human fibroblasts arrest in either G1, G2, or G2/M, yeast that senesce due to telomeric dysfunction arrest in G2/M (Campisi and d'Adda di Fagagna 2007; IJpma and Greider 2003; Johnson et al. 2001; Pignolo et al. 1998; Jullien et al. 2013; Mao et al. 2012). In addition, the frequency of survivors during senescence and the rate of senescence bypass are much higher in yeast as compared to mammalian cells. During a senescence assay, up to one-in-10,000 yeast cells are survivors (unfortunately the precise frequency is not known) (Campisi 2001; Teixeira 2013; Dimri 2005; Wright and Shay 2001). Conversely, primary human cells rarely bypass senescence, though the frequency increases in the absence of p53/p21 and RB/$p16^{INK4a}$ pathways (it is estimated that 1 in 10^7 cells can by bypass crisis and maintain their telomeres without upregulating telomerase activity) (Baker et al. 2011; Reddel 2000; Molofsky et al. 2006; Rogan et al. 1995; Krishnamurthy et al. 2006; Shay and Wright 1989; Shay et al. 1993).

Finally, some characteristics of senescent human cells have not been reported in senescent yeast. For example, senescent yeast have not been shown to have SASP- of SAHF-like phenotype (though there are gross changes in chromatin at senescence) (Campisi 2012; Kozak et al. 2010; Adams 2009; Platt et al. 2013; Collins and Sedivy 2003). Though it is possible that these questions have not been addressed experimentally, it is also possible that these changes are not seen in senescent yeast.

The three models of yeast aging and senescence

To add to the complexity of senescence, there are three different ways to study senescence in yeast. In addition to genetically inactivating telomerase, yeast aging and senescence can be assayed by measuring replicative lifespan or chronologic lifespan (Mortimer and Johnston 1959; Takeuchi et al. 2010; Longo et al. 1999; Zhang et al. 2006; Longo et al. 1996; Yamakoshi et al. 2009; Fabrizio et al. 2001). Because yeast divide asymmetrically (that is the budded daughter cell is smaller than the mother cell), one can count the number of offspring that come from a single yeast cell. Mortimer and Johnston showed that individual yeast cells do not divide forever (Mortimer and Johnston 1959) and so replicative lifespan is a measurement of how many daughter cells can be budded from a mother cell during

the course of its life. Conversely, the chronologic lifespan of a yeast cell is a measurement of how long a population of yeast remains viable in stationary phase.

Though each assay is very different, the chronological and replicative lifespan models have some similarities. First, whereas telomere shortening triggers senescence when telomerase is inactivated, telomeric dysfunction does not drive replicative or chronological lifespan (Smeal et al. 1996; D'Mello and Jazwinski 1991; Burtner et al. 2009; Chen et al. 2009). Second, many pathways regulate both chronological and replicative lifespan including caloric restriction, mitochondrial dysfunction, and ROS (of note, many of these pathways either do not affect or have yet to be shown to affect the pace of telomere dysfunction induced senescence in yeast; Pang and Chen 1994; Longo et al. 2012). However, the replicative and chronologic lifespan assays are still very different. For example, the cells are not even cycling in the chronologic assay. In addition, some pathways – including the *SIR2*/*FOB1* pathway that results in extrachromosomal rDNA circles (ERC) – are unique to yeast replicative lifespan and do not affect chronologic aging (or even human aging for that matter) (Bitterman et al. 2003).

Rap1

We considered the possibility that telomere shortening might cause relocalization of normally telomere-bound proteins to new genomic loci and thus

regulate senescence, an idea long hypothesized but never demonstrated directly (Campisi 1997). A prime candidate for such a factor in *S. cerevisiae* is Rap1 (Repressor activator protein 1), which binds directly to telomere repeat DNA in a sequence-specific fashion *via* two tandem Myb-type homeodomains which are connected by a short peptide linker (Konig et al. 1996). Rap1 controls telomere function and maintenance including telomere capping, length regulation, localization to the nuclear periphery, and heterochromatin formation (which silences the expression of subtelomeric loci) (Bonetti et al. 2010; Marcand et al. 1997; Kyrion et al. 1993; Pardo and Marcand 2005; Marcand et al. 2008; Vodenicharov and Wellinger 2006; Negrini et al. 2007; Hofmann et al. 1989; Klein et al. 1992; Palladino et al. 1993). Rap1 mediates telomere silencing by recruiting the Sir protein complex, which it also does at the silent mating loci *HML* and *HMR* (Moretti and Shore 2001; Moretti et al. 1994). In contrast, at hundreds of genomic loci Rap1 functions as a transcriptional activator, *via* binding to upstream promoter regions and interacting with various coactivator proteins (e.g. Gcr1 and Gcr2 at glycolytic genes, and Fhl1 and Ifh1 at ribosomal protein genes) (Zhao et al. 2006; Tornow et al. 1993; López et al. 1998; Schawalder et al. 2004; Wade et al. 2004). These dual sets of Rap1 functions - at telomeres and at genomic loci - raise the possibility that if Rap1 were lost from shortened telomeres it might expand its roles at extra-telomeric loci. Several considerations support this idea. First, Rap1 is an abundant protein (~4000 molecules per haploid cell: Buchman et al. 1988;

Ghaemmaghami et al. 2003), and a significant fraction (at least 10-15%) localizes to telomeres, which by fluorescence microscopy are visualized as prominent foci at the nuclear periphery that appear to be the primary sites of Rap1 localization (Gotta et al. 1996; Klein et al. 1992). Thus the telomeric pool of Rap1 is large enough to have the potential for significant effects upon redistribution. Second, there are many low affinity Rap1 binding sites that unoccupied throughout the genome. Rap1 binds tightly ($K_d \sim 10^{-11}$ M) to its highest affinity DNA binding sites, which follow the approximate consensus RMAYCCRMNCAYY and comprise two hemisites (ACAYC and ACAYM) linked by a trinucleotide (CRM) (Lieb et al. 2001; Vignais et al. 1990). These DNA sequence elements are each bound respectively by the homeodomain-linker peptide-homeodomain amino acid sequences within each Rap1 monomer(Konig et al. 1996). Rap1 can also bind with significant affinity to a single hemisite paired with a linker sequence(Del Vescovo et al. 2004). *In vivo*, many loci with consensus or hemisite-linker sequences are not bound by Rap1 in normal cells, raising the possibility that these sites might be bound by Rap1 under conditions that increase the available pool of Rap1, or alternatively increase accessibility of the sites to Rap1. Third, Rap1 has been observed previously to relocalize in the G2 phase of the cell cycle (Laroche et al. 2000) and under conditions of stress, including low glucose (Buck and Lieb 2006) and DNA damage by the alkylating agent methyl methanesulfonate (MMS; Tomar et al. 2008). Finally, senescence itself may be a Rap1-relocalizing stress because cytological studies indicate that critical telomere

shortening in telomerase deficient cells causes an apparent loss in intensity of telomere-associated Rap1 along with elevation in its overall nucleoplasmic localization (Palladino et al. 1993; Straatman and Louis 2007). However, whether Rap1 relocalizes to particular genomic targets at senescence and how such relocalization might impact cell physiology have not been addressed. Here we experimentally addressed if Rap1 relocalizes to new sites throughout the genome at senescence and how it affects gene expression at senescence.

REFERENCES

Abdallah P, Luciano P, Runge KW, Lisby M, Géli V, Gilson E, Teixeira MT. 2009. A two-step model for senescence triggered by a single critically short telomere. *Nature Cell Biology* **11**: 988–993.

Adams PD. 2009. Healing and hurting: molecular mechanisms, functions, and pathologies of cellular senescence. *Mol Cell* **36**: 2–14.

Baker DJ, Wijshake T, Tchkonia T, Lebrasseur NK, Childs BG, Van De Sluis B, Kirkland JL, Van Deursen JM. 2011. Clearance of p16Ink4a-positive senescent cells delays ageing-associated disorders. *Nature* **479**: 232–236.

Benetti R, García-Cao M, Blasco MA. 2007. Telomere length regulates the epigenetic status of mammalian telomeres and subtelomeres. *Nat Genet* **39**: 243–250.

Bitterman KJ, Medvedik O, Sinclair DA. 2003. Longevity regulation in Saccharomyces cerevisiae: linking metabolism, genome stability, and heterochromatin. *Microbiol Mol Biol Rev* **67**: 376–99– table of contents.

Blasco MA, Lee HW, Hande MP, Samper E, Lansdorp PM, DePinho RA, Greider CW. 1997. Telomere shortening and tumor formation by mouse cells lacking telomerase RNA. *Cell* **91**: 25–34.

Bonetti D, Clerici M, Anbalagan S, Martina M, Lucchini G, Longhese MP. 2010.

Shelterin-like proteins and Yku inhibit nucleolytic processing of Saccharomyces cerevisiae telomeres. *PLoS Genet* **6**: e1000966.

Buchman AR, Lue NF, Kornberg RD. 1988. Connections between transcriptional activators, silencers, and telomeres as revealed by functional analysis of a yeast DNA-binding protein. *Mol Cell Biol* **8**: 5086–5099.

Buck MJ, Lieb JD. 2006. A chromatin-mediated mechanism for specification of conditional transcription factor targets. *Nat Genet* **38**: 1446–1451.

Burtner CR, Murakami CJ, Kennedy BK, Kaeberlein M. 2009. A molecular mechanism of chronological aging in yeast. *Cell Cycle* **8**: 1256–1270.

Campisi J. 2012. Aging, Cellular Senescence, and Cancer. *Annu Rev Physiol* **75**: 121109133849001.

Campisi J. 2001. Cellular senescence as a tumor-suppressor mechanism. *Trends Cell Biol* **11**: S27–31.

Campisi J. 1997. The biology of replicative senescence. *European Journal of Cancer* **33**: 703–709.

Campisi J, d'Adda di Fagagna F. 2007. Cellular senescence: when bad things happen to good cells. *Nat Rev Mol Cell Biol* **8**: 729–740.

Carrel A. 1912. On the Permanent Life of Tissues Outside of the Organism. *J Exp Med*

15: 516–528.

Chandra T, Kirschner K, Thuret J-Y, Pope BD, Ryba T, Newman S, Ahmed K, Samarajiwa SA, Salama R, Carroll T, et al. 2012. Independence of repressive histone marks and chromatin compaction during senescent heterochromatic layer formation. *Mol Cell* **47**: 203–214.

Chang H-Y, Lawless C, Addinall SG, Oexle S, Taschuk M, Wipat A, Wilkinson DJ, Lydall D. 2011. Genome-wide analysis to identify pathways affecting telomere-initiated senescence in budding yeast. *G3 (Bethesda)* **1**: 197–208.

Chau BN, Wang JYJ. 2003. Coordinated regulation of life and death by RB. *Nat Rev Cancer* **3**: 130–138.

Chen X-F, Meng F-L, Zhou J-Q. 2009. Telomere recombination accelerates cellular aging in Saccharomyces cerevisiae. *PLoS Genet* **5**: e1000535.

Collins CJ, Sedivy JM. 2003. Involvement of the INK4a/Arf gene locus in senescence. *Aging Cell* **2**: 145–150.

D'Mello NP, Jazwinski SM. 1991. Telomere length constancy during aging of Saccharomyces cerevisiae. *J Bacteriol* **173**: 6709–6713.

Del Vescovo V, De Sanctis V, Bianchi A, Shore D, Di Mauro E, Negri R. 2004. Distinct DNA elements contribute to Rap1p affinity for its binding sites. *Journal of*

Molecular Biology **338**: 877–893.

Dhahbi JM, Atamna H, Boffelli D, Magis W, Spindler SR, Martin DIK. 2011. Deep sequencing reveals novel microRNAs and regulation of microRNA expression during cell senescence. *PLoS ONE* **6**: e20509.

Dimri GP. 2005. What has senescence got to do with cancer? *Cancer Cell* **7**: 505–512.

Dionne I, Wellinger RJ. 1996. Cell cycle-regulated generation of single-stranded G-rich DNA in the absence of telomerase. *Proc Natl Acad Sci USA* **93**: 13902–13907.

Du X, Shen J, Kugan N, Furth EE, Lombard DB, Cheung C, Pak S, Luo G, Pignolo RJ, DePinho RA, et al. 2004. Telomere shortening exposes functions for the mouse Werner and Bloom syndrome genes. *Mol Cell Biol* **24**: 8437–8446.

Espinosa JM, Verdun RE, Emerson BM. 2003. p53 functions through stress- and promoter-specific recruitment of transcription initiation components before and after DNA damage. *Mol Cell* **12**: 1015–1027.

Fabrizio P, Pozza F, Pletcher SD, Gendron CM, Longo VD. 2001. Regulation of longevity and stress resistance by Sch9 in yeast. *Science* **292**: 288–290.

Fajkus J, Sýkorová E, Leitch AR. 2005. Telomeres in evolution and evolution of telomeres. *Chromosome Res* **13**: 469–479.

Faragher RG, Kill IR, Hunter JA, Pope FM, Tannock C, Shall S. 1993. The gene

responsible for Werner syndrome may be a cell division "counting" gene. *Proc Natl Acad Sci USA* **90**: 12030–12034.

Freund A, Laberge R-M, Demaria M, Campisi J. 2012. Lamin B1 loss is a senescence-associated biomarker. *Mol Biol Cell* **23**: 2066–2075.

Funayama R, Saito M, Tanobe H, Ishikawa F. 2006. Loss of linker histone H1 in cellular senescence. *J Cell Biol* **175**: 869–880.

Ghaemmaghami S, Huh W-K, Bower K, Howson RW, Belle A, Dephoure N, O'Shea EK, Weissman JS. 2003. Global analysis of protein expression in yeast. *Nature* **425**: 737–741.

Gotta M, Laroche T, Formenton A, Maillet L, Scherthan H, Gasser SM. 1996. The clustering of telomeres and colocalization with Rap1, Sir3, and Sir4 proteins in wild-type Saccharomyces cerevisiae. *J Cell Biol* **134**: 1349–1363.

Greider CW, Blackburn EH. 1985. Identification of a specific telomere terminal transferase activity in Tetrahymena extracts. *Cell* **43**: 405–413.

Griffith JD, Comeau L, Rosenfield S, Stansel RM, Bianchi A, Moss H, de Lange T. 1999. Mammalian telomeres end in a large duplex loop. *Cell* **97**: 503–514.

Hackett JA, Feldser DM, Greider CW. 2001. Telomere dysfunction increases mutation rate and genomic instability. *Cell* **106**: 275–286.

Hagelstrom RT, Blagoev KB, Niedernhofer LJ, Goodwin EH, Bailey SM. 2010. Hyper telomere recombination accelerates replicative senescence and may promote premature aging. *Proceedings of the National Academy of Sciences* **107**: 15768–15773.

Harley CB, Futcher AB, Greider CW. 1990. Telomeres shorten during ageing of human fibroblasts. *Nature* **345**: 458–460.

Hayflick L, Moorhead PS. 1961. The serial cultivation of human diploid cell strains. *Experimental cell research* **25**: 585–621.

Herbig U, Jobling WA, Chen BPC, Chen DJ, Sedivy JM. 2004. Telomere shortening triggers senescence of human cells through a pathway involving ATM, p53, and p21(CIP1), but not p16(INK4a). *Mol Cell* **14**: 501–513.

Hofmann JF, Laroche T, Brand AH, Gasser SM. 1989. RAP-1 factor is necessary for DNA loop formation in vitro at the silent mating type locus HML. *Cell* **57**: 725–737.

Howard BH. 1996. Replicative senescence: considerations relating to the stability of heterochromatin domains. *Experimental Gerontology* **31**: 281–293.

IJpma AS, Greider CW. 2003. Short telomeres induce a DNA damage response in Saccharomyces cerevisiae. *Mol Biol Cell* **14**: 987–1001.

Jackson JG, Pereira-Smith OM. 2006. p53 is preferentially recruited to the promoters of growth arrest genes p21 and GADD45 during replicative senescence of normal human fibroblasts. *Cancer Res* **66**: 8356–8360.

Jacob NK, Kirk KE, Price CM. 2003. Generation of telomeric G strand overhangs involves both G and C strand cleavage. *Mol Cell* **11**: 1021–1032.

Johnson FB, Marciniak RA, McVey M, Stewart SA, Hahn WC, Guarente L. 2001. The Saccharomyces cerevisiae WRN homolog Sgs1p participates in telomere maintenance in cells lacking telomerase. *EMBO J* **20**: 905–913.

Jullien L, Mestre M, Roux P, Gire V. 2013. Eroded human telomeres are more prone to remain uncapped and to trigger a G2 checkpoint response. *Nucleic Acids Res* **41**: 900–911.

Klein F, Laroche T, Cardenas ME, Hofmann JF, Schweizer D, Gasser SM. 1992. Localization of RAP1 and topoisomerase II in nuclei and meiotic chromosomes of yeast. *J Cell Biol* **117**: 935–948.

Konig P, Giraldo R, Chapman L, Rhodes D. 1996. The crystal structure of the DNA-binding domain of yeast RAP1 in complex with telomeric DNA. *Cell* **85**: 125–136.

Kozak ML, Chavez A, Dang W, Berger SL, Ashok A, Guo X, Johnson FB. 2010. Inactivation of the Sas2 histone acetyltransferase delays senescence driven by

telomere dysfunction. *EMBO J* **29**: 158–170.

Krishnamurthy J, Ramsey MR, Ligon KL, Torrice C, Koh A, Bonner-Weir S, Sharpless NE. 2006. p16INK4a induces an age-dependent decline in islet regenerative potential. *Nature* **443**: 453.

Kyrion G, Liu K, Liu C, Lustig AJ. 1993. RAP1 and telomere structure regulate telomere position effects in Saccharomyces cerevisiae. *Genes Dev* **7**: 1146–1159.

Lafferty-Whyte K, Cairney CJ, Jamieson NB, Oien KA, Keith WN. 2009. Pathway analysis of senescence-associated miRNA targets reveals common processes to different senescence induction mechanisms. *Biochim Biophys Acta* **1792**: 341–352.

Laroche T, Martin SG, Tsai-Pflugfelder M, Gasser SM. 2000. The dynamics of yeast telomeres and silencing proteins through the cell cycle. *J Struct Biol* **129**: 159–174.

Lee HW, Blasco MA, Gottlieb GJ, Horner JW, Greider CW, DePinho RA. 1998. Essential role of mouse telomerase in highly proliferative organs. *Nature* **392**: 569–574.

Lieb JD, Liu X, Botstein D, Brown PO. 2001. Promoter-specific binding of Rap1 revealed by genome-wide maps of protein-DNA association. *Nat Genet* **28**: 327–334.

Longo VD, Gralla EB, Valentine JS. 1996. Superoxide dismutase activity is essential for stationary phase survival in Saccharomyces cerevisiae. Mitochondrial production of toxic oxygen species in vivo. *J Biol Chem* **271**: 12275–12280.

Longo VD, Liou LL, Valentine JS, Gralla EB. 1999. Mitochondrial superoxide decreases yeast survival in stationary phase. *Arch Biochem Biophys* **365**: 131–142.

Longo VD, Shadel GS, Kaeberlein M, Kennedy B. 2012. Replicative and chronological aging in Saccharomyces cerevisiae. *Cell Metab* **16**: 18–31.

López MC, Smerage JB, Baker HV. 1998. Multiple domains of repressor activator protein 1 contribute to facilitated binding of glycolysis regulatory protein 1. *Proc Natl Acad Sci USA* **95**: 14112–14117.

Lundblad V, Szostak JW. 1989. A mutant with a defect in telomere elongation leads to senescence in yeast. *Cell* **57**: 633–643.

Mao Z, Ke Z, Gorbunova V, Seluanov A. 2012. Replicatively senescent cells are arrested in G1 and G2 phases. *Aging (Albany NY)* **4**: 431–435.

Marcand S, Gilson E, Shore D. 1997. A protein-counting mechanism for telomere length regulation in yeast. *Science* **275**: 986–990.

Marcand S, Pardo B, Gratias A, Cahun S, Callebaut I. 2008. Multiple pathways inhibit

NHEJ at telomeres. *Genes Dev* **22**: 1153–1158.

Maringele L, Lydall D. 2004. Telomerase- and recombination-independent immortalization of budding yeast. *genesdevcshlporg* **18**: 2663–2675. http://eutils.ncbi.nlm.nih.gov/entrez/eutils/elink.fcgi?dbfrom=pubmed&id=15489288&retmode=ref&cmd=prlinks.

McClintock B. 1941. The Stability of Broken Ends of Chromosomes in Zea Mays. *Genetics* **26**: 234–282.

McElligott R, Wellinger RJ. 1997. The terminal DNA structure of mammalian chromosomes. *EMBO J* **16**: 3705–3714.

Michishita E, McCord RA, Berber E, Kioi M, Padilla-Nash H, Damian M, Cheung P, Kusumoto R, Kawahara TLA, Barrett JC, et al. 2008. SIRT6 is a histone H3 lysine 9 deacetylase that modulates telomeric chromatin. *Nature* **452**: 492–496.

Molofsky AV, Slutsky SG, Joseph NM, He S, Pardal R, Krishnamurthy J, Sharpless NE, Morrison SJ. 2006. Increasing p16INK4a expression decreases forebrain progenitors and neurogenesis during ageing. *Nature* **443**: 448.

Moretti P, Freeman K, Coodly L, Shore D. 1994. Evidence that a complex of SIR proteins interacts with the silencer and telomere-binding protein RAP1. *Genes Dev* **8**: 2257–2269.

Moretti P, Shore D. 2001. Multiple Interactions in Sir Protein Recruitment by Rap1p at Silencers and Telomeres in Yeast. *Mol Cell Biol* **21**: 8082–8094.

Mortimer RK, Johnston JR. 1959. Life span of individual yeast cells. *Nature* **183**: 1751–1752.

Muller HJ. 1941. INDUCED MUTATIONS IN DROSOPHILA. *Cold Spring Harbor Symposia on Quantitative Biology* **9**: 151–167.

Muñoz-Jordán JL, Cross GA, de Lange T, Griffith JD. 2001. t-loops at trypanosome telomeres. *EMBO J* **20**: 579–588.

Narita M, Narita M, Krizhanovsky V, Nuñez S, Chicas A, Hearn SA, Myers MP, Lowe SW. 2006. A novel role for high-mobility group a proteins in cellular senescence and heterochromatin formation. *Cell* **126**: 503–514.

Narita M, Nuñez S, Heard E, Narita M, Lin AW, Hearn SA, Spector DL, Hannon GJ, Lowe SW. 2003. Rb-mediated heterochromatin formation and silencing of E2F target genes during cellular senescence. *Cell* **113**: 703–716.

Nautiyal S, DeRisi JL, Blackburn EH. 2002. The genome-wide expression response to telomerase deletion in Saccharomyces cerevisiae. *Proc Natl Acad Sci USA* **99**: 9316–9321.

Negrini S, Ribaud V, Bianchi A, Shore D. 2007. DNA breaks are masked by multiple

Rap1 binding in yeast: implications for telomere capping and telomerase regulation. *Genes Dev* **21**: 292–302.

Neyret-Kahn H, Benhamed M, Ye T, Le Gras S, Cossec J-C, Lapaquette P, Bischof O, Ouspenskaia M, Dasso M, Seeler J, et al. 2013. Sumoylation at chromatin governs coordinated repression of a transcriptional program essential for cell growth and proliferation. *Genome Research*.

O'Sullivan RJ, Kubicek S, Schreiber SL, Karlseder J. 2010. Reduced histone biosynthesis and chromatin changes arising from a damage signal at telomeres. *Nat Struct Mol Biol* **17**: 1218–1225.

Olovnikov AM. 1973. A theory of marginotomy: The incomplete copying of template margin in enzymic synthesis of polynucleotides and biological significance of the phenomenon. *Journal of Theoretical Biology* **41**: 181–190.

Olsen CL, Gardie B, Yaswen P, Stampfer MR. 2002. Raf-1-induced growth arrest in human mammary epithelial cells is p16-independent and is overcome in immortal cells during conversion. *Oncogene* **21**: 6328–6339.

Palladino F, Laroche T, Gilson E, Axelrod A, Pillus L, Gasser SM. 1993. SIR3 and SIR4 proteins are required for the positioning and integrity of yeast telomeres. *Cell* **75**: 543–555.

Palm W, de Lange T. 2008. How shelterin protects mammalian telomeres. *Annu Rev Genet* **42**: 301–334.

Pang JH, Chen KY. 1994. Global change of gene expression at late G1/S boundary may occur in human IMR-90 diploid fibroblasts during senescence. *J Cell Physiol* **160**: 531–538.

Pardo B, Marcand S. 2005. Rap1 prevents telomere fusions by nonhomologous end joining. *EMBO J* **24**: 3117–3127.

Pignolo RJ, Martin BG, Horton JH, Kalbach AN, Cristofalo VJ. 1998. The pathway of cell senescence: WI-38 cells arrest in late G1 and are unable to traverse the cell cycle from a true G0 state. *Experimental Gerontology* **33**: 67–80.

Platt JM, Ryvkin P, Wanat JJ, Donahue G, Ricketts MD, Barrett SP, Waters HJ, Song S, Chavez A, Abdallah KO, et al. 2013. Rap1 relocalization contributes to the chromatin-mediated gene expression profile and pace of cell senescence. *Genes Dev* **27**: 1406–1420.

Reddel RR. 2000. The role of senescence and immortalization in carcinogenesis. *Carcinogenesis* **21**: 477–484.

Ritchie KB, Mallory JC, Petes TD. 1999. Interactions of TLC1 (which encodes the RNA subunit of telomerase), TEL1, and MEC1 in regulating telomere length in the

yeast Saccharomyces cerevisiae. *Mol Cell Biol* **19**: 6065–6075.

Rogan EM, Bryan TM, Hukku B, Maclean K, Chang AC, Moy EL, Englezou A, Warneford SG, Dalla-Pozza L, Reddel RR. 1995. Alterations in p53 and p16INK4 expression and telomere length during spontaneous immortalization of Li-Fraumeni syndrome fibroblasts. *Mol Cell Biol* **15**: 4745–4753.

Sadaie M, Salama R, Carroll T, Tomimatsu K, Chandra T, Young ARJ, Narita M, Pérez-Mancera PA, Bennett DC, Chong H, et al. 2013. Redistribution of the Lamin B1 genomic binding profile affects rearrangement of heterochromatic domains and SAHF formation during senescence. *Genes Dev* **27**: 1800–1808.

Schaetzlein S, Kodandaramireddy NR, Ju Z, Lechel A, Stepczynska A, Lilli DR, Clark AB, Rudolph C, Kuhnel F, Wei K, et al. 2007. Exonuclease-1 deletion impairs DNA damage signaling and prolongs lifespan of telomere-dysfunctional mice. *Cell* **130**: 863–877.

Schawalder SB, Kabani M, Howald I, Choudhury U, Werner M, Shore D. 2004. Growth-regulated recruitment of the essential yeast ribosomal protein gene activator Ifh1. *Nature* **432**: 1058.

Seshadri T, Campisi J. 1990. Repression of c-fos transcription and an altered genetic program in senescent human fibroblasts. *Science* **247**: 205–209.

Sfeir A, de Lange T. 2012. Removal of shelterin reveals the telomere end-protection problem. *Science* **336**: 593–597.

Shah PP, Donahue G, Otte GL, Capell BC, Nelson DM, Cao K, Aggarwala V, Cruickshanks HA, Rai TS, McBryan T, et al. 2013. Lamin B1 depletion in senescent cells triggers large-scale changes in gene expression and the chromatin landscape. *Genes Dev* **27**: 1787–1799.

Shelton DN, Chang E, Whittier PS, Choi D, Funk WD. 1999. Microarray analysis of replicative senescence. *Curr Biol* **9**: 939–945.

Shimi T, Butin-Israeli V, Adam SA, Hamanaka RB, Goldman AE, Lucas CA, Shumaker DK, Kosak ST, Chandel NS, Goldman RD. 2011. The role of nuclear lamin B1 in cell proliferation and senescence. *Genes Dev* **25**: 2579–2593.

Singer MS, Gottschling DE. 1994. TLC1: template RNA component of Saccharomyces cerevisiae telomerase. *Science* **266**: 404–409.

Smeal T, Claus J, Kennedy B, Cole F, Guarente L. 1996. Loss of transcriptional silencing causes sterility in old mother cells of S. cerevisiae. *Cell* **84**: 633–642.

Stansel RM, de Lange T, Griffith JD. 2001. T-loop assembly in vitro involves binding of TRF2 near the 3′ telomeric overhang. *EMBO J* **20**: 5532.

Stein GH, Drullinger LF, Robetorye RS, Pereira-Smith OM, Smith JR. 1991. Senescent

cells fail to express cdc2, cycA, and cycB in response to mitogen stimulation. *Proc Natl Acad Sci USA* **88**: 11012–11016.

Straatman KR, Louis EJ. 2007. Localization of telomeres and telomere-associated proteins in telomerase-negative Saccharomyces cerevisiae. *Chromosome Res* **15**: 1033–1050.

Sun F, Fu H, Liu Q, Tie Y, Zhu J, Xing R, Sun Z, Zheng X. 2008. Downregulation of CCND1 and CDK6 by miR-34a induces cell cycle arrest. *FEBS Lett* **582**: 1564–1568.

Takeuchi S, Takahashi A, Motoi N, Yoshimoto S, Tajima T, Yamakoshi K, Hirao A, Yanagi S, Fukami K, Ishikawa Y, et al. 2010. Intrinsic cooperation between p16INK4a and p21Waf1/Cip1 in the onset of cellular senescence and tumor suppression in vivo. *Cancer Res* **70**: 9381–9390.

Tazawa H, Tsuchiya N, Izumiya M, Nakagama H. 2007. Tumor-suppressive miR-34a induces senescence-like growth arrest through modulation of the E2F pathway in human colon cancer cells. *Proc Natl Acad Sci USA* **104**: 15472–15477.

Teixeira MT. 2013. Saccharomyces cerevisiae as a Model to Study Replicative Senescence Triggered by Telomere Shortening. *Front Oncol* **3**: 101.

Tomar RS, Zheng S, Brunke-Reese D, Wolcott HN, Reese JC. 2008. Yeast Rap1

contributes to genomic integrity by activating DNA damage repair genes. *EMBO J* **27**: 1575–1584.

Tornow J, Zeng X, Gao W, Santangelo GM. 1993. GCR1, a transcriptional activator in Saccharomyces cerevisiae, complexes with RAP1 and can function without its DNA binding domain. *EMBO J* **12**: 2431–2437.

Vignais ML, Huet J, Buhler JM, Sentenac A. 1990. Contacts between the factor TUF and RPG sequences. *J Biochem* **265**: 14669–14674.

Vodenicharov MD, Wellinger RJ. 2006. DNA degradation at unprotected telomeres in yeast is regulated by the CDK1 (Cdc28/Clb) cell-cycle kinase. *Mol Cell* **24**: 127–137.

Wade JT, Hall DB, Struhl K. 2004. The transcription factor Ifh1 is a key regulator of yeast ribosomal protein genes. *Nature* **432**: 1054–1058.

Wellinger RJ, Ethier K, Labrecque P, Zakian VA. 1996. Evidence for a new step in telomere maintenance. *Cell* **85**: 423–433.

Wright WE, Shay JW. 2001. Cellular senescence as a tumor-protection mechanism: the essential role of counting. *Curr Opin Genet Dev* **11**: 98–103.

Xu D, Takeshita F, Hino Y, Fukunaga S, Kudo Y, Tamaki A, Matsunaga J, Takahashi R-U, Takata T, Shimamoto A, et al. 2011. miR-22 represses cancer progression by

inducing cellular senescence. *J Cell Biol* **193**: 409–424.

Yamakoshi K, Takahashi A, Hirota F, Nakayama R, Ishimaru N, Kubo Y, Mann DJ, Ohmura M, Hirao A, Saya H, et al. 2009. Real-time in vivo imaging of p16Ink4a reveals cross talk with p53. *J Cell Biol* **186**: 393–407.

Yoon IK, Kim HK, Kim YK, Song I-H, Kim W, Kim S, Baek S-H, Kim JH, Kim J-R. 2004. Exploration of replicative senescence-associated genes in human dermal fibroblasts by cDNA microarray technology. *Experimental Gerontology* **39**: 1369–1378.

Zglinicki von T. 2002. Oxidative stress shortens telomeres. *Trends Biochem Sci* **27**: 339–344.

Zhang H. 2003. Senescence-specific gene expression fingerprints reveal cell-type-dependent physical clustering of up-regulated chromosomal loci. *Proceedings of the National Academy of Sciences* **100**: 3251–3256.

Zhang J, Pickering CR, Holst CR, Gauthier ML, Tlsty TD. 2006. p16INK4a modulates p53 in primary human mammary epithelial cells. *Cancer Res* **66**: 10325–10331.

Zhang R, Chen W, Adams PD. 2007. Molecular dissection of formation of senescence-associated heterochromatin foci. *Mol Cell Biol* **27**: 2343–2358.

Zhao Y, McIntosh KB, Rudra D, Schawalder S, Shore D, Warner JR. 2006. Fine-

structure analysis of ribosomal protein gene transcription. *Mol Cell Biol* **26**: 4853–4862.

Zwerschke W, Mazurek S, Stöckl P, Hütter E, Eigenbrodt E, Jansen-Dürr P. 2003. Metabolic analysis of senescent human fibroblasts reveals a role for AMP in cellular senescence. *Biochem J* **376**: 403–411.

CHAPTER 2: Rap1 relocalization contributes to the chromatin-mediated gene expression profile and pace of cell senescence

INTRODUCTION

Mammalian cell senescence is an active response to stresses that put cells at risk for neoplastic transformation, including DNA damage, oncogenic signals, dramatic chromatin changes, and critically shortened or dysfunctional telomeres (Campisi 2013). Accordingly, cell senescence limits carcinogenesis in a cell autonomous fashion. Senescence may also have negative consequences, including contributing to carcinogenesis in a non-cell autonomous manner and to age-related degenerative pathologies (Baker et al. 2011). Telomere shortening and uncapping are particularly important drivers of human cell senescence, as evidenced by the capacity of the telomerase enzyme to immortalize human cells and by associations between dysfunctional telomeres and age-related diseases and progeroid syndromes (Armanios 2013). Senescent cells are characterized by persistent cell cycle arrest mediated by DNA damage checkpoint factors, and also display profound changes in gene expression, chromatin organization, metabolism, and secretory behavior (Campisi 2013). The mechanisms underlying these changes are not well understood, but such knowledge promises to enhance our understanding of cancer and other age-related diseases.

In the budding yeast *S. cerevisiae* telomere length is maintained by telomerase, and thus yeast cells do not naturally senesce as a consequence of gradual telomere shortening. Telomere-driven senescence can be modeled in yeast by genetic inactivation of telomerase, leading eventually to critical telomere shortening and mitotic arrest (Lundblad and Szostak 1989). It is important to distinguish yeast senescence from yeast replicative aging and from chronological aging. Replicative aging is measured by the number of daughters produced by a mother cell prior to her death, and chronological aging by the time a yeast cell can survive under conditions of nutrient deprivation; however, neither of these aging models are driven by telomere shortening. Senescent yeast display several features remarkably similar to mammalian cells that have senesced due to telomere shortening. For example both involve DDRs and cell cycle arrest dependent on PI3-kinase-type kinases (IJpma and Greider 2003; Herbig et al. 2004). Both also involve activation of stress responses, inhibition of glycolysis, and downregulation of mRNAs encoding the core histones (Nautiyal et al. 2002; O'Sullivan et al. 2010; Zwerschke et al. 2003). Critical telomere shortening in both settings causes loss of heterochromatic histone marks and subtelomeric gene silencing (Benetti et al. 2007; Kozak et al. 2010), and the telomere ends can fuse to one another (Hackett et al. 2001; Blasco et al. 1997; Capper et al. 2007). Furthermore, similar factors modulate the pace of senescence in both systems. For example, telomere-driven senescence in mammals is promoted by ATM, ATR and EXO1, and is delayed by the WRN and

BLM helicases, and in yeast the orthologous proteins Tel1, Mec1, Exo1, and Sgs1 function similarly (IJpma and Greider 2003; Herbig et al. 2004; Schaetzlein et al. 2007; Ritchie et al. 1999; Abdallah et al. 2009; Maringele and Lydall 2004; Johnson et al. 2001). Thus, yeast telomerase mutants provide a valuable model for understanding several features of cell senescence.

We considered the possibility that telomere shortening might cause relocalization of normally telomere-bound proteins to new genomic loci and thus contribute to senescence, an idea long hypothesized but never demonstrated (Campisi 1997). A prime candidate for such a factor in *S. cerevisiae* is Rap1 (Repressor activator protein 1). Rap1 binds directly to telomere repeat DNA in a sequence-specific fashion *via* two tandem Myb-type homeodomains linked by a short peptide (Konig et al. 1996). At telomeres, Rap1 contributes to capping and length regulation, localization to the nuclear periphery, and formation of heterochromatin (Marcand et al. 1997; Kyrion et al. 1993; Pardo and Marcand 2005; Vodenicharov et al. 2010; Negrini et al. 2007; Klein et al. 1992; Palladino et al. 1993). Rap1 mediates telomere silencing by recruiting the Sir protein complex (Moretti and Shore 2001). In contrast, at hundreds of genes Rap1 functions as a transcriptional activator, *via* binding to upstream promoter regions and interacting with various coactivator proteins (Zhao et al. 2006; Tornow et al. 1993; Schawalder et al. 2004). These dual sets of Rap1 functions - at telomeres and at genomic loci -

raise the possibility that if Rap1 were lost from shortened telomeres it might expand its roles at extra-telomeric loci. Several considerations support this idea. First, Rap1 is an abundant protein (~4000 molecules per haploid cell: Buchman et al. 1988), and a significant fraction (at least 10-15%) localizes to telomeres, which by fluorescence microscopy are visualized as prominent foci at the nuclear periphery that appear to be the primary sites of Rap1 localization (Gotta et al. 1996; Klein et al. 1992). Thus the telomeric pool of Rap1 is large enough to have the potential for significant effects upon redistribution. Second, many loci with consensus or near-consensus Rap1 target sequences are not bound by the protein in normal cells, raising the possibility that these sites might be bound under conditions that increase the available pool of Rap1 or that increase site accessibility. Third, Rap1 relocalizes to some degree in the G2 phase of the cell cycle (Laroche et al. 2000) and under conditions of stress, including low glucose (Buck and Lieb 2006) and DNA damage by methyl methanesulfonate (MMS: Tomar et al. 2008). Finally, senescence itself may be a Rap1-relocalizing stress because fluorescence microscopy studies indicate that critical telomere shortening causes an apparent loss in intensity of telomere-associated Rap1 along with enhanced localization of Rap1 in numerous other nuclear regions (Straatman and Louis 2007; Palladino et al. 1993). Yet the questions of whether Rap1 relocalizes to particular genomic targets at senescence and how such relocalization might impact gene expression and the rate of senescence have not been addressed.

Here we demonstrate that at senescence Rap1 is lost from subtelomeric regions and localizes to upstream promoter regions of hundreds of new target genes. This redistribution of Rap1 depends on the Mec1 DDR kinase, and plays direct roles in senescence-related gene expression. Remarkably, the genes encoding the core histones are among the new targets of Rap1, and Rap1 contributes to a global decline in histone levels and also decreases nucleosome occupancy selectively at the promoters of genes that are upregulated at senescence. Moreover, this Rap1-histone interplay impacts not only gene expression but also the pace of senescence.

RESULTS

Rap1 targets new loci in senescent cells

Chromatin immunoprecipitation (ChIP) using anti-Rap1 antibodies was performed in wild type and senescent *tlc1Δ* cells, and the genomic distributions of enriched fragments were assessed using high resolution tiling arrays (ChIP-chip; Figs. 1A and S1). Enrichment was calculated with respect to non-specific IgG control ChIP, although essentially identical results were obtained when the comparison was made to input chromatin (data not shown). Using a conservative MAT cutoff of 10^{-5} (see Methods), 798 Rap1 target genes were identified in wild type cells. These

targets were highly similar to those identified previously (Fig. S2; $p = 2.5 \times 10^{-123}$) (Harbison et al. 2004). At senescence, three major types of changes in Rap1 localization were apparent. First, there is increased enrichment at many sites already targeted by Rap1 in wild type cells (Figs. 1A and S1). Second, and more strikingly, there are many new Rap1 target peaks (Figs. 1A and S1). Third, Rap1 occupancy declines at subtelomeres (Figs. 1B, 7B and S3). These changes do not reflect alterations in overall Rap1 levels, which remain nearly constant per cell (Fig. 1C which compares equal cell numbers, data not shown, and see Fig. 7D). All three types of changes were confirmed *via* ChIP-qPCR against multiple targets (Figs. 1D-F; Rap1 ChIP enrichment was in comparison to *ACT1*, and was normalized to IgG and input controls).

We found that Rap1 localizes to 491 new target genes at senescence, and we refer to these as NRTS ("New Rap1 Targets at Senescence"; Fig 2A). Similar to Rap1 targets in normal cells, NRTS were localized primarily in upstream promoter regions (Figs. 2B and 2C; Fig S4). We searched for enriched sequence motifs within the NRTS promoters using HOMER, a *de novo* motif discovery program (Heinz et al. 2010). Whereas the previously defined Rap1 consensus CACCCA(A/C)ACA (Lieb et al. 2001) was the most significant motif identified in the wild type targets (798 genes), it was not found in the NRTS target set (Fig 2D). Instead, the most significant NRTS motif ($p = 10^{-12}$) was TTTTTTGCG(C/G), which may have weak nucleosome destabilizing activity (Segal and Widom 2009; Wu and Li 2010).

Consistent with this possibility, at senescence Rap1 preferentially targets regions of the genome where histones have been found to have high turnover under normal conditions (p-value = 1.4×10^{-84}, Table S1). Even though NRTS are not enriched for consensus Rap1 binding sites, they are enriched for suboptimal Rap1 binding sites (Table S2A, B). The tandem Myb domains of Rap1 each bind hemisites within consensus targets, and the peptide linking the Myb domains binds a three nucleotide spacer linking the hemisites (Konig et al. 1996). Rap1 can also bind with significant affinity (reduced five to ten-fold from its optimal 10^{-11} M Kd) to a single hemisite paired with a linker sequence (cf. Table S2A; Del Vescovo et al. 2004). Such hemisite-linker sites were enriched within NRTS; $p = 2.7 \times 10^{-4}$ for the presence of at least one such site (Table S2). Furthermore, in vitro Rap1 binding data (Mukherjee et al. 2004) indicate that Rap1 binds NRTS promoters with an affinity lower than for natural Rap1 targets but substantially higher than non-Rap1 targets (Fig. 2E). Thus DNA binding by Rap1 may contribute to NRTS occupancy. Overall it appears that the forces dictating Rap1 occupancy at the NRTS *vs.* normal targets differ due to changes in Rap1, its cofactors, or the chromatin structure of the target sites themselves.

NRTS are preferentially upregulated by Rap1 at senescence

In wild type cells, Rap1 activates transcription at most of its target genes, but also contributes to transcriptional silencing at subtelomeres and the silent mating

loci. To address whether Rap1 affects gene expression of the NRTS, we first examined microarray-based mRNA expression analyses for senescent *tlc1Δ* mutants (Nautiyal et al. 2002) . Remarkably, the NRTS preferentially overlap the set of genes that are upregulated at senescence ($p = 1.9x10^{-5}$; Fig 3A). Furthermore, Rap1 specifically targets some of the most highly upregulated genes at senescence, e.g. *HSP26, NCA3*, and *GAC1*, Fig. 2B, S4A). In contrast, there is no enrichment for NRTS within the set of genes downregulated at senescence ($p = 1$). We note also that the majority of NRTS are not regulated significantly at senescence, and so Rap1 binding is apparently not sufficient to confer regulation in all cases. In other words, although some NRTS are upregulated, others are downregulated, and most are not regulated at senescence, overall the set of NRTS genes shows a statistical tendency to be upregulated.

To test whether Rap1 activates expression of the NRTS that are upregulated at senescence, we elevated Rap1 levels in wild type cells two-fold by introducing a single copy plasmid with *RAP1* expression driven by the *NOP1* promoter (*NOP1p-RAP1*; Figs. 3B and S5) and then measured changes in Rap1 occupancy and gene expression at NRTS. Although high levels of Rap1 are toxic (Freeman et al. 1995), the two-fold increase in Rap1 inhibited cell growth only slightly (Fig. S5C). In comparison to the non-targeted *ACT1* locus, Rap1 overexpression caused significant elevations in Rap1 binding at the upstream promoter regions of senescence-upregulated NRTS (Fig. 3C, *vs. ACT1*) and in the levels of mRNA from these genes

(Fig 3D) in all cases tested. Control experiments confirmed that Rap1 does not regulate the *ACT1* locus (Fig S5D, E). Therefore, increasing the level of Rap1 is sufficient to mimic the effects of senescence on upregulated NRTS. We confirmed the importance of Rap1 in the upregulation of these NRTS by decreasing the levels of Rap1 at senescence. Because *RAP1* is essential, we could not test the effects of deleting *RAP1* entirely, but we were able to decrease Rap1 levels ~40% using the hypomorphic *rap1 DAmP* (Decreased Abundance by mRNA Perturbation) allele (Breslow et al. 2008) (Figs. 3E and S5E). *rap1 DAmP* blunted the upregulation in NRTS mRNA levels at senescence, and in contrast did not affect mRNA levels from the non-targeted *ACT1* and *SPC42* control loci (Fig. 3F); and control ChIP experiments confirmed that the allele also reduced Rap1 levels at these NRTS at senescence (Fig. 3G, *vs. ACT1*). Therefore for NRTS that are activated at senescence, Rap1 relocalization to these loci apparently contributes to their upregulation.

Because senescence results in a G2/M cell cycle arrest, we wondered if altered expression of NRTS might be a secondary effect of the arrest. Comparison of the NRTS genes that are senescence-regulated (Nautiyal et al. 2002) to those that are mitotic arrest-regulated (Spellman et al. 1998) revealed a non-significant overlap between upregulated datasets ($p = 1$, Fig. S6A) and downregulated datasets ($p = 0.65$, Fig. S6B). And qPCR analyses showed that expression of senescence-upregulated NRTS genes either did not change or was diminished with nocodazole-

mediated arrest (Fig S6C). These findings suggest that the Rap1-dependent regulation of NRTS is largely independent of G2/M arrest *per se*.

Rap1 targets and represses the core histone genes at senescence

Gene ontology (GO) analysis of the NRTS revealed enrichment for genes involved in metabolism, stress responses, and aspects of DDRs (Table S3). These broadly reflect the functional categories of genes with altered expression noted previously for senescent *tlc1Δ* mutants (Nautiyal et al. 2002), indicating that Rap1 does not target a narrow functional subset of senescence-regulated genes. However, we were surprised to find that the second most significant GO category for the NRTS was the *nuclear nucleosome* ($p = 2.2 \times 10^{-4}$), including all of the genes encoding the core histone proteins H2A, H2B, H3 and H4. Indeed, direct inspection of ChIP-chip data for the loci encoding these proteins, *HTA1-HTB1, HTA2-HTB2, HHT1-HHF1,* and *HHT2-HHF2*, revealed significant Rap1 binding in senescent cells (Fig. 4A). *HTZ1* (encoding the only *S. cerevisiae* H2A variant histone) was also strongly targeted by Rap1 at senescence, whereas *HHO1* (encoding the H1-like protein) was weakly targeted, and *CSE4* (encoding the centromere-specific H3 variant histone) was not (Fig. S7A). These findings were confirmed using Rap1 ChIP-qPCR (Figs S7B). Diminished expression of the core histone loci at senescence was noted previously (Nautiyal et al. 2002), but these loci have never been identified as Rap1 targets. In keeping with these observations, we found that the levels of histone proteins H2A,

H2B, H3, and H4 were significantly reduced at senescence (Figs 4B and S7C-D). The decline in histone levels was not a simple consequence of G2/M arrest, because except for small reductions in H3 and H4, histone levels remained largely steady following treatment of wild type cells with nocodazole (Fig. S7E).

Even though NRTS are not enriched overall for genes that are downregulated at senescence, it was still possible that Rap1 contributes to the senescence-related downregulation of histone genes. We found that Rap1 overexpressed by two-fold (*via* plasmid-based *NOP1p-RAP1*) in wild type cells led to elevated Rap1 binding at all histone promoters (Fig. 4C), along with repression of histone gene expression and protein levels in cells that had been arrested with nocodazole (Fig. 4D; Fig S7F). This Rap1-dependent repression was not observed unless cells were arrested in this fashion (not shown), consistent with the requirement for normal histone levels to support cell cycle progression and with the natural arrest of senescent cells in G2/M. Moreover, reduction in Rap1 levels at senescence, *via rap1 DAmP,* reduced Rap1 occupancy at the histone loci (Fig. 4E) and blunted histone gene down regulation (Fig 4F). Therefore, Rap1 binds and inhibits the expression of the core histone genes at senescence.

Rap1 requires the Sir2/3/4 protein complex to silence telomeres and the silent mating loci (Strahl-Bolsinger et al. 1997), and furthermore, the Sir complex has been found to relocalize from telomeres to genomic loci under various stresses (Martin et al. 1999). We therefore asked whether repression of the histone loci

might depend on the Sir complex. However, repression proved to be Sir-independent, as deletion of *SIR2*, *SIR3* or *SIR4* did not affect downregulation of the core histone loci in senescent cells (Fig. S8).

Histone losses contribute to altered gene expression at senescence, and connect to reciprocal occupancy of Rap1 and histones at NRTS

Because histone RNA and protein levels are dramatically downregulated at senescence, we wondered if these processes might contribute to selective gene expression changes at senescence. To address this question, we first compared genes that change in expression following acute histone H4 depletion (Wyrick et al. 1999) to 1) genes that are differentially expressed at senescence (Nautiyal et al. 2002) and 2) genes that are differentially expressed at senescence and are also NRTS. These comparisons revealed a significant overlap in all cases (upregulated with H4 depletion and senescence: $p = 4.5 \times 10^{-18}$, downregulated with H4 depletion and senescence: $p= 1.7 \times 10^{-49}$, and the same up and downregulated datasets restricted to NRTS: $p = 3.1 \times 10^{-4}$ and $p = 3.5 \times 10^{-7,}$ respectively; Tables S4A-B). The reduced significance of the NRTS subset is a consequence of the smaller number of loci involved. In fact, the fraction of genes up/downregulated at senescence that are also up/downregulated with H4 depletion is greater when restricted to the NRTS (29% and 42%, for up and downregulated loci, respectively) than for genes overall (20% and 34%, for up and downregulated loci, respectively). In addition, we

discovered that genes upregulated at senescence tend to display rapid histone turnover in wild type cells (Table S5), indicating that they naturally contain low stability nucleosomes; and as noted above (Table S1), such high turnover regions are preferentially targeted by Rap1 at senescence. Finally, we found that overexpression of the four core histone proteins in senescent cells (*via GAL1-10* driven expression of *HTA1-HTB1* and *HHT2-HHF2*: Feser et al. 2010) blunts the activation of NRTS at senescence (Fig. 4G). Therefore, histone loss appears to be an important contributor to changes in gene expression at senescence, particularly those governed by redistribution of Rap1 to new target genes.

Rap1 and nucleosome occupancy have been found to correlate inversely at many genomic loci, which might reflect an ability of Rap1 to compete directly with nucleosomes for some DNA sites or might instead be an indirect consequence of nucleosome losses associated with transcriptional activation by Rap1 at target genes (Ganapathi et al. 2011; Yu and Morse 1999; Koerber et al. 2009; Lickwar et al. 2012; Rhee and Pugh 2011). ChIP-qPCR analyses for Rap1 and histone H3 demonstrated reciprocal changes for the proteins at NRTS that are activated at senescence, in comparison to the *ACT1* locus, which is not targeted by *RAP1* (Fig 5A). Thus histones are not lost uniformly from chromatin at senescence, and loss is more pronounced at activated NRTS. Rap1 is required for these losses, because senescent cells containing the *rap1-DAmP* allele accumulated reduced levels of Rap1 at these loci, and the loss of histone H3 from these loci was blunted or blocked completely

(Fig. 5B). In addition, and consistent with a reciprocal relationship between Rap1 and nucleosome occupancy, overexpression of the four core histone proteins in senescent cells similarly inhibited accumulation of Rap1 and the loss of histone H3 at these activated NRTS (Fig. 5C). To rule out the possibility that histone losses at these loci was an indirect consequence of decreased histone levels overall, we performed a timecourse of Rap1 overexpression in wild type cells and demonstrated that histone H3 is lost from activated NRTS with more rapid kinetics than any reduction in overall histone protein levels (Fig. S9).

Because the core histone loci are a class of NRTS that are repressed by Rap1 at senescence, we explored how senescence affects the relationships between Rap1 and histones at the promoters of these loci. Although ChIP-qPCR tests confirmed that Rap1 accumulates at the upstream promoter regions of the histone genes at senescence, histone H3 was actually retained (in contrast to H3 losses at the activated NRTS; Fig 5D). Furthermore, although senescent *rap1-DAmP* cells accumulated reduced levels of Rap1 at the histone loci, H3 actually became slightly enriched in comparison to senescent cells with normal levels of Rap1 (Fig. 5E), even though histone gene repression at senescence is alleviated, i.e. derepressed, by *rap1-DAmP* (cf. Fig. 4F)). Therefore Rap1-dependent repression of the histone loci at senescence is associated with retention of histones in histone gene promoter regions but also must involve additional Rap1-dependent repressive mechanisms.

Rap1 drives the rate of senescence

Although Rap1 targets new loci and drives gene expression changes in senescent cells, it did not necessarily follow that such events would impact the rate of senescence. To test this possibility we compared senescence in cells with wild type to reduced levels of Rap1 (i.e. *tlc1Δ vs. rap1-DAmP tlc1Δ*). As in all our comparisons of senescence in cells of different genotype, we performed this experiment with the haploid progeny derived from a single *TLC1/tlc1Δ* diploid that was also heterozygous for the allele to be tested (i.e. *RAP1*/*rap1-DAmP* in this case); thus the different haploids inherit telomeres of similar lengths, enabling fair comparisons between genotypes. Remarkably, the *rap1-DAmP tlc1Δ* cells senesced significantly more slowly than the control *tlc1Δ* cells (Fig. 6A; $p = 0.0012$). This is not an effect of early activation of the homologous recombination (HR)-dependent survivor pathway of telomere maintenance (Lundblad and Blackburn 1993) because the *rap1-DAmP tlc1Δ* mutants reached their growth nadir and formed survivors after more, rather than fewer, population doublings (approximately 85 vs. 70 PDs). The delayed senescence is a somewhat surprising result because Rap1 naturally contributes to telomere capping (Negrini et al. 2007; Vodenicharov et al. 2010; Pardo and Marcand 2005), and thus a reduction in Rap1 levels might be expected to exacerbate telomere dysfunction. We infer that the Rap1 proteins bound tightly to telomere repeat DNA (Kd $\sim 10^{-11}$ M: Vignais et al. 1990) are unaffected by the small reduction in Rap1 levels, whereas it is clear that Rap1 binding at NRTS loci, which

lack canonical Rap1 binding sites, is diminished (Fig. 3G). This inference is supported by our finding that there are normal levels of Rap1 at telomere repeats in the DAmP strain, as indicated by ChIP (Figs. S5F, G), and by the capacity of the DAmP allele to maintain normal telomere length and to prevent end-fusions (Lescasse et al. 2013; Ungar et al. 2009). Overall, our findings indicate that Rap1 drives not only the gene expression phenotype but also the pace of senescence.

Histone overexpression delays senescence

We wondered if the antagonistic relationships between Rap1 and histones also apply to the rate of senescence. We compared cells with normal histone loci to those also overexpressing the four core histones (using histone genes under *GAL1-10* control as above), and found that histone overexpression delays senescence (Fig 6B). Therefore, the pace of senescence is apparently propelled by the histone losses that accompany it, and the pro-senescence role of Rap1 may be explained by its capacity to inhibit histone expression and function.

Rap1 relocalization and function at senescence depends on *MEC1*

The loss of Rap1 binding sites caused by telomere shortening might contribute to its relocalization in senescent cells. However, critically shortened telomeres in senescent cells activate a DDR, and Rap1 has previously been found to localize to the *RNR3* locus in cells exposed MMS in a fashion that depends on the

DDR checkpoint kinases Mec1 and Dun1 (Tomar et al. 2008), raising the possibility that the DDR contributes to Rap1 relocalization at senescence. We therefore investigated what DDR factors are involved in Rap1 functions at senescence, including the PI3-type kinases Mec1 and Tel1, and the Dun1 kinase. Dun1 acts downstream of the Rad53 kinase, which itself is partially responsible for mediating signaling from Mec1 and Tel1 (Putnam et al. 2009). Tel1 localizes to short telomeres (Sabourin et al. 2007), and can contribute to the pace of senescence (Abdallah et al. 2009; Ritchie et al. 1999), but the G2/M arrest at senescence depends on Mec1 and is independent of Tel1 and Rad53 (Enomoto et al. 2002; IJpma and Greider 2003). Therefore, one or more of these DDR factors might affect the action of Rap1 at senescence.

We examined the expression of upregulated NRTS at senescence by qPCR, and found that for all eight loci examined, deletion of *MEC1* substantially blunted their upregulation, but deletion of *TEL1* or *DUN1* had no effect (Figs. 7A and S10). In addition, *MEC1* deletion partially or completely rescued histone downregulation at senescence (Fig. 7A). In keeping with these results, Rap1 ChIP-qPCR demonstrated that *MEC1* is required at senescence for full loss of Rap1 at subtelomeres (Fig. 7B) and for enrichment at NRTS (Fig. 7C). Our findings indicate that Mec1 is necessary to remove Rap1 from subtelomeres and deposit it at its novel target sites at senescence. The dependence on Mec1, but not Tel1 and Dun1, correlates with the requirements for G2/M arrest at senescence. In addition, TCA-extracted Rap1

displayed reduced-mobility forms at senescence, which are also dependent on *MEC1* (Fig. 7D). Therefore, although additional studies will be required to understand the nature and functional significance of these apparent Rap1 modifications, these findings raise the possibility that post-translational modification of Rap1 is involved in its relocalization.

DISCUSSION

Our experimental findings show that Rap1 targets the upstream promoter regions of hundreds of novel targets at senescence (the NRTS), and that it plays important roles in the regulation of these targets. NRTS tend to be upregulated at senescence overall, but some NRTS are downregulated, most notably the genes encoding the core histone proteins. This was a surprising finding because, although Rap1 normally targets at least five percent of all genes, it has never before been observed at the histone genes. Consistent with the downregulation of histone transcripts in senescent yeast (Nautiyal et al. 2002), we show for the first time that histone protein levels also decline significantly. Histone losses appear to be critical mediators of senescence, because the gene expression changes in senescent cells are remarkably similar to those following acute depletion of histone H4, and because senescence can be delayed by overexpression of the core histone genes. Histone losses have also been observed recently in other aging-related settings, including replicatively aged yeast mother cells and senescent cultured human fibroblasts,

suggesting histone losses may be a conserved feature of aging and senescence (Feser et al. 2010; O'Sullivan et al. 2010). Importantly, the mechanisms underlying histone losses in these other settings are not known, and therefore our demonstration that Rap1 plays a role in transducing the DDR signals at critically shortened telomeres into histone losses reveals the most detailed mechanism known to date.

Rap1 leads to histone losses in two ways. First, it represses histone gene expression by targeting the upstream promoter regions of the histone loci, thus contributing to global downregulation of histones. Second, it contributes to site-specific losses in nucleosome occupancy at the promoters of NRTS that are upregulated at senescence (as reflected by ChIPed histone H3 levels). It will be important in future studies to explore the detailed mechanisms underlying these two effects of Rap1, but there are already clues to possible mechanisms.

In the case of histone gene downregulation, it is clear that Rap1 does not repress expression *via* recruitment of the Sir2/3/4 protein complex, nor is repression explained by increased nucleosome occupancy at the histone gene promoters. The regulation of histone gene expression in normal cells is under tight control, and involves a large number of regulators, both positive (Spt10, Swi4, Mbp1, Rtt109 and the SWI/SNF complex) and negative (the HIR and RSC complexes, Asf1 and Rtt106) (Eriksson et al. 2012). Rap1 may either inhibit or facilitate the

action of one or more of these regulators, for example by competing with the binding of a positive regulator.

In the case of site-specific histone losses at upregulated NRTS, nucleosome losses may simply be an indirect consequence of the elevated expression of these genes. However, we favor a more direct role for Rap1 in competing with nucleosomes for site occupancy, based on several longstanding and recent findings in wild type cells. For example, Rap1 can interfere with nucleosome positioning and can facilitate gene activation by the Gcn4 transcription factor, which by itself cannot function efficiently at binding site ensconced within a nucleosome (Yu and Morse 1999), and experimental depletion of Rap1 leads to rapid elevations in nucleosome occupancy selectively at sites to which it was previously bound (Ganapathi et al. 2011). Furthermore, Rap1 binding sites are enriched at the entry/exit points for the DNA wrapped around of the majority of nucleosomes to which it binds, where it may gain access to relatively free DNA, thus weakening histone-DNA interactions; and indeed these nucleosomes display particularly low occupancy and high turnover rates (Koerber et al. 2009; Rhee and Pugh 2011; Dion et al. 2007). Finally, sites to which Rap1 binds with the longest residence time (i.e. slowest off-rate) are those with the least nucleosome occupancy (Lickwar et al. 2012). Regardless of whether the competition between Rap1 and nucleosomes at upregulated NRTS is direct or indirect, it clearly plays important roles in the regulation of gene expression in senescent cells.

Mammalian Rap1 might also have similar effects on chromatin, nucleosome occupancy, and gene expression. For example, overexpression of Trf2, which recruits hRap1 to DNA, can reduce nucleosome density within telomere chromatin, which suggests that the hRap1:Trf2 complex may modify chromatin (Galati et al. 2012). Also, the recent demonstrations that mammalian Rap1 localizes not only to telomeres but also can bind with some affinity to DNA itself, contribute to the transcriptional regulation of sites throughout the genome, and bind several histone proteins raise the possibility that mammalian Rap1 may contribute to changes in chromatin and gene expression in senescent cells (Martinez et al. 2010; Yang et al. 2011; Arat and Griffith 2012; Lee et al. 2011).

Our findings provide insight into how Rap1 selectively targets NRTS. Many sites containing sequences to which Rap1 binds with optimal affinity *in vitro* are not occupied by Rap1 in wild type cells, indicating the chromatin context contributes to Rap1 occupancy (Lieb et al. 2001). The promoters of NRTS are not enriched for optimal Rap1 binding sites, but rather tend to contain hemisite plus linker sequences to which Rap1 binds selectively but with reduced affinity *in vitro* (Del Vescovo et al. 2004). In addition, the most highly enriched motif present within NRTS promoters is TTTTTTGCGC, which is similar to the so-called G/C-capped poly(dA:dT) tracts that normally associate with the centers of nucleosome-free regions in yeast promoters (Wu and Li 2010). Poly(dA:dT) tract length is inversely correlated with nucleosome stability (Segal and Widom 2009), and so we propose

that the short tracts found within NRTS are not sufficient to exclude nucleosomes substantially in wild type cells, but as histone levels decline at senescence the local effects of these tracts are uncovered by a global shift in equilibrium toward nucleosome loss. Thus, nucleosome destabilization together with increased Rap1 availability and binding to nearby hemisites would conspire to drive the observed nucleosome losses selectively at NRTS.

Senescence is accompanied by the association of Rap1 with hundreds of new target loci, along with increased Rap1 levels at most of the targets to which it normally localizes in wild type cells (see Supplemental Material, including Figure S11 for additional analyses and discussion of the normal targets of Rap1). This raises the question: from where do these additional Rap1 proteins arise? Elevated levels of Rap1 are not the answer, because total cell levels of Rap1 remain relatively constant. It seems reasonable that as the telomere repeat tracts shorten with senescence, telomere-bound Rap1 should be liberated. But telomeres contain approximately one Rap1 protein per 18 bp of DNA (Gilson et al. 1993), and if we assume that the 32 telomeres in a haploid cell each lose on average 275 bp of DNA by senescence, this would liberate only 130 Rap1 proteins, which is not enough to account for approximately 500 NRTS along with increases at normal Rap1 targets. Another potential reservoir of Rap1 is provided by the subtelomeric regions, from which we found Rap1 is lost at senescence; although normal subtelomeric levels of

Rap1 have not been carefully measured, there are indications that they may be substantial. For example, this is illustrated by the dramatic delocalization of Rap1 from telomere-associated foci visualized by fluorescence microscopy in *sir* mutants (Gotta et al. 1996). Because Rap1 associates indirectly with subtelomeres, *via* binding to nucleosome-bound Sir3 and Sir4 (Moretti and Shore 2001; Strahl-Bolsinger et al. 1997), and because the direct binding of Rap1 to telomere repeat DNA, with Kd $\sim 10^{-11}$ M, is presumably independent of Sir proteins, this dramatic loss suggests that a greater number of Rap1 proteins are associated with subtelomeric than telomeric sequences. The Sir proteins are known to delocalize from subtelomeres at senescence, as demonstrated by fluorescence microscopy (Straatman and Louis 2007) and as indicated by the increased acetylation of subtelomeric histone H4K16, which destabilizes Sir3 binding to nucleosomes (Kozak et al. 2010). Therefore, our finding that Rap1 leaves subtelomeres at senescence is in keeping with previous observations. We note also that even though relocalization of the Sir silencing proteins from telomeres to other loci, either from engineered redistribution or following DNA damage, have been found to have important functional consequences (Marcand et al. 1996; Martin et al. 1999; Maillet et al. 1996), we did not detect roles for the Sir proteins at downregulated targets of Rap1 (Fig. S8 and unpublished data). In addition to delocalization of Rap1 from telomeres and subtelomeres at senescence, the increase in the number of Rap1-targeted loci may also reflect a shift in the general equilibrium from nucleoplasmic

to chromosome-associated Rap1, perhaps aided by increased exposure of binding sites secondary to nucleosome losses.

Consistent with the new localization of Rap1 not being a simple mass action-based consequence of its liberation from shortened telomere repeat DNA, the loss of Rap1 from subtelomeres and its new localization at NRTS depends on the DDR kinase Mec1. However, many of these changes are unique to senescence and not just a generic stress or DDR (see Supplemental Material, including Figs. S12, S13 and Table S6, for comparisons of roles for Rap1 during senescence, DDR, and other stress responses). In addition, these events correlate with Mec1-dependent post-translational modification of Rap1, and the identity and potential functional role of such modification is currently under investigation. Furthermore, deletion of *MEC1* delays senescence (Abdallah et al. 2009), consistent with the Mec1-dependence of Rap1 action at senescence.

In the setting of critically shortened telomeres, what might be the purpose of a DDR-regulated redistribution of Rap1 leading to activation of stress response genes and downregulation of histone genes? Although telomerase naturally maintains steady-state telomere length in yeast, telomere loss events can still occur, e.g. at broken replication forks, and this response might be of benefit in such cases. However, the response may be only one manifestation of a mechanism having broader importance for the repair of DNA breaks in other genomic regions. In cells lacking telomerase, critically shortened telomeres are similar to double stranded

breaks that are slowly repaired or are irreparable, i.e. DSBs that do not have a readily available homologous target sequence (e.g. a sister chromatid), or no homologous target sequence, from which to template HR-dependent repair. For example, both types of lesions can eventually translocate to the nuclear pore complex, where it is thought that checkpoint responses and alternative HR pathways are activated (Khadaroo et al. 2009; Oza et al. 2009; Nagai et al. 2008). Slowly repaired breaks have also been found recently to activate chromatin mobility, not only of the break site itself but apparently also of other genomic regions, which is thought to enhance the search of the broken end for a homologous target (Dion et al. 2012; Miné-Hattab and Rothstein 2012). The increased mobility requires both Mec1 signaling and the action of the Ino80 chromatin remodeling complex, which can evict nucleosomes and may thus facilitate chromatin mobility (Neumann et al. 2012). Rap1-dependent stimulation of nucleosome losses at particular genomic sites together with downregulation of global histone levels could contribute to this mechanism. This hypothesis is consistent with the similar patterns of NRTS gene expression in MMS-treated and senescent cells, including downregulation of histone genes (Gasch et al. 2001), and indicates that roles for Rap1 in the repair of DNA breaks throughout the genome should be explored.

REFERENCES

Abdallah P, Luciano P, Runge KW, Lisby M, Géli V, Gilson E, Teixeira MT. 2009. A

two-step model for senescence triggered by a single critically short telomere. *Nature Cell Biology* **11**: 988–993.

Arat NÖ, Griffith JD. 2012. Human Rap1 Interacts Directly with Telomeric DNA and Regulates TRF2 Localization at the Telomere. *Journal of Biological Chemistry* **287**: 41583–41594.

Armanios M. 2013. Telomeres and age-related disease: how telomere biology informs clinical paradigms. *J Clin Invest* **123**: 996–1002.

Baker DJ, Wijshake T, Tchkonia T, Lebrasseur NK, Childs BG, Van De Sluis B, Kirkland JL, Van Deursen JM. 2011. Clearance of p16Ink4a-positive senescent cells delays ageing-associated disorders. *Nature* **479**: 1–6.

Benetti R, García-Cao M, Blasco MA. 2007. Telomere length regulates the epigenetic status of mammalian telomeres and subtelomeres. *Nat Genet* **39**: 243–250.

Blasco MA, Lee H-W, Hande MP, Samper E, Lansdorp PM, DePinho RA, Greider CW. 1997. Telomere Shortening and Tumor Formation by Mouse Cells Lacking Telomerase RNA. *Mol Cell* **91**: 25–34.

Breslow DK, Cameron DM, Collins SR, Schuldiner M, Stewart-Ornstein J, Newman HW, Braun S, Madhani HD, Krogan NJ, Weissman JS. 2008. A comprehensive strategy enabling high-resolution functional analysis of the yeast genome. *Nat*

Methods **5**: 711–718.

Buchman AR, Lue NF, Kornberg RD. 1988. Connections between transcriptional activators, silencers, and telomeres as revealed by functional analysis of a yeast DNA-binding protein. *Mol Cell Biol* **8**: 5086–5099.

Buck MJ, Lieb JD. 2006. A chromatin-mediated mechanism for specification of conditional transcription factor targets. *Nat Genet* **38**: 1446–1451.

Campisi J. 2013. Aging, cellular senescence, and cancer. *Annual Review of Physiology* **75**: 685–705.

Campisi J. 1997. The biology of replicative senescence. *European Journal of Cancer* **33**: 703–709.

Capper R, Britt-Compton B, Tankimanova M, Rowson J, Letsolo B, Man S, Haughton M, Baird DM. 2007. The nature of telomere fusion and a definition of the critical telomere length in human cells. *Genes Dev* **21**: 2495–2508.

Del Vescovo V, De Sanctis V, Bianchi A, Shore D, Di Mauro E, Negri R. 2004. Distinct DNA elements contribute to Rap1p affinity for its binding sites. *Journal of Molecular Biology* **338**: 877–893.

Dion MF, Kaplan T, Kim M, Buratowski S, Friedman N, Rando OJ. 2007. Dynamics of Replication-Independent Histone Turnover in Budding Yeast. *Science* **315**:

1405–1408.

Dion V, Kalck V, Horigome C, Towbin BD, Gasser SM. 2012. Increased mobility of double-strand breaks requires Mec1, Rad9 and the homologous recombination machinery. *Nature Cell Biology* **14**: 502–509.

Enomoto S, Glowczewski L, Berman J. 2002. MEC3, MEC1, and DDC2 are essential components of a telomere checkpoint pathway required for cell cycle arrest during senescence in Saccharomyces cerevisiae. *Mol Biol Cell* **13**: 2626–2638.

Eriksson PR, Ganguli D, Nagarajavel V, Clark DJ. 2012. Regulation of histone gene expression in budding yeast. *Genetics* **191**: 7–20.

Feser J, Truong D, Das C, Carson JJ, Kieft J, Harkness T, Tyler JK. 2010. Elevated histone expression promotes life span extension. *Mol Cell* **39**: 724–735.

Freeman K, Gwadz M, Shore D. 1995. Molecular and genetic analysis of the toxic effect of RAP1 overexpression in yeast. *Genetics* **141**: 1253–1262.

Galati A, Magdinier F, Colasanti V, Bauwens S, Pinte S, Ricordy R, Giraud-Panis M-J, Pusch MC, Savino M, Cacchione S, et al. 2012. TRF2 controls telomeric nucleosome organization in a cell cycle phase-dependent manner. *PLoS ONE* **7**: e34386.

Ganapathi M, Palumbo MJ, Ansari SA, He Q, Tsui K, Nislow C, Morse RH. 2011.

Extensive role of the general regulatory factors, Abf1 and Rap1, in determining genome-wide chromatin structure in budding yeast. *Nucleic Acids Res* **39**: 2032–2044.

Gasch AP, Huang M, Metzner S, Botstein D, Elledge SJ, Brown PO. 2001. Genomic expression responses to DNA-damaging agents and the regulatory role of the yeast ATR homolog Mec1p. *Mol Biol Cell* **12**: 2987–3003.

Gilson E, Roberge M, Giraldo R, Rhodes D, Gasser SM. 1993. Distortion of the DNA double helix by RAP1 at silencers and multiple telomeric binding sites. *Journal of Molecular Biology* **231**: 293–310.

Gotta M, Laroche T, Formenton A, Maillet L, Scherthan H, Gasser SM. 1996. The clustering of telomeres and colocalization with Rap1, Sir3, and Sir4 proteins in wild-type Saccharomyces cerevisiae. *J Cell Biol* **134**: 1349–1363.

Hackett JA, Feldser DM, Greider CW. 2001. Telomere dysfunction increases mutation rate and genomic instability. *Cell* **106**: 275–286.

Harbison CT, Gordon DB, Lee TI, Rinaldi NJ, Macisaac KD, Danford TW, Hannett NM, Tagne J-B, Reynolds DB, Yoo J, et al. 2004. Transcriptional regulatory code of a eukaryotic genome. *Nature* **431**: 99.

Heinz S, Benner C, Spann N, Bertolino E, Lin YC, Laslo P, Cheng JX, Murre C, Singh H,

Glass CK. 2010. Simple combinations of lineage-determining transcription factors prime cis-regulatory elements required for macrophage and B cell identities. *Mol Cell* **38**: 576–589.

Herbig U, Jobling WA, Chen BPC, Chen DJ, Sedivy JM. 2004. Telomere shortening triggers senescence of human cells through a pathway involving ATM, p53, and p21(CIP1), but not p16(INK4a). *Mol Cell* **14**: 501–513.

IJpma AS, Greider CW. 2003. Short telomeres induce a DNA damage response in Saccharomyces cerevisiae. *Mol Biol Cell* **14**: 987–1001.

Johnson FB, Marciniak RA, McVey M, Stewart SA, Hahn WC, Guarente L. 2001. The Saccharomyces cerevisiae WRN homolog Sgs1p participates in telomere maintenance in cells lacking telomerase. *EMBO J* **20**: 905–913.

Khadaroo B, Teixeira MT, Luciano P, Eckert-Boulet N, Germann SM, Simon MN, Gallina I, Abdallah P, Gilson E, Géli V, et al. 2009. The DNA damage response at eroded telomeres and tethering to the nuclear pore complex. *Nature Cell Biology* **11**: 980–987.

Klein F, Laroche T, Cardenas ME, Hofmann JF, Schweizer D, Gasser SM. 1992. Localization of RAP1 and topoisomerase II in nuclei and meiotic chromosomes of yeast. *J Cell Biol* **117**: 935–948.

Koerber RT, Rhee HS, Jiang C, Pugh BF. 2009. Interaction of transcriptional regulators with specific nucleosomes across the Saccharomyces genome. *Mol Cell* **35**: 889–902.

Konig P, Giraldo R, Chapman L, Rhodes D. 1996. The crystal structure of the DNA-binding domain of yeast RAP1 in complex with telomeric DNA. *Cell* **85**: 125–136.

Kozak ML, Chavez A, Dang W, Berger SL, Ashok A, Guo X, Johnson FB. 2010. Inactivation of the Sas2 histone acetyltransferase delays senescence driven by telomere dysfunction. *EMBO J* **29**: 158–170.

Kyrion G, Liu K, Liu C, Lustig AJ. 1993. RAP1 and telomere structure regulate telomere position effects in Saccharomyces cerevisiae. *Genes Dev* **7**: 1146–1159.

Laroche T, Martin SG, Tsai-Pflugfelder M, Gasser SM. 2000. The dynamics of yeast telomeres and silencing proteins through the cell cycle. *J Struct Biol* **129**: 159–174.

Lee O-H, Kim H, He Q, Baek HJ, Yang D, Chen L-Y, Liang J, Chae HK, Safari A, Liu D, et al. 2011. Genome-wide YFP fluorescence complementation screen identifies new regulators for telomere signaling in human cells. *Mol Cell Proteomics* **10**: M110.001628.

Lescasse R, Pobiega S, Callebaut I, Marcand S. 2013. End-joining inhibition at

telomeres requires the translocase and polySUMO-dependent ubiquitin ligase Uls1. *EMBO J* **32**: 805–815.

Lickwar CR, Mueller F, Hanlon SE, McNally JG, Lieb JD. 2012. Genome-wide protein–DNA binding dynamics suggest a molecular clutch for transcription factor function. *Nature* **484**: 251–255.

Lieb JD, Liu X, Botstein D, Brown PO. 2001. Promoter-specific binding of Rap1 revealed by genome-wide maps of protein-DNA association. *Nat Genet* **28**: 327–334.

Lundblad V, Blackburn EH. 1993. An alternative pathway for yeast telomere maintenance rescues est1- senescence. *Cell* **73**: 347–360.

Lundblad V, Szostak JW. 1989. A mutant with a defect in telomere elongation leads to senescence in yeast. *Cell* **57**: 633–643.

Maillet L, Boscheron C, Gotta M, Marcand S, Gilson E, Gasser SM. 1996. Evidence for silencing compartments within the yeast nucleus: a role for telomere proximity and Sir protein concentration in silencer-mediated repression. *Genes Dev* **10**: 1796–1811.

Marcand S, Buck SW, Moretti P, Gilson E, Shore D. 1996. Silencing of genes at nontelomeric sites in yeast is controlled by sequestration of silencing factors at

telomeres by Rap 1 protein. *Genes Dev* **10**: 1297–1309.

Marcand S, Gilson E, Shore D. 1997. A protein-counting mechanism for telomere length regulation in yeast. *Science* **275**: 986–990.

Maringele L, Lydall D. 2004. Telomerase- and recombination-independent immortalization of budding yeast. *Genes Dev* **18**: 2663–2675.

Martin SG, Laroche T, Suka N, Grunstein M, Gasser SM. 1999. Relocalization of telomeric Ku and SIR proteins in response to DNA strand breaks in yeast. *Cell* **97**: 621–633.

Martinez P, Thanasoula M, Carlos AR, Gómez-López G, Tejera AM, Schoeftner S, Dominguez O, Pisano DG, Tarsounas M, Blasco MA. 2010. Mammalian Rap1 controls telomere function and gene expression through binding to telomeric and extratelomeric sites. *Nature Cell Biology* **12**: 768–780.

Miné-Hattab J, Rothstein R. 2012. Increased chromosome mobility facilitates homology search during recombination. *Nature Cell Biology* **14**: 510–517.

Moretti P, Shore D. 2001. Multiple Interactions in Sir Protein Recruitment by Rap1p at Silencers and Telomeres in Yeast. *Mol Cell Biol* **21**: 8082–8094.

Mukherjee S, Berger MF, Jona G, Wang XS, Muzzey D, Snyder M, Young RA, Bulyk ML. 2004. Rapid analysis of the DNA-binding specificities of transcription factors

with DNA microarrays. *Nat Genet* **36**: 1331–1339.

Nagai S, Dubrana K, Tsai-Pflugfelder M, Davidson MB, Roberts TM, Brown GW, Varela E, Hediger F, Gasser SM, Krogan NJ. 2008. Functional targeting of DNA damage to a nuclear pore-associated SUMO-dependent ubiquitin ligase. *Science* **322**: 597–602.

Nautiyal S, DeRisi JL, Blackburn EH. 2002. The genome-wide expression response to telomerase deletion in Saccharomyces cerevisiae. *Proc Natl Acad Sci USA* **99**: 9316–9321.

Negrini S, Ribaud V, Bianchi A, Shore D. 2007. DNA breaks are masked by multiple Rap1 binding in yeast: implications for telomere capping and telomerase regulation. *Genes Dev* **21**: 292–302.

Neumann FR, Dion V, Gehlen LR, Tsai-Pflugfelder M, Schmid R, Taddei A, Gasser SM. 2012. Targeted INO80 enhances subnuclear chromatin movement and ectopic homologous recombination. *Genes Dev* **26**: 369–383.

O'Sullivan RJ, Kubicek S, Schreiber SL, Karlseder J. 2010. Reduced histone biosynthesis and chromatin changes arising from a damage signal at telomeres. *Nat Struct Mol Biol* **17**: 1218–1225.

Oza P, Jaspersen SL, Miele A, Dekker J, Peterson CL. 2009. Mechanisms that regulate

localization of a DNA double-strand break to the nuclear periphery. *Genes Dev* **23**: 912–927.

Palladino F, Laroche T, Gilson E, Axelrod A, Pillus L, Gasser SM. 1993. SIR3 and SIR4 proteins are required for the positioning and integrity of yeast telomeres. *Cell* **75**: 543–555.

Pardo B, Marcand S. 2005. Rap1 prevents telomere fusions by nonhomologous end joining. *EMBO J* **24**: 3117–3127.

Putnam CD, Jaehnig EJ, Kolodner RD. 2009. Perspectives on the DNA damage and replication checkpoint responses in Saccharomyces cerevisiae. *DNA Repair* **8**: 974–982.

Rhee HS, Pugh BF. 2011. Comprehensive genome-wide protein-DNA interactions detected at single-nucleotide resolution. *Cell* **147**: 1408–1419.

Ritchie KB, Mallory JC, Petes TD. 1999. Interactions of TLC1 (which encodes the RNA subunit of telomerase), TEL1, and MEC1 in regulating telomere length in the yeast Saccharomyces cerevisiae. *Mol Cell Biol* **19**: 6065–6075.

Sabourin M, Tuzon CT, Zakian VA. 2007. Telomerase and Tel1p preferentially associate with short telomeres in S. cerevisiae. *Mol Cell* **27**: 550–561.

Schaetzlein S, Kodandaramireddy NR, Ju Z, Lechel A, Stepczynska A, Lilli DR, Clark

AB, Rudolph C, Kuhnel F, Wei K, et al. 2007. Exonuclease-1 Deletion Impairs DNA Damage Signaling and Prolongs Lifespan of Telomere-Dysfunctional Mice. *Cell* **130**: 863–877.

Schawalder SB, Kabani M, Howald I, Choudhury U, Werner M, Shore D. 2004. Growth-regulated recruitment of the essential yeast ribosomal protein gene activator Ifh1. *Nature* **432**: 1058.

Segal E, Widom J. 2009. Poly(dA:dT) tracts: major determinants of nucleosome organization. *Curr Opin Struct Biol* **19**: 65–71.

Spellman PT, Sherlock G, Zhang MQ, Iyer VR, Anders K, Eisen MB, Brown PO, Botstein D, Futcher B. 1998. Comprehensive identification of cell cycle-regulated genes of the yeast Saccharomyces cerevisiae by microarray hybridization. *Mol Biol Cell* **9**: 3273–3297.

Straatman KR, Louis EJ. 2007. Localization of telomeres and telomere-associated proteins in telomerase-negative Saccharomyces cerevisiae. *Chromosome Res* **15**: 1033–1050.

Strahl-Bolsinger S, Hecht A, Luo K, Grunstein M. 1997. SIR2 and SIR4 interactions differ in core and extended telomeric heterochromatin in yeast. *Genes Dev* **11**: 83–93.

Tomar RS, Zheng S, Brunke-Reese D, Wolcott HN, Reese JC. 2008. Yeast Rap1 contributes to genomic integrity by activating DNA damage repair genes. *EMBO J* **27**: 1575–1584.

Tornow J, Zeng X, Gao W, Santangelo GM. 1993. GCR1, a transcriptional activator in Saccharomyces cerevisiae, complexes with RAP1 and can function without its DNA binding domain. *EMBO J* **12**: 2431–2437.

Ungar L, Yosef N, Sela Y, Sharan R, Ruppin E, Kupiec M. 2009. A genome-wide screen for essential yeast genes that affect telomere length maintenance. *Nucleic Acids Res* **37**: 3840–3849.

Vignais ML, Huet J, Buhler JM, Sentenac A. 1990. Contacts between the factor TUF and RPG sequences. *J Biol Chem* **265**: 14669–14674.

Vodenicharov MD, Laterreur N, Wellinger RJ. 2010. Telomere capping in non-dividing yeast cells requires Yku and Rap1. *EMBO J* **29**: 3007–3019.

Wu R, Li H. 2010. Positioned and G/C-capped poly(dA:dT) tracts associate with the centers of nucleosome-free regions in yeast promoters. *Genome Research* **20**: 473–484.

Wyrick JJ, Holstege FC, Jennings EG, Causton HC, Shore D, Grunstein M, Lander ES, Young RA. 1999. Chromosomal landscape of nucleosome-dependent gene

expression and silencing in yeast. *Nature* **402**: 418–421.

Yang D, Xiong Y, Kim H, He Q, Li Y, Chen R, Songyang Z. 2011. Human telomeric proteins occupy selective interstitial sites. *Cell Res* **21**: 1013–1027.

Yu L, Morse RH. 1999. Chromatin opening and transactivator potentiation by RAP1 in Saccharomyces cerevisiae. *Mol Cell Biol* **19**: 5279–5288.

Zhao Y, McIntosh KB, Rudra D, Schawalder S, Shore D, Warner JR. 2006. Fine-structure analysis of ribosomal protein gene transcription. *Mol Cell Biol* **26**: 4853–4862.

Zwerschke W, Mazurek S, Stöckl P, Hutter E, Eigenbrodt E, Jansen-Durr P. 2003. Metabolic analysis of senescent human fibroblasts reveals a role for AMP in cellular senescence. *Biochem J* **376**: 403–411.

Supplemental Material

Materials and Methods

Yeast strains and plasmids

All experiments were performed in the BY4741/2 background (Brachmann et al. 1998) and mutant alleles are deletions unless otherwise specified. See Supplemental Table 7 for strain details. Double and triple mutants were made by either deleting *TLC1* in a diploid heterozygous for the other mutation(s) or by mating haploids of interest with a *tlc1* mutant early after telomerase loss (< 35 PD) followed by serial streaking of colonies to equilibrate telomere length. All strains were genotyped using auxotrophy or drug resistance, along with PCR-based verification. Cells were grown at 30°C in YPAD or in SC-based selective drop-out media (Amberg et al. 2005).

All plasmids were made using standard Gateway cloning methods (Alberti et al. 2007). pAG413-*NOP1*-ccdB, pAG423-*NOP1*-ccdB, pAG413-*NOP1-RAP1,* and pAG423-*NOP1-RAP1* contain the sequences extending upstream from the *NOP1* ORF for 400bp as previously described (Chavez et al. 2011), and the last two plasmids contains the full *RAP1* ORF in place of ccdB. pAG426-*GAL1*-ccdB came from the Advanced Gateway Library (Alberti et al. 2007) from which we made pAG426-*GAL1-RAP1*.

Senescence assays

Senescence assays were performed in YPAD using fresh spore products from dissection plates, with growth in liquid starting approximately 25 PD after loss of telomerase. All comparisons between different genotypes were performed using spore products obtained from the same *TLC1/tlc1Δ* diploid possessing any other heterozygous genetic changes of interest (e.g. *RAP1/rap1 DAmP*) to ensure that the haploid cells being compared had inherited telomeres of similar length and from the same epigenetic environment. Spore products (N=4 per genotype unless otherwise specified) were passaged serially in fresh liquid media. 10^6 cells were inoculated into 5 mL of media, were grown for 22 hours, counted using a Coulter counter and then re-inoculated at 10^6 cells/5 ml media. Cell counts were used to determine elapsed PDs (PD = $\log_2$(final/starting concentration)). *P*-values for differences between rates of senescence were calculated using the PD at the nadir of the curves for individual cultures and using a Student's *t*-test. Samples for mRNA expression and ChIP assays of senescent cells were obtained ~5 PDs prior to the nadir to avoid contributions from survivors of senescence, and cells were harvested under optimal growth conditions (i.e. at < 2 x 10^7 cells/ml after 12-16 hours of growth for senescent cultures after an initial inoculation at ≤ 2 x 10^6 cells/ml in fresh medium, while carefully following their growth and doubling times).

Chromatin immunoprecipitation and analysis

ChIP was performed as previously described (Kozak et al. 2010). Briefly, $2x10^8$ cells were harvested during exponential growth, crosslinked with formaldehyde and sonicated to an average 100-200 bp DNA fragment size. Chromatin (750 μg total protein, measured using the BCA method) was immunoprecipitated using rabbit anti-Rap1 (Y-300, Santa Cruz), rabbit anti-total H3 (ab1791, Abcam), or rabbit IgG (31207, Pierce). Purified DNA was quantified using qPCR and standard curves, and the enrichment for specific ChIP signals (Rap1 or histone H3) at specific target loci were calculated by normalization to input (obtained from 50 μg total protein), rabbit IgG controls, and an unaffected reference locus (*ACT1*), as follows using Rap1 ChIP as an example: Enrichment for Rap1 at target locus = $[(Rap1_{target} - IgG_{target})/Input_{target}] / [(Rap1_{reference} - IgG_{reference})/Input_{reference}]$. Overall ChIP patterns were similar when the IgG control and reference locus normalization were omitted from calculations. Primers are listed in Supplemental Table S8. ChIP telomere dot blots were based on previous methods (LeBel et al. 2006). ChIP samples were denatured with 1M NaOH to final concentration of 0.4M for 20' at 65°C. Using the Minifold-1 Dot Blot System (Whatman, GE Healthcare) samples were blotted onto nylon membranes (Hybond-XL, GE Healthcare) prewashed with 300 μl 10X SCP (1M NaCl, 0.3M Na2HPO4, 0.02M EDTA, pH 6.8). Following blotting membrane was washed 3X with 300 μl 10X SCP and crosslinked with UV StratalinkerTM 2400 (Stratagene, Agilent) set at

600 µJx100. Membrane was prehybridized for 1hr at 50°C with 20ml of Church's Buffer (1mM EDTA, 0.5mM NaH2PO4, 0.5mM Na2HPO4, 7% SDS, 1% BSA) and then hybridized overnight at 37°C 32P endlabled CA oligo = CCCACCACACACACCCACACCC in 20mL of Church's Buffer. Membrane was washed 3X 5' with 2X SSC / 1% SDS at RT and 2X 20' with 0.5X SSC / 0.2% SDS at 50°C and then exposed overnight with a phosphorimager screen (Molecular Dynamics, GE Healthcare). For some analyses, immunoprecipitated and input DNA samples were quantified by hybridization to Affymetrix S. cerevisiae 1.0R tiling arrays, as described (Dowell et al. 2010). Hybridization data were analyzed using the MAT (Model-based Analysis of Tiling-array) algorithm (Johnson et al. 2006) or area under the curve (AUC). Rap1 peaks were defined as those with a MAT significance of $p < 10\text{-}5$. Yeast gene promoters were defined as the region from 1kb upstream of transcription start to 500 bp downstream from transcription start. A promoter was considered to contain a Rap1 binding site if at least 50% of the peak interval fell within the promoter. To determine the AUC, ChIP array data was imported into Partek, GC-RMA normalized, and quantile normalized, then the log2 ratio of Rap1 to IgG was taken for each probe. Probe scores were summed in 25 base-pair bins by multiplying the score for each probe overlapping a bin by the proportion of the probe that overlapped. Binned data was used to make Rap1 enrichment tracks for the UCSC Genome Browser. Raw data files and MAT processed data are available at http://tesla.pcbi.upenn.edu/~pry/johnsonlab/rap1_senescence.html . To generate

topographical profiles of Rap1 enrichment over shared Rap1 targets and NRTS genes, each gene in a given set was partitioned into 20 equal-sized parts and the average bin score for each part was computed. Vectors for each gene in a set were then averaged together to give Rap1 set enrichment. The HOMER (Hypergeometric Optimization of Motif EnRichment) program was used to find de novo consensus sequences at Rap1 targets, as previously described (Heinz et al. 2010).

Statistics

p-values for overlap between sets of genes and target sites, and for differences between measurements, were calculated using Fisher's exact test and Student's t-test (2-tailed), respectively. All error bars are standard errors of the mean (SEM).

Cell extract preparation and immunoblotting

Cells were counted using a Coulter counter, harvested during exponential growth by centrifugation and pellets containing ~ 1-2x10^8 cells were frozen in liquid N_2 and then stored at -80^0 C. For whole cell extracts, cell pellets were resuspended in 800 µl of FA lysis buffer (50 mM HEPES-KOH pH 7.5, 140 mM NaCl, 1 mM EDTA, 0.1% Triton X-100, 1 mM PMSF, 2 µg/mL aprotinin, 2 µg/mL leupeptin, 2 µg/mL pepstatin A) and disrupted with ~500 µl cold 0.5 mm zirconia/silica beads (BioSpec) using a mini–beadbeater (BioSpec) for 6 x 60 sec at 4°C. Samples were

centrifuged at 10,000 rpm for 15 min at 4°C. Protein concentrations were measured using the BCA method. For trichloroacetic acid (TCA) extraction, 20% TCA-washed cell pellets were resuspended in 200 µl of 20% TCA along with 400 µl acid-washed glass beads (soda lime; BioSpec), disrupted with a mini–beadbeater for 3 x 90 sec at 4°C, and extracts were centrifuged at 14,000 rpm for 10 min. Pellets were resuspended in 100 µl Laemmli buffer and ~50 µl 2 M Tris base to neutralize pH. Samples were recentrifuged at 14,000 rpm for 10 min, boiled, and loaded by equal cell number.

Extracts were run on 4–12% Bis-Tris gels (NuPAGE, Invitrogen) and transferred to nitrocellulose membranes. Membranes were blotted with anti-Rap1 antibody (Y-300, Santa Cruz), anti-tubulin antibody (ab6160, Abcam), anti-H2A antibody (39235, Active Motif), anti-H2B antibody (39237, Active Motif), anti-H3 antibody (ab1791, Abcam), or anti-H4 antibody (#04-858, Millipore). Membranes were blocked with TBS-T (0.1% Tween-20) with 5% milk and all wash steps were performed with TBS–T.

Yeast spot essays

Spot assays were performed using cells from log phase liquid cultures grown at 30°C . 10-fold serial dilutions of cells, beginning with $4x10^5$ cells, were spotted on YPAD plates and imaged after 1.5 days of growth.

Quantitation of mRNA expression

Cells were harvested during exponential growth and frozen in liquid N_2 and stored at -80^0 C. RNA was extracted using the RNeasy Mini protocol (Qiagen), including the on column DNaseI digestion. 0.5 μg of RNA was reverse transcribed using the TaqMan Reverse Transcription Kit (ABI) at 25°C for 10', 42°C for 30', and 48°C for 20'. cDNA was analyzed using qPCR analysis on a Roche Applied Sciences Light Cycler 480 using SYBR Green Jumpstart Taq ReadyMix (Sigma) according to kit directions. Samples were run in triplicate in a 384-well format. A standard curve was run for each PCR reaction, using 4–fold serial dilutions of pooled cDNA samples. In most cases, the following qPCR program was run: 95°C 10', followed by 50 cycles of [95°C 15", 60°C 59", 60°C 1" with signal acquisition], followed by signal acquisition during melting up to 95°C to ensure single species amplification; for histone transcripts the following qPCR program was used: 95°C 10', followed by 50 cycles of [95°C 10", 57°C 15", 72°C 14", 72°C 1" with signal acquisition], followed by signal acquisition during melting up to 95°C to ensure single species amplification as described (Feser et al. 2010). Primers are listed in Supplemental Table S8.

Preliminary investigation of Rap1 activities in senescent cells at genes normally targeted in wild type cells

Rap1 normally binds to hundreds of target sites throughout the genome, usually at the upstream promoter regions of genes from which it typically contributes to gene activation. Indeed, aside from its repressive role at subtelomeres and the silent mating loci, Rap1 binds strongly to the promoters of the majority of the most highly transcribed yeast genes (Lieb et al. 2001), and these also tend to be sites with the lowest nucleosome occupancy in wild type cells (Lickwar et al. 2012; Ganapathi et al. 2011). Our ChIP-chip analyses of Rap1 binding in wild type compared to senescent *tlc1Δ* cells indicated an elevation in Rap1 occupancy at senescence at most normal targets of Rap1 (e.g. Fig. S11A). To address the potential role for Rap1 in regulation of these genes at senescence, we tested the effect of two-fold Rap1 overexpression in wild type cells, and found that in comparison to *ACT1*, Rap1 occupancy increased at promoters of these genes and resulted in downregulation of mRNA levels from these genes (Fig. S11B and C). These findings are consistent with a genome-wide comparison of normal Rap1 target genes and genes that are regulated at senescence; the set of genes upregulated at senescence do not overlap significantly with normal targets of Rap1, but genes downregulated at senescence do show significant overlap ($p = 0.99$ and 1.02×10^{-7}, respectively). We emphasize that this result is different from the new Rap1 target genes at senescence (i.e. the NRTS), which do show significant overlap with senescence

upregulated genes. The senescence-related downregulation of the tested normal Rap1 target genes does not depend on the Sir2/3/4 complex, and therefore involves a mechanism distinct from the normal Rap1 and Sir complex-dependent repression of subtelomeres and the silent mating loci (Fig. S11D).

We do not yet understand how Rap1 contributes to downregulation of its normal target genes in senescent cells, and mechanisms different from those that contribute to NRTS regulation may be at play. One possibility is that too much Rap1 binding to promoters can interfere with access of positively acting transcription factors. A second possibility is that higher levels of chromatin-associated Rap1 results in greater competition for Rap1-associated transcriptional coactivators, leading to downregulation of the normal targets of Rap1 (which are highly expressed in wild type cells) as activated NRTS loci compete for limiting coactivators. A third possibility is that it is a simple consequence of the fact that in wild type cells the normal targets of Rap1 are the most highly expressed genes and have the lowest levels of promoter histone occupancy. Therefore, the Rap1-dependent reduction in global histone levels at senescence cannot lead to any additional upregulation at these genes, and so in comparison to most other genes (which can experience different degrees of upregulation, per cell, from the global decline in histone levels), the normal Rap1 targets appear to be downregulated. These possibilities are not mutually exclusive, and additional work will be required

to understand the extent to which they or additional mechanisms lead to downregulation of normal Rap1 target genes at senescence.

Comparison of the Rap1-dependent gene expression profile at senescence with Rap1-dependent roles during the DDR and other stress responses

Because Rap1 has previously been found to relocalize under conditions of stress (Martin et al. 1999; Buck and Lieb 2006; Tomar et al. 2008), we wondered if the activities of Rap1 at senescence might reflect a generic role in stress responses. We therefore compared the gene sets that are up or downregulated at senescence and are also newly targeted by Rap1 (NRTS) with the gene sets up or downregulated in cells damaged by MMS or grown in low glucose.

MMS evokes a DDR, similar to the DDR displayed in senescent cells. Gene expression profiles in senescent and MMS treated cells were previously found to be similar but nonetheless distinct (Nautiyal et al. 2002). For example, the senescent gene expression profile includes changes in the environmental stress response and metabolic genes not seen under conditions of DNA damage. Comparison of NRTS expression changes with MMS-regulated genes (Gasch et al. 2001) revealed significant overlap between the upregulated and downregulated data sets ($p = 1.7x10^{-7}$, and 5.3×10^{-9}, respectively; Table S6A,B). These overlaps were most significant after maximal exposure to MMS and were highly dependent on *MEC1*

(not shown). Of particular note, expression of the core histone genes is downregulated in both cases. However, at most only forty percent of senescence-regulated NRTS overlap the DDR gene expression profile, and thus the majority of senescence-regulated NRTS are not part of the DDR, indicating differences between the two responses. Similarly, the single new target of Rap1 that has been studied in MMS treated cells, *RNR3* (Tomar et al. 2008), was not identified in our Rap1 ChIP-chip analysis as a NRTS (Fig. S12), and furthermore, the targeting of Rap1 to *RNR3* was reported to be *DUN1*-dependent, whereas we find that the regulation of NRTS is *DUN1*-independent (Fig. S10B). Buck and Lieb demonstrated Rap1 relocalization to novel target genes under conditions of low glucose (Buck and Lieb 2006). Comparison of these genes with NRTS revealed no significant overlap ($p = 0.23$, Fig S13), indicating Rap1 binds different target genes in the two stress conditions.

Overall, it appears that Rap1 relocalization and target regulation in senescent cells does not reflect a generic role for Rap1 in stress responses, although there are significant similarities between Rap1 activities at senescence and in the DDR induced by MMS.

Supplemental References

Alberti S, Gitler AD, Lindquist S. 2007. A suite of Gateway cloning vectors for high-throughput genetic analysis in Saccharomyces cerevisiae. *Yeast* **24**: 913–919.

Amberg DC, Amberg DC, Burke D, Burke D, Strathern JN, Strathern JN. 2005. *Methods in yeast genetics*. Cold Spring Harbor Laboratory Press.

Brachmann CB, Davies A, Cost GJ, Caputo E, Li J, Hieter P, Boeke JD. 1998. Designer deletion strains derived from Saccharomyces cerevisiae S288C: a useful set of strains and plasmids for PCR-mediated gene disruption and other applications. *Yeast* **14**: 115–132.

Buck MJ, Lieb JD. 2006. A chromatin-mediated mechanism for specification of conditional transcription factor targets. *Nat Genet* **38**: 1446–1451.

Chavez A, Agrawal V, Johnson FB. 2011. Homologous Recombination-dependent Rescue of Deficiency in the Structural Maintenance of Chromosomes (Smc) 5/6 Complex. *Journal of Biological Chemistry* **286**: 5119–5125.

Dion MF, Kaplan T, Kim M, Buratowski S, Friedman N, Rando OJ. 2007. Dynamics of Replication-Independent Histone Turnover in Budding Yeast. *Science* **315**: 1405–1408.

Dowell NL, Sperling AS, Mason MJ, Johnson RC. 2010. Chromatin-dependent binding of the S. cerevisiae HMGB protein Nhp6A affects nucleosome dynamics and transcription. *Genes Dev* **24**: 2031–2042.

Feser J, Truong D, Das C, Carson JJ, Kieft J, Harkness T, Tyler JK. 2010. Elevated

histone expression promotes life span extension. *Mol Cell* **39**: 724–735.

Ganapathi M, Palumbo MJ, Ansari SA, He Q, Tsui K, Nislow C, Morse RH. 2011. Extensive role of the general regulatory factors, Abf1 and Rap1, in determining genome-wide chromatin structure in budding yeast. *Nucleic Acids Res* **39**: 2032–2044.

Gasch AP, Huang M, Metzner S, Botstein D, Elledge SJ, Brown PO. 2001. Genomic expression responses to DNA-damaging agents and the regulatory role of the yeast ATR homolog Mec1p. *Mol Biol Cell* **12**: 2987–3003.

Harbison CT, Gordon DB, Lee TI, Rinaldi NJ, Macisaac KD, Danford TW, Hannett NM, Tagne J-B, Reynolds DB, Yoo J, et al. 2004. Transcriptional regulatory code of a eukaryotic genome. *Nature* **431**: 99.

Heinz S, Benner C, Spann N, Bertolino E, Lin YC, Laslo P, Cheng JX, Murre C, Singh H, Glass CK. 2010. Simple combinations of lineage-determining transcription factors prime cis-regulatory elements required for macrophage and B cell identities. *Mol Cell* **38**: 576–589.

Huang DW, Sherman BT, Lempicki RA. 2009. Systematic and integrative analysis of large gene lists using DAVID bioinformatics resources. *Nat Protoc* **4**: 44–57.

Lickwar CR, Mueller F, Hanlon SE, McNally JG, Lieb JD. 2012. Genome-wide protein–

DNA binding dynamics suggest a molecular clutch for transcription factor function. *Nature* **484**: 251–255.

Lieb JD, Liu X, Botstein D, Brown PO. 2001. Promoter-specific binding of Rap1 revealed by genome-wide maps of protein-DNA association. *Nat Genet* **28**: 327–334.

Johnson WE, Li W, Meyer CA, Gottardo R, Carroll JS, Brown M, Liu XS. 2006. Model-based analysis of tiling-arrays for ChIP-chip. *Proc Natl Acad Sci USA* **103**: 12457–12462.

Kozak ML, Chavez A, Dang W, Berger SL, Ashok A, Guo X, Johnson FB. 2010. Inactivation of the Sas2 histone acetyltransferase delays senescence driven by telomere dysfunction. *EMBO J* **29**: 158–170.

LeBel C, Larrivée M, Bah A, Laterreur N, Lvesque N, Wellinger RJ. 2006. Assessing telomeric phenotypes. *Methods Mol Biol* **313**: 265–316.

Martin SG, Laroche T, Suka N, Grunstein M, Gasser SM. 1999. Relocalization of telomeric Ku and SIR proteins in response to DNA strand breaks in yeast. *Cell* **97**: 621–633.

Nautiyal S, DeRisi JL, Blackburn EH. 2002. The genome-wide expression response to telomerase deletion in Saccharomyces cerevisiae. *Proc Natl Acad Sci USA* **99**:

9316–9321.

Spellman PT, Sherlock G, Zhang MQ, Iyer VR, Anders K, Eisen MB, Brown PO, Botstein D, Futcher B. 1998. Comprehensive identification of cell cycle-regulated genes of the yeast Saccharomyces cerevisiae by microarray hybridization. *Mol Biol Cell* **9**: 3273–3297.

Tomar RS, Zheng S, Brunke-Reese D, Wolcott HN, Reese JC. 2008. Yeast Rap1 contributes to genomic integrity by activating DNA damage repair genes. *EMBO J* **27**: 1575–1584.

Wyrick JJ, Holstege FC, Jennings EG, Causton HC, Shore D, Grunstein M, Lander ES, Young RA. 1999. Chromosomal landscape of nucleosome-dependent gene expression and silencing in yeast. *Nature* **402**: 418–421.

Figure 2-1

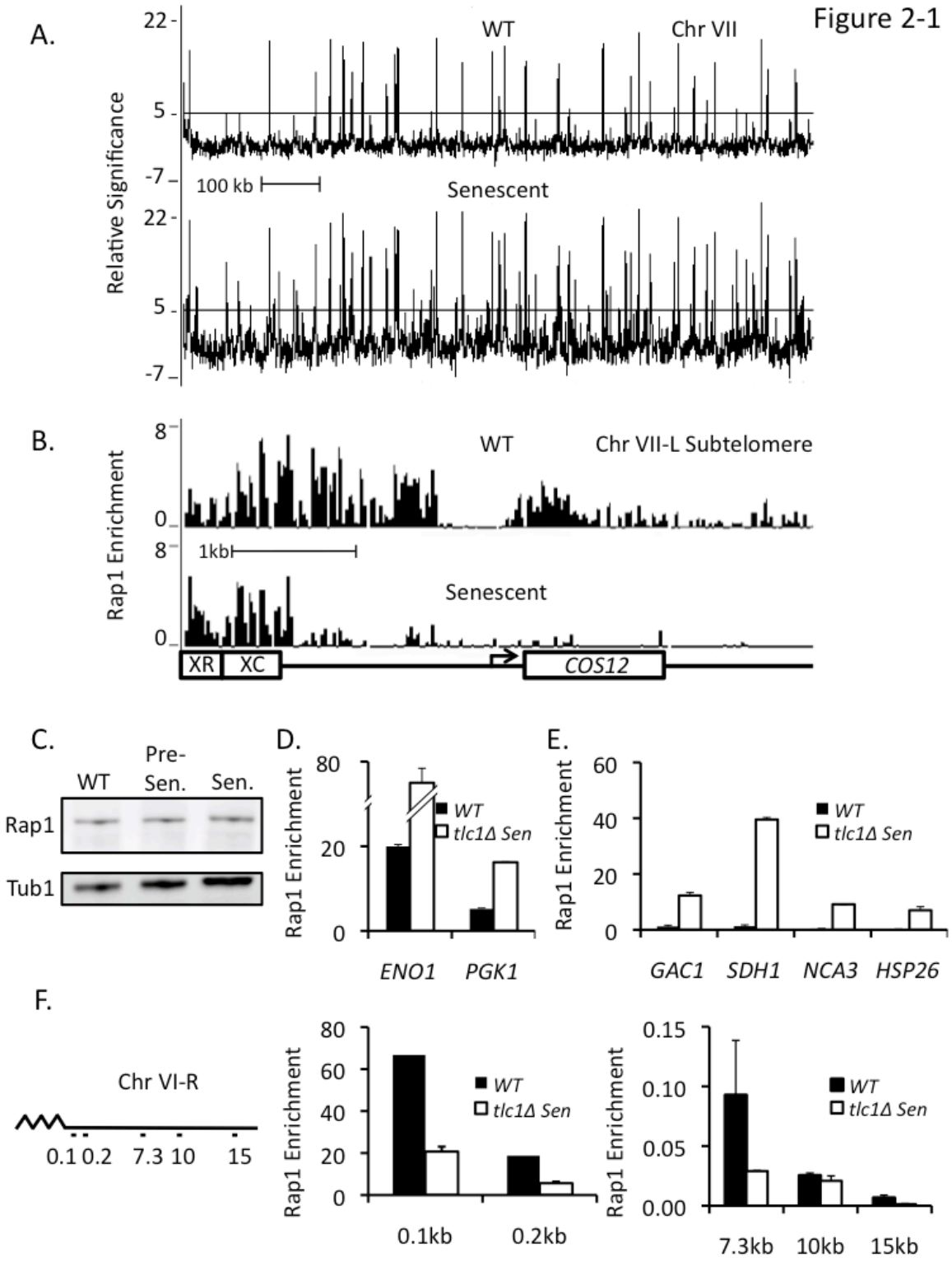
A.
WT
Chr VII
22
5
-7
100 kb
Senescent
Relative Significance
B.
WT
Chr VII-L Subtelomere
8
0
1kb
Senescent
Rap1 Enrichment
XR
XC
COS12
C.
WT
Pre-Sen.
Sen.
Rap1
Tub1
D.
Rap1 Enrichment
WT
tlc1Δ Sen
ENO1
PGK1
E.
GAC1
SDH1
NCA3
HSP26
F.
Chr VI-R
0.1 0.2 7.3 10 15
0.1kb
0.2kb
7.3kb
10kb
15kb

Figure 1. Rap1 leaves subtelomeres and redistributes to new genomic loci at senescence.

(A) Chromosomal distribution of Rap1 in wildtype and senescent cells. Rap1 ChIP-tiling array data, normalized to control rabbit IgG ChIP data, are shown for chromosome VII (see Fig. S1 for all chromosomes). Data are plotted by relative significance using MAT algorithm ($-\log_{10}$(p-value)). Senescent cells were obtained 5 population doublings (PD) prior to the nadir in growth rate to avoid contributions by survivors of senescence. **(B)** Rap1 leaves subtelomeres at senescence. Rap1 ChIP-tiling array data are shown for subtelomere VII-L. Data are plotted as the $\log_2$ ratio of the Rap1 and control rabbit IgG ChIP signal intensities. **(C)** Rap1 protein levels do not change substantially at senescence. Rap1 and tubulin immunoblots of whole cell extracts from equal numbers of cells from wildtype and *tlc1Δ* cultures at ~PD30 (*pre-senescent*) and ~PD70 (*senescent*). Note that tubulin levels per cell increase at senescence, consistent with increased cell volume (Nautiyal et al. 2002). **(D-F)** Rap1 ChIP-qPCR analyses confirming that at senescence Rap1 displays enhanced enrichment at sites naturally targeted in WT cells (D) and at new Rap1 targets at senescence (*NRTS*; E), whereas Rap1 occupancy decreases at subtelomeres (F). Rap1 enrichment is the ratio of the Rap1 level at each targeted locus compared to *ACT1,* normalized to non-specific IgG and input controls. The locations of qPCR probes along subtelomere VI-R are shown. All qPCR data are

means (N=3), and similar results were obtained in two other experiments using independent biological replicates.

Figure 2-2

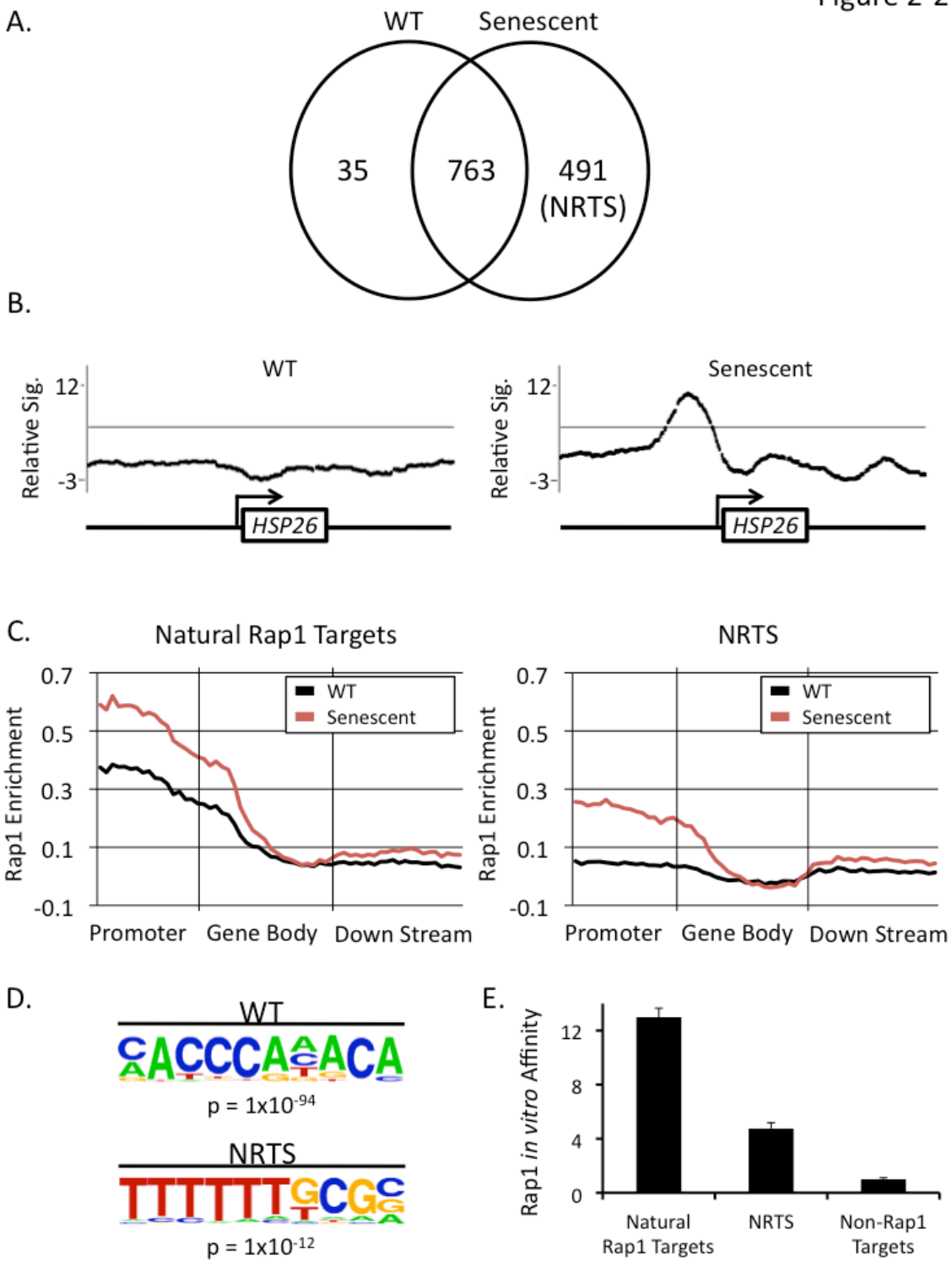
A.
WT
Senescent
35
763
491
(NRTS)
B.
WT
Senescent
Relative Sig.
12
-3
HSP26
C.
Natural Rap1 Targets
NRTS
Rap1 Enrichment
0.7
0.5
0.3
0.1
-0.1
WT
Senescent
Promoter
Gene Body
Down Stream
D.
WT
p = 1x10-94
NRTS
p = 1x10-12
E.
Rap1 in vitro Affinity
12
8
4
0
Natural Rap1 Targets
NRTS
Non-Rap1 Targets

Figure 2. New Rap1 targets at senescence (NRTS).

(A) Venn diagram comparing Rap1 target genes in wild type and senescent cells. The 35 targets lost at senescence are largely from subtelomeric regions (Fig S3B). **(B)** *HSP26* is an example of a NRTS. Data are plotted as in Fig 1A. **(C)** Rap1 occupancy at senescence increases preferentially both at the promoters of sites naturally targeted in WT cells (*Natural Rap1 Targets*, n=763) and of *NRTS* (n=491). Data are plotted as the average ChIP intensities ($\log_2$(Rap1 ChIP/rabbit IgG ChIP)) for the genes in each category within and flanking each gene. *Promoter* is the 500bp region upstream of the open reading frame (ORF), *gene body* is the ORF, and *downstream* is the 500bp region downstream of the ORF. **(D)** NRTS are not enriched for the consensus Rap1 binding sequence. The most significant motif identified using HOMER among WT target genes is the Rap1 binding consensus, and the most significant motif among NRTS is shown. **(E)** Rap1 binds sequences in NRTS promoters. Rap1 in vitro affinity was measured by protein binding microarrays (Mukherjee et al. 2004).

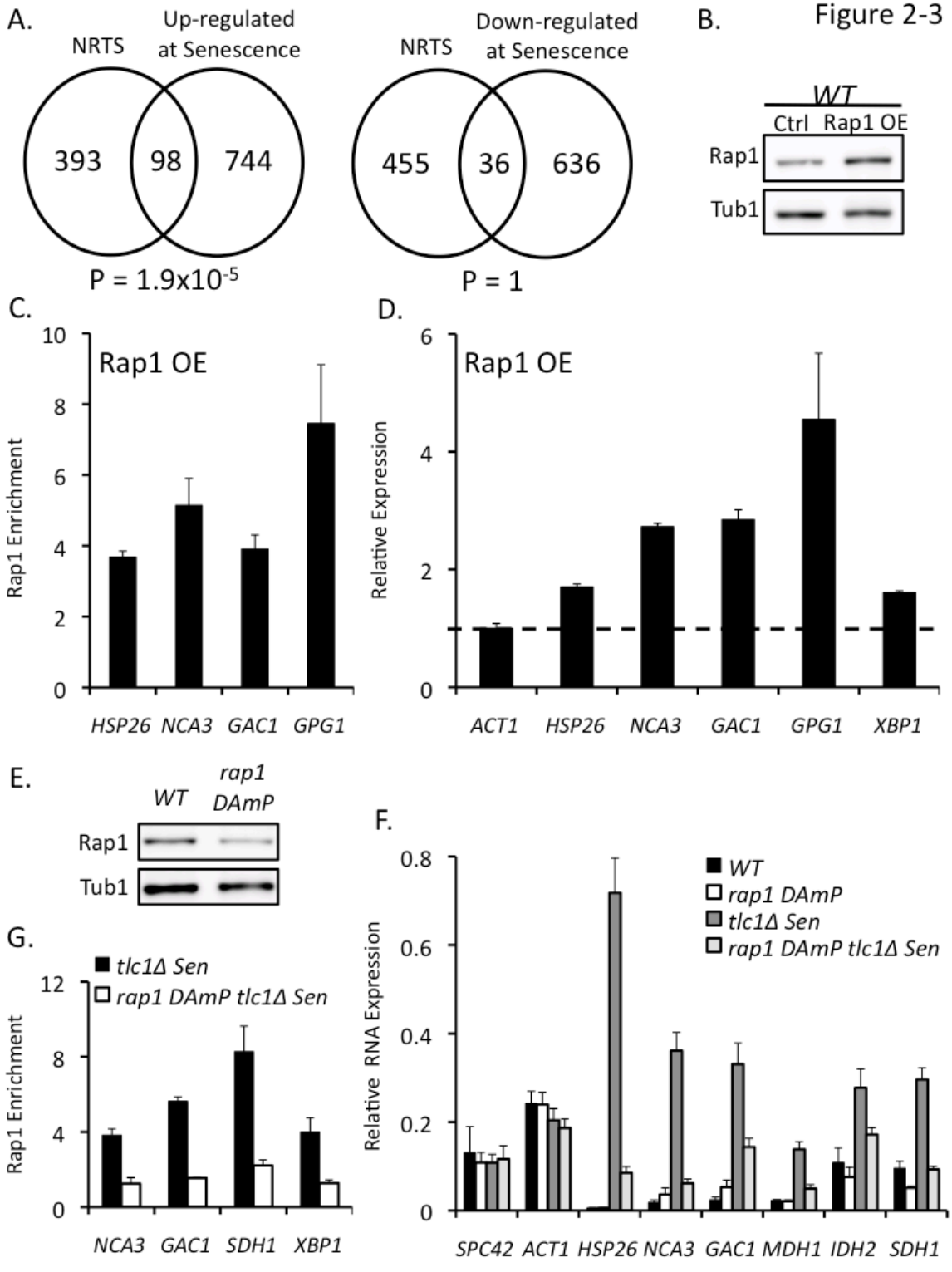
A.
NRTS
Up-regulated at Senescence
393
98
744
P = 1.9x10-5
NRTS
Down-regulated at Senescence
455
36
636
P = 1
B.
WT
Ctrl
Rap1 OE
Rap1
Tub1
C.
Rap1 OE
Rap1 Enrichment
HSP26
NCA3
GAC1
GPG1
D.
Rap1 OE
Relative Expression
ACT1
HSP26
NCA3
GAC1
GPG1
XBP1
E.
WT
rap1 DAmP
Rap1
Tub1
F.
WT
rap1 DAmP
tlc1Δ Sen
rap1 DAmP tlc1Δ Sen
Relative RNA Expression
SPC42
ACT1
HSP26
NCA3
GAC1
MDH1
IDH2
SDH1
G.
tlc1Δ Sen
rap1 DAmP tlc1Δ Sen
Rap1 Enrichment
NCA3
GAC1
SDH1
XBP1

Figure 2-3

Figure 3. NRTS are preferentially upregulated by Rap1 at senescence.

(A) Venn diagram comparing NRTS to genes that are differentially expressed (≥ 1.5-fold) at senescence (among 6178 genes total). **(B-D)** A two-fold elevation in Rap1 levels is sufficient to mimic effects of senescence at upregulated NRTS in WT cells. **(B)** Immunoblots of TCA extracts from equal numbers of cells carrying the *NOP1p-RAP1* plasmid (*Rap1 OE*) or the vector control (*Ctrl*). **(C)** Rap1 levels at the promoters of upregulated NRTS. Rap1 enrichment is the ratio of Rap1 levels measured by qPCR in *NOP1p-RAP1 vs.* vector control cells normalized to *ACT1*. **(D)** Upregulated NRTS are activated by Rap1 overexpression. Data are RNA levels in Rap1 OE cells relative to control cells and normalized to *ACT1* transcripts. **(E-G)** Rap1 contributes to upregulation of NRTS at senescence. **(E)** Rap1 levels are reduced in *rap1 DAmP* cells. Immunoblots of TCA extracts from equal numbers of wild type and *rap1 DAmP* cells. **(F)** Rap1 contributes to activation at senescence of upregulated NRTS. mRNA levels were measured by qPCR in wild type (*WT*, n=2), *rap1 DAmP* (n=2), and senescent (*tlc1Δ Sen*, n=4; *rap1 DAmP tlc1Δ Sen*, n=4) cultures. **(G)** Reduced Rap1 levels blunt Rap1 occupancy at the upstream promoters of NRTS at senescence. Data are plotted as fold change in Rap1 enrichment in senescent cells relative to wild type cells and normalized to occupancy at the *ACT1* locus, as measured by qPCR. All qPCR data are means (N=3, except as noted), and similar results were obtained in two other experiments using independent biological replicates.

Figure 2-4

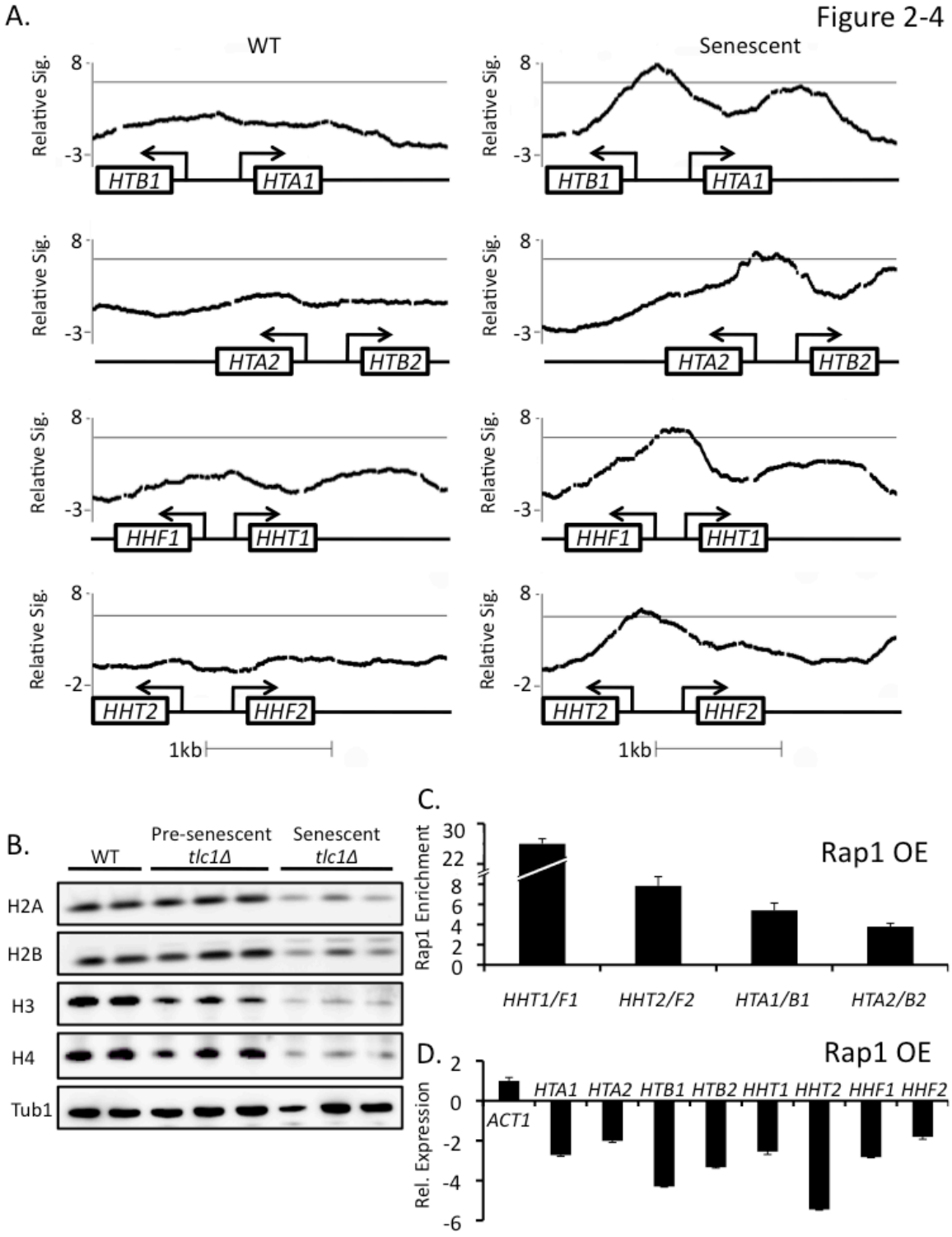
A.
WT
Senescent
Relative Sig.
8
-3
-2
HTB1
HTA1
HTA2
HTB2
HHF1
HHT1
HHT2
HHF2
1kb
B.
WT
Pre-senescent
tlc1Δ
Senescent
tlc1Δ
H2A
H2B
H3
H4
Tub1
C.
Rap1 Enrichment
30
22
8
6
4
2
0
Rap1 OE
HHT1/F1
HHT2/F2
HTA1/B1
HTA2/B2
D.
Rel. Expression
2
0
-2
-4
-6
Rap1 OE
ACT1
HTA1
HTA2
HTB1
HTB2
HHT1
HHT2
HHF1
HHF2

Figure 2-4 Cont

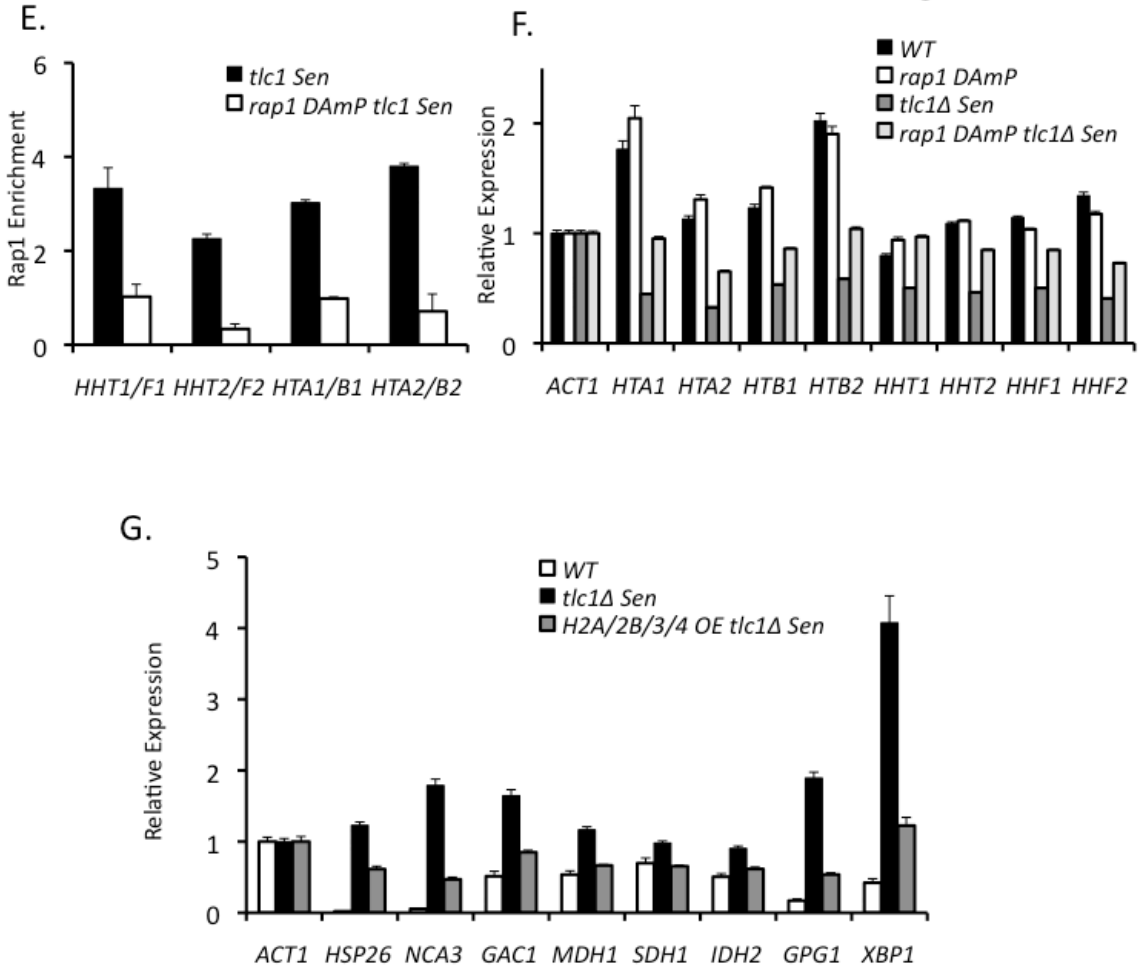

Figure 4. Rap1 targets and represses core histone gene expression at senescence.

(A) Rap1 binds all core histone promoters at senescence. Data are plotted as in Fig 1A. **(B)** Histone protein levels decrease at senescence. Immunoblots of whole cell extracts from the indicated wildtype (n=2) and *tlc1Δ* cultures at ~PD 30 (*pre-senescent*, n=3) and ~PD 70 (*senescent*, n=3). Lanes were loaded by equal protein and stained with anti-H2A, anti-H2B, anti-H3, anti-H4 or anti-tubulin antibodies. **(C-D)** Increased levels of Rap1 are sufficient to repress histone gene expression. **(C)** Rap1 occupancy at core histone promoters is increased in wild type cells carrying the *NOP1p-RAP1* plasmid. Data are plotted as in Fig 3C. **(D)** Increased Rap1 levels blunt histone gene expression. qPCR data are fold changes in mRNA expression in nocodazole-arrested WT cells carrying the *NOP1p-RAP1* plasmid (n=3) relative to arrested vector control strains (n=3), normalized to *ACT1* transcripts. **(E-F)** Rap1 contributes to core histone gene repression at senescence. **(E)** Reduced levels of Rap1 in *rap1 DAmP* mutants blunt Rap1 occupancy at histone promoters at senescence. Data are plotted as in Fig 3G. **(F)** Repression of core histone genes depends on Rap1. mRNA levels were measured by qPCR normalized to *ACT1* transcripts using RNA from wild type (*WT*, n=2), *rap1 DAmP* (n=2), senescent (*tlc1Δ Sen*, n=4), and senescent *rap1 DAmP* (*rap1 DAmP tlc1Δ Sen*, n=4) cultures. **(G)** Histone overexpression blunts upregulation of NRTS at senescence. mRNA levels

were measured by qPCR in wild type (n=2), senescent *tlc1Δ* (n=4), and senescent *H2A/H2B/H3/H4*-overexpressing *tlc1Δ* (n=4) cultures.

Figure 2-5

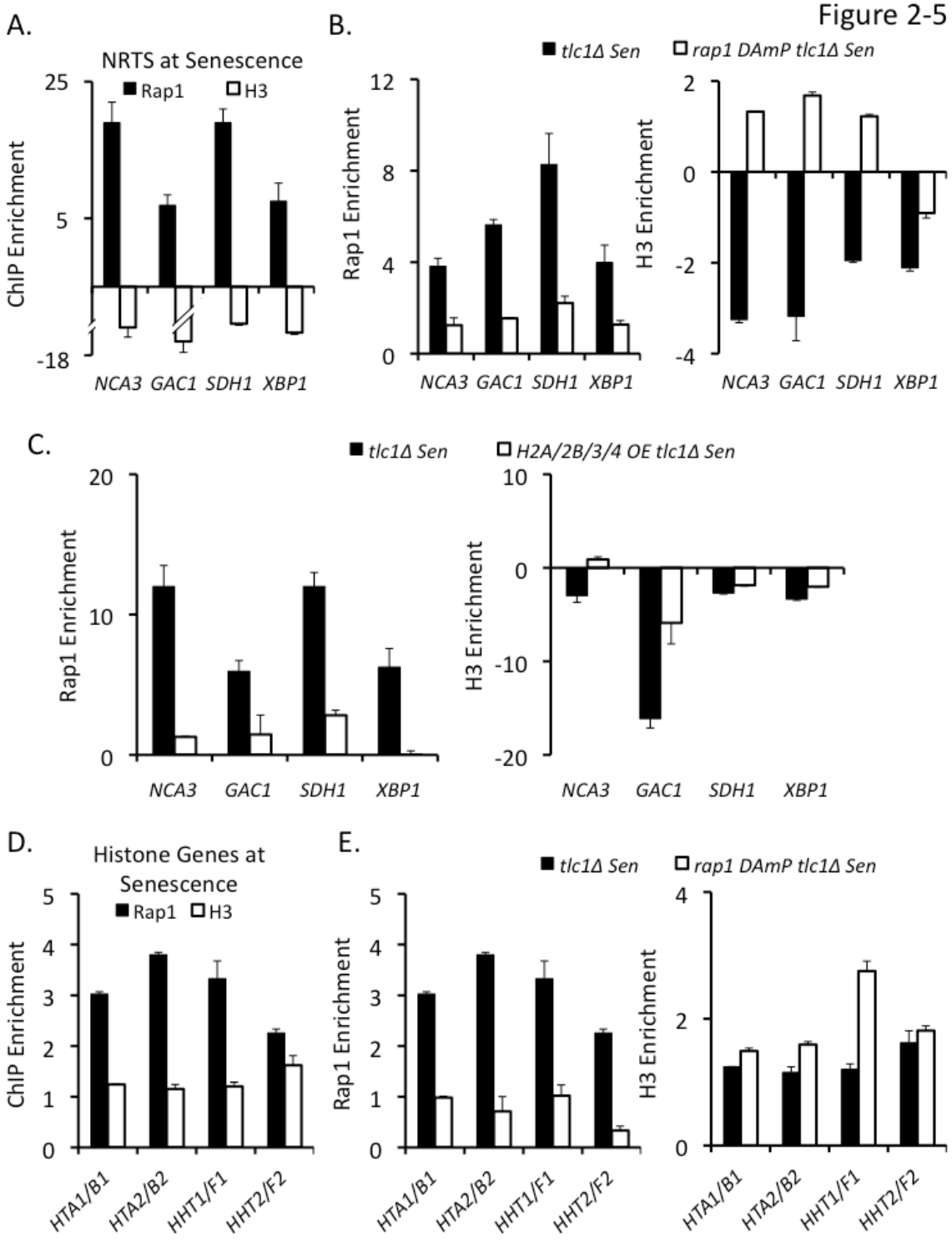
A.
NRTS at Senescence
Rap1
H3
ChIP Enrichment
25
5
-18
NCA3 GAC1 SDH1 XBP1
B.
tlc1Δ Sen
rap1 DAmP tlc1Δ Sen
Rap1 Enrichment
12
8
4
0
H3 Enrichment
2
0
-2
-4
NCA3 GAC1 SDH1 XBP1
C.
tlc1Δ Sen
H2A/2B/3/4 OE tlc1Δ Sen
Rap1 Enrichment
20
10
0
H3 Enrichment
10
0
-10
-20
NCA3 GAC1 SDH1 XBP1
D.
Histone Genes at Senescence
Rap1
H3
ChIP Enrichment
5
4
3
2
1
0
HTA1/B1 HTA2/B2 HHT1/F1 HHT2/F2
E.
tlc1Δ Sen
rap1 DAmP tlc1Δ Sen
Rap1 Enrichment
5
4
3
2
1
0
H3 Enrichment
4
2
0
HTA1/B1 HTA2/B2 HHT1/F1 HHT2/F2

Figure 5. A reciprocal relationship exists between Rap1 and histone occupancy at activated NRTS.

Rap1 or H3 ChIP-qPCR data are plotted as fold changes in Rap1 and H3 enrichment in senescent cells relative to wild type cells, normalized to *ACT1*. **(A)** Histones are preferentially lost at activated NRTS. **(B)** Rap1 contributes to histone loss at activated NRTS, because such losses are reduced in *rap1 DAmP* cells at senescence. **(C)** Overexpression of the core histone loci blunts elevated Rap1 occupancy and histone loss at activated NRTS. **(D)** Histones are not preferentially lost at core histone promoters at senescence. **(E)** Rap1 does not significantly affect histone occupancy at the core histone promoters at senescence. All qPCR data are means (N=3); similar results were obtained in three other experiments using independent biological replicates and also when data were normalized to *RSP5* (a non-Rap1 targeted locus) instead of *ACT1*.

Figure 2-6

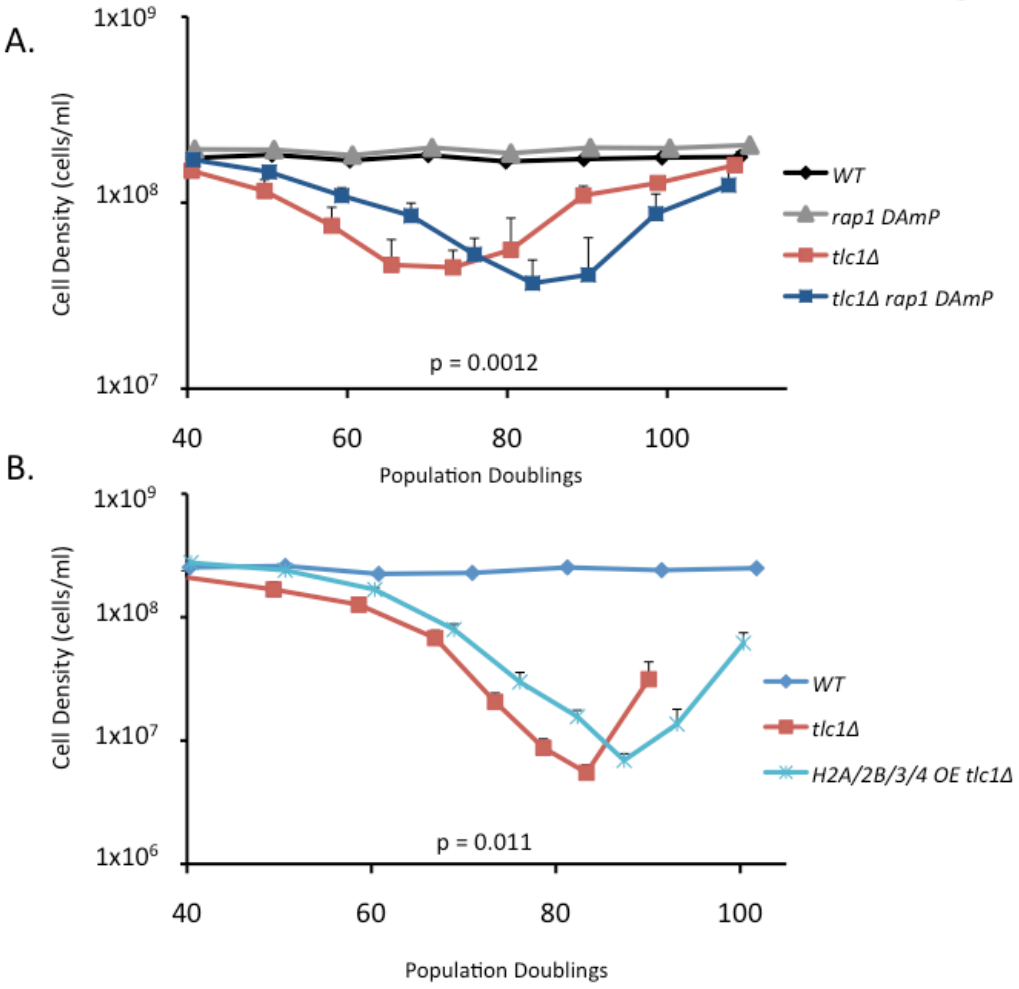
A.
1x10^9
1x10^8
1x10^7
Cell Density (cells/ml)
p = 0.0012
40
60
80
100
Population Doublings
WT
rap1 DAmP
tlc1Δ
tlc1Δ rap1 DAmP
B.
1x10^9
1x10^8
1x10^7
1x10^6
Cell Density (cells/ml)
p = 0.011
40
60
80
100
Population Doublings
WT
tlc1Δ
H2A/2B/3/4 OE tlc1Δ

Figure 6. Reduced Rap1 levels or increased histone levels delay senescence.

(A) Rap1 drives senescence. Senescence assay of *WT* (n=2), *rap1 DAmP* (n=2), *tlc1Δ* (n=4), and *rap1 DAmP tlc1Δ* (n=4) cultures. p = 0.0012 for delayed senescence by *rap1 DAmP*. **(B)** Increased histone levels delay senescence. Senescence assay comparing *WT* (n=1), *tlc1Δ* (n=7), and *tlc1Δ* cells overexpressing core histone proteins (*H2A/2B/3/4 tlc1Δ;* n=5). p = 0.011 for delayed senescence by histone overexpression.

Figure 2-7

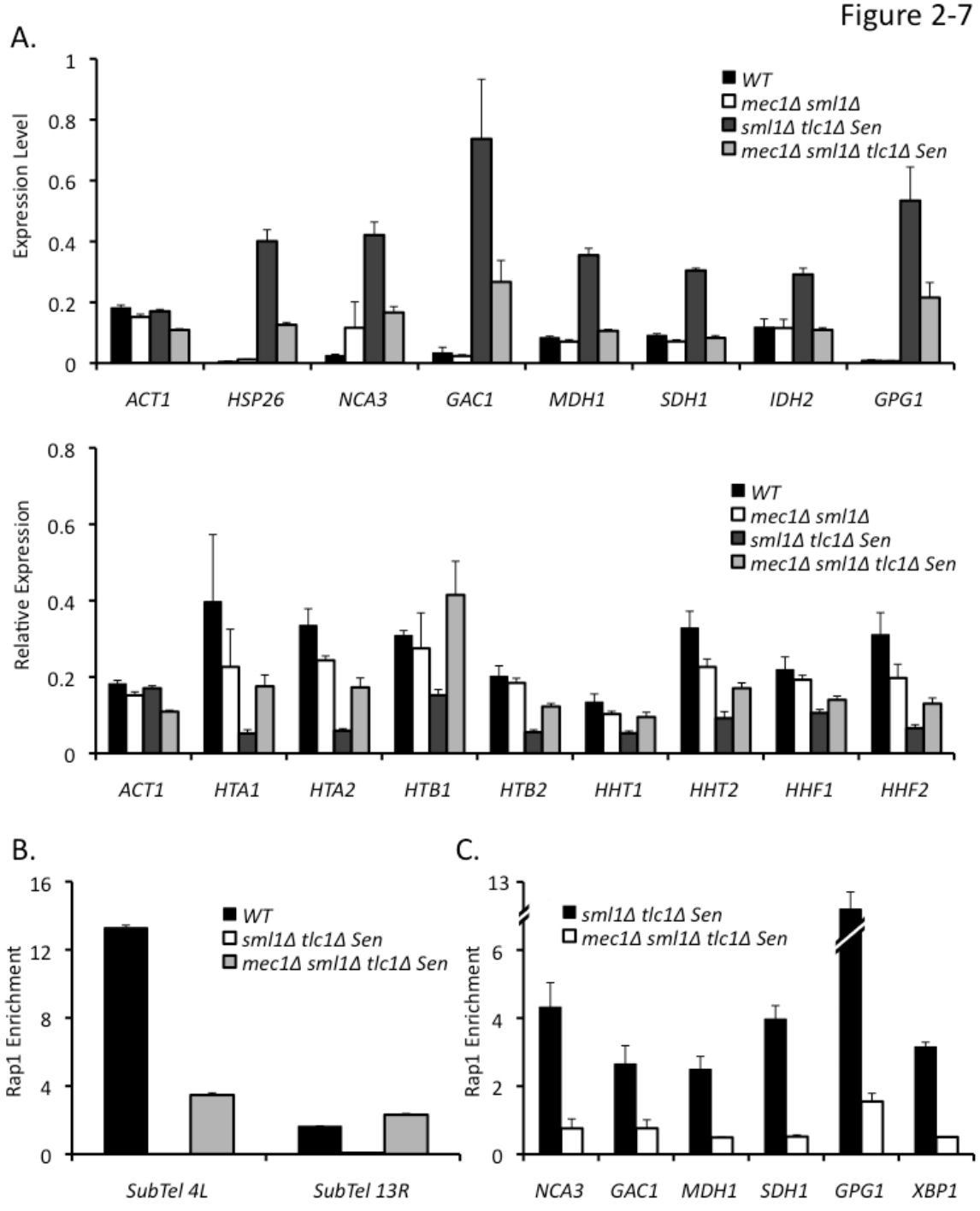
A.
Expression Level
1
0.8
0.6
0.4
0.2
0
WT
mec1Δ sml1Δ
sml1Δ tlc1Δ Sen
mec1Δ sml1Δ tlc1Δ Sen
ACT1
HSP26
NCA3
GAC1
MDH1
SDH1
IDH2
GPG1
Relative Expression
0.8
0.6
0.4
0.2
0
WT
mec1Δ sml1Δ
sml1Δ tlc1Δ Sen
mec1Δ sml1Δ tlc1Δ Sen
ACT1
HTA1
HTA2
HTB1
HTB2
HHT1
HHT2
HHF1
HHF2
B.
Rap1 Enrichment
16
12
8
4
0
WT
sml1Δ tlc1Δ Sen
mec1Δ sml1Δ tlc1Δ Sen
SubTel 4L
SubTel 13R
C.
Rap1 Enrichment
13
6
4
2
0
sml1Δ tlc1Δ Sen
mec1Δ sml1Δ tlc1Δ Sen
NCA3
GAC1
MDH1
SDH1
GPG1
XBP1

Figure 2-7 Cont

D.

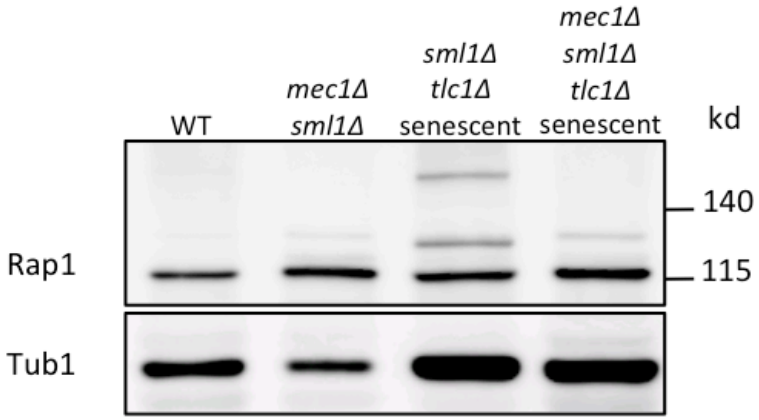

Figure 7. Rap1 relocalization and function at senescence requires *MEC1*.

(A) Activation of NRTS and repression of histones at senescence depends on *MEC1*. qPCR measurements of mRNA from wild type (n=2), *mec1Δ sml1Δ* (n=2), senescent *sml1Δ tlc1Δ* (n=4), and senescent *mec1Δ sml1 Δtlc1Δ* (n=4) cultures. **(B)** Rap1 loss from subtelomeres depends on *MEC1*. ChIP data are plotted as in Fig 1F. Subtelomere 4L and 13R qPCR amplicons are respectively 0.11 and 0.2 kb away from the base of the telomeric repeats. **(C)** Rap1 localization to activated NRTS depends on *MEC1*. ChIP data are plotted as in Fig 3G. **(D)** Slower mobility species of Rap1 present at senescence depend on *MEC1*. Immunoblots of TCA extracts, loaded by equal cell number and stained with anti-Rap1 or anti-tubulin antibodies. For all experiments, senescent cultures were harvested 5 PD prior to the growth nadir, which for *sml1Δ tlc1Δ* was ~PD 70 and for *mec1Δ sml1Δ tlc1Δ* was ~PD 80.

Figure 2-S1

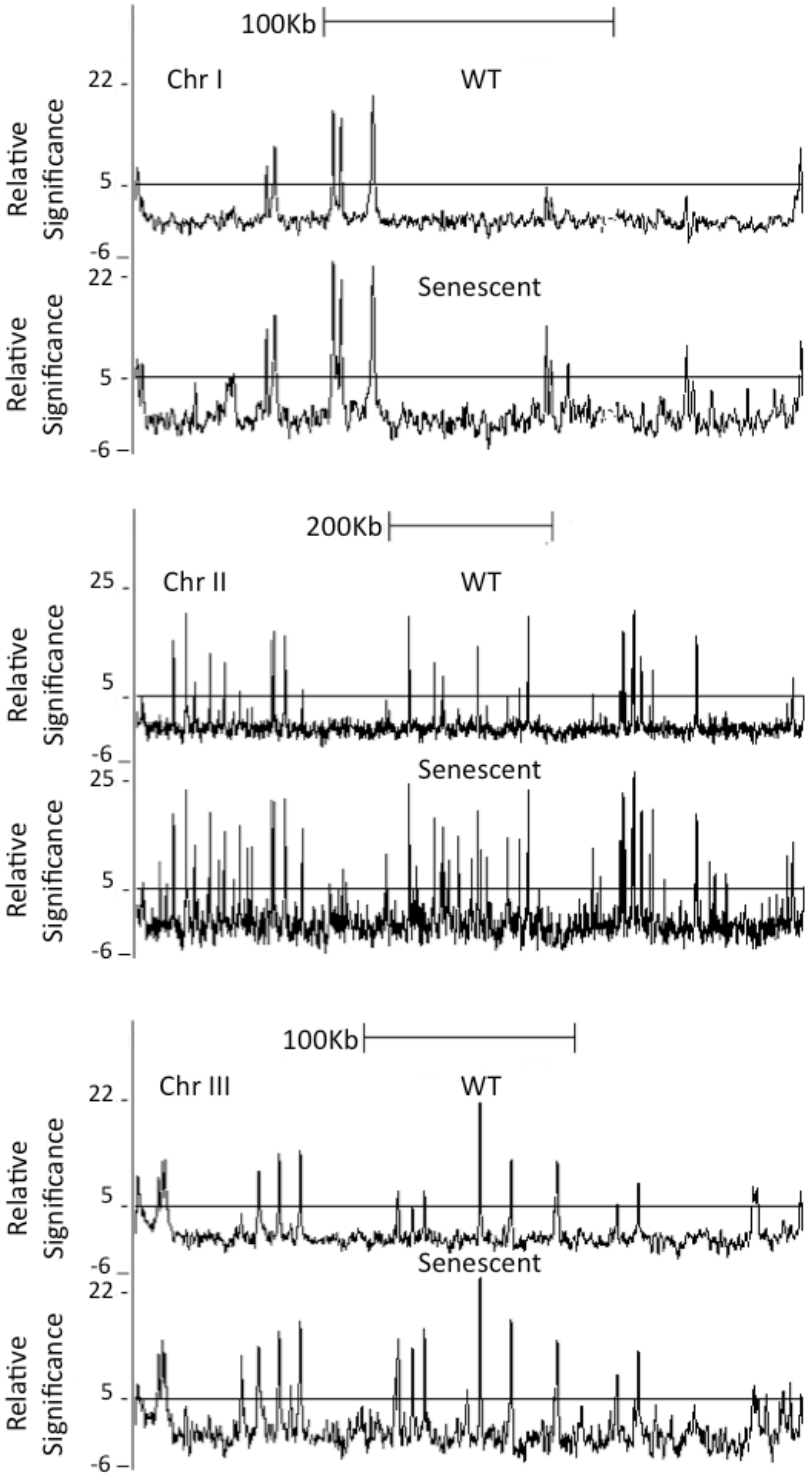
100Kb
Chr I
WT
Relative Significance
22
5
-6
Senescent
200Kb
Chr II
25
100Kb
Chr III

Figure 2-S1 Cont

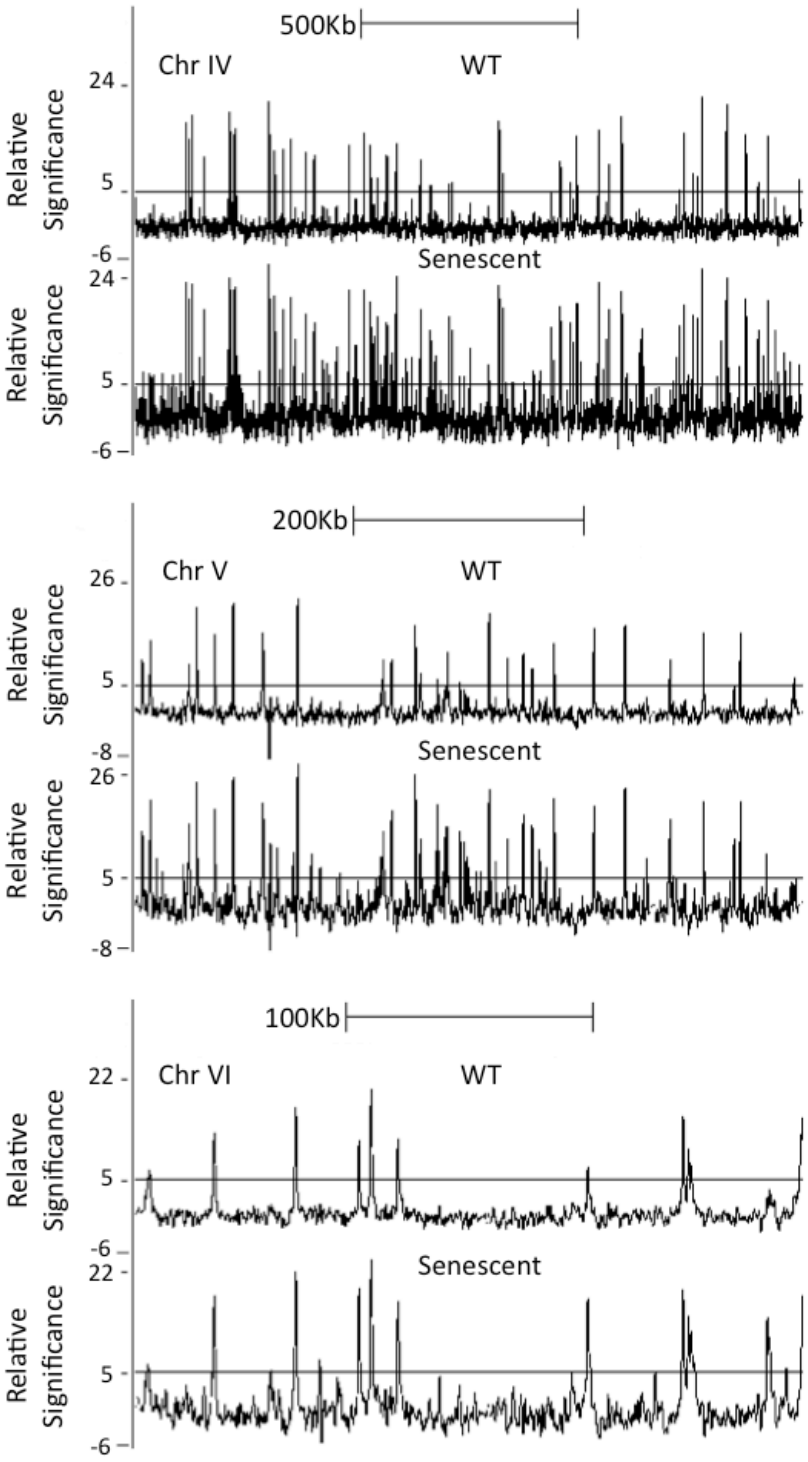

Figure 2-S1 Cont

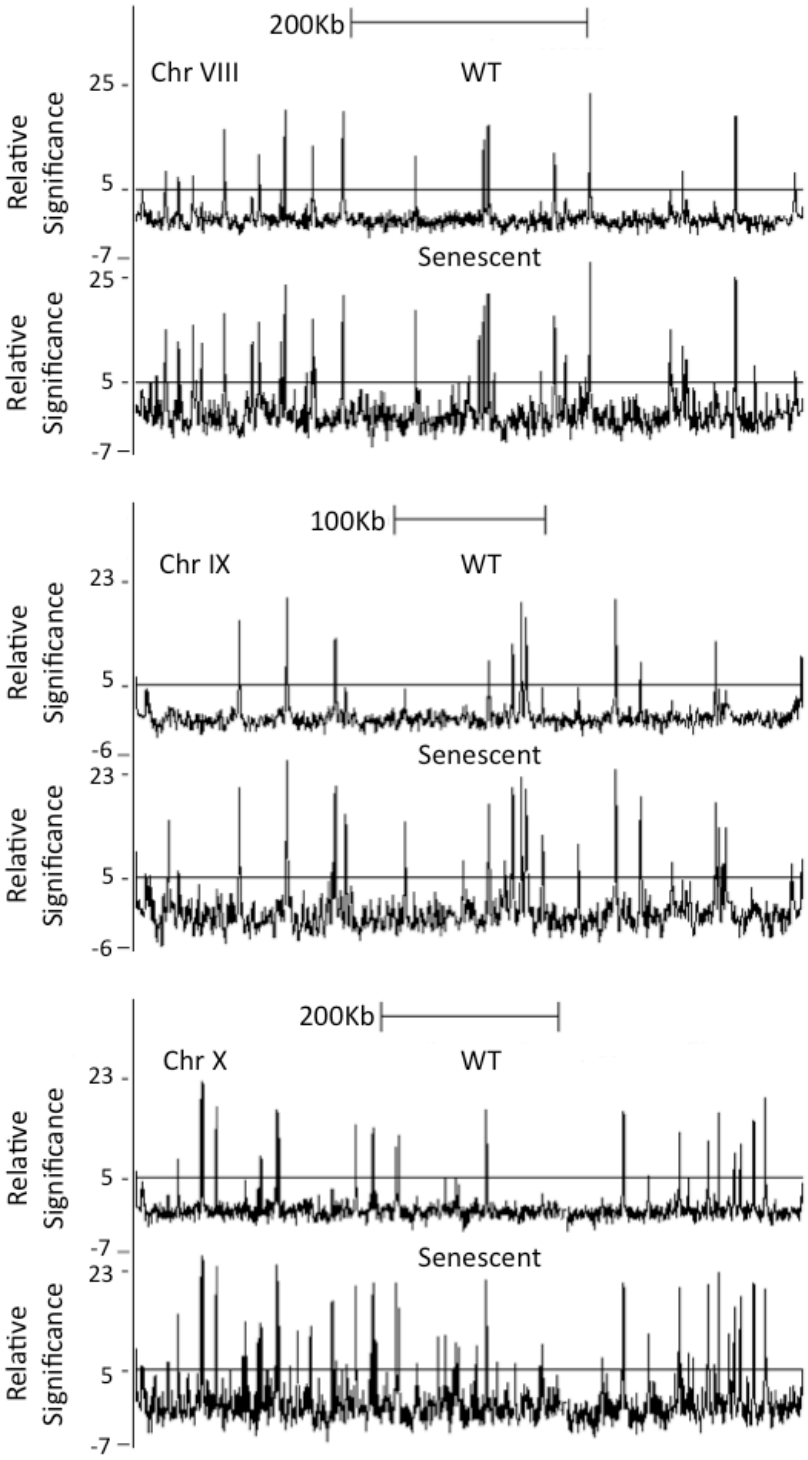

Figure 2-S1 Cont

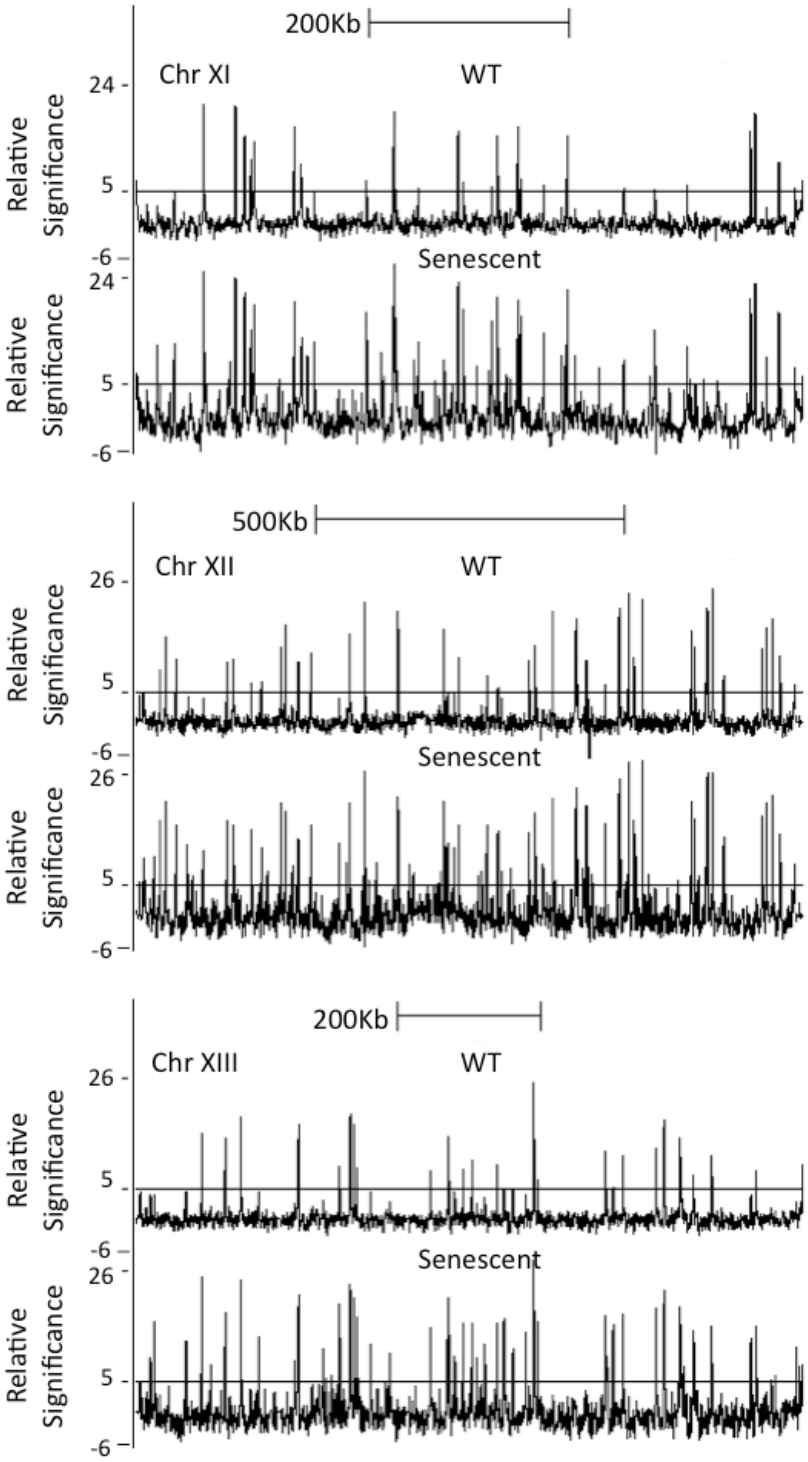

Figure 2-S1 Cont

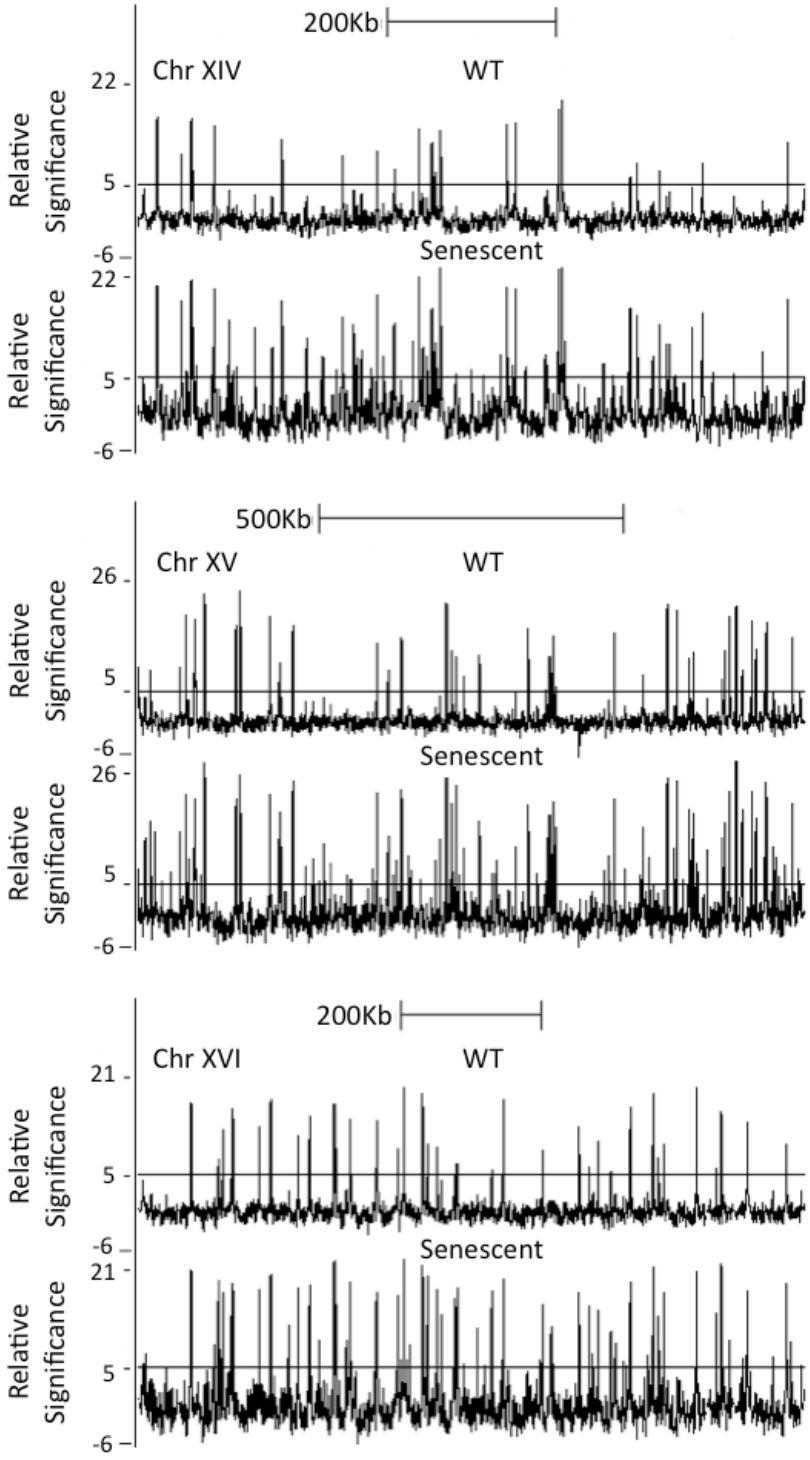

Figure S1.

Rap1 ChIP-tiling array data are shown for chromosomes I-XVI. Data are plotted as in Fig 1A.

Figure 2-S2

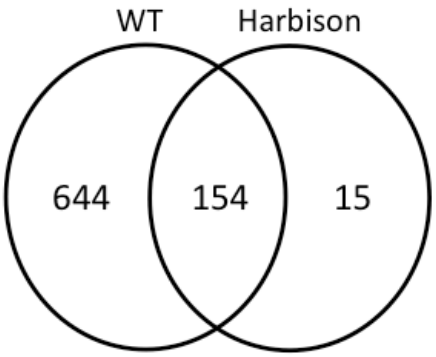

$p = 2.5 \times 10^{-123}$

Figure S2.

Rap1 target gene localization in wild type cells is similar to that observed in previous studies (Harbison et al. 2004). The p-value was calculated using Fisher's exact test from a total universe of 6178 genes.

Figure 2-S3

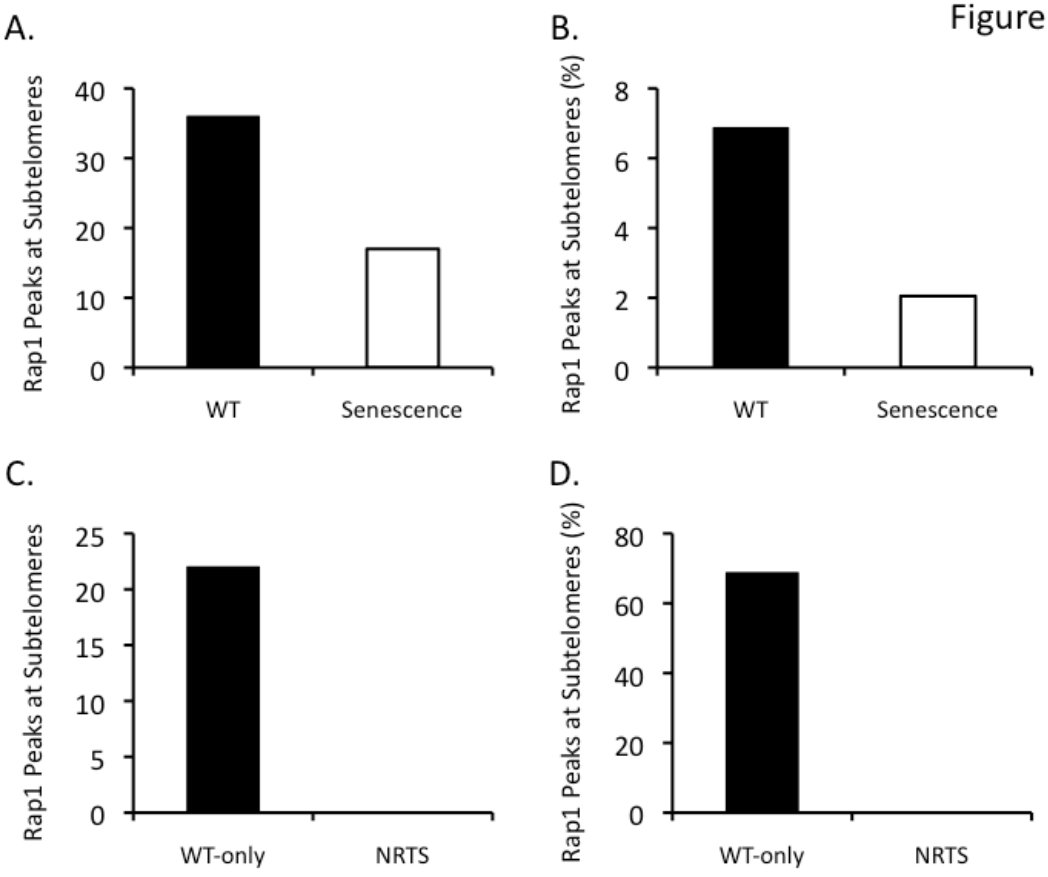

E.

Subtelomeric

YAR075W
COS2
COS7
COS4
YFR057W
COS12
COS6
YHL048C-A
COS8
YIL177C
YJL225C
COS5
YLR462W
COS3
COS1
YRF1-6
AAD15

Figure S3.

Rap1 leaves subtelomeres at senescence. **(A, B)** Rap1 enrichment at subtelomeres decreases at senescence. The total number (A) and percentage (B) Rap1 binding peaks at subtelomeres in WT and senescent cells. **(C, D)** No NRTS-associated Rap1 peaks are located in subtelomeres (0%, 0/346). Most Rap1 peaks that are present in WT but not in senescent cells (*WT-only*) are located at subtelomeres (69%, 22/32). Data are plotted as in Fig S3A-B. **(E)** List of WT-only genes that classified as *subtelomeric* (lying within 10kb of the telomere repeats). Note that these 17 genes are fewer than the 22 Rap1 WT-only subtelomeric peaks because some peaks are not associated with genes. In addition, note that the ten WT-only peaks associated with non-subtelomeric genes are a consequence of subtle changes in apparent Rap1 binding that caused the peaks not to be considered by our criteria as overlapping the promoters of the associated genes in senescent cells, but upon direct inspection is was apparent that these peaks are not substantially altered at senescence.

Figure 2-S4

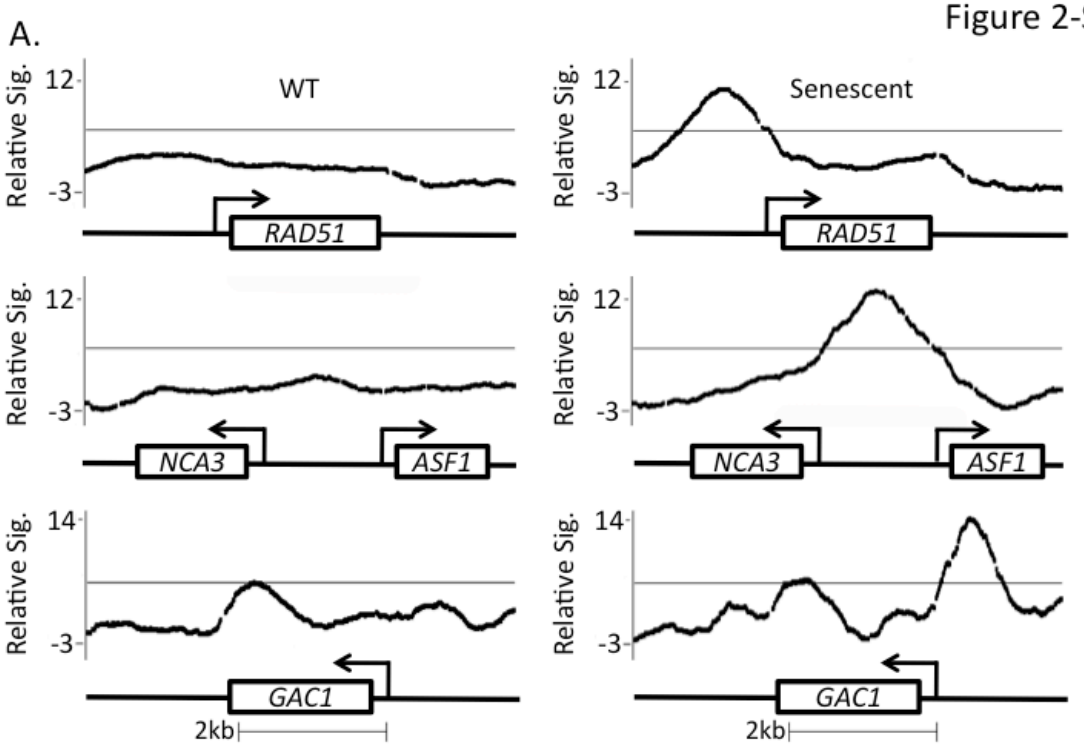

Figure S4.

At senescence, Rap1 binds preferentially upstream from the promoters of NRTS, e.g. *RAD51*, *NCA3*, *ASF1*, and *GAC1* (*cf*. Figs 2B and 2C). Data are plotted as in Fig. 1A.

Figure 2-S5

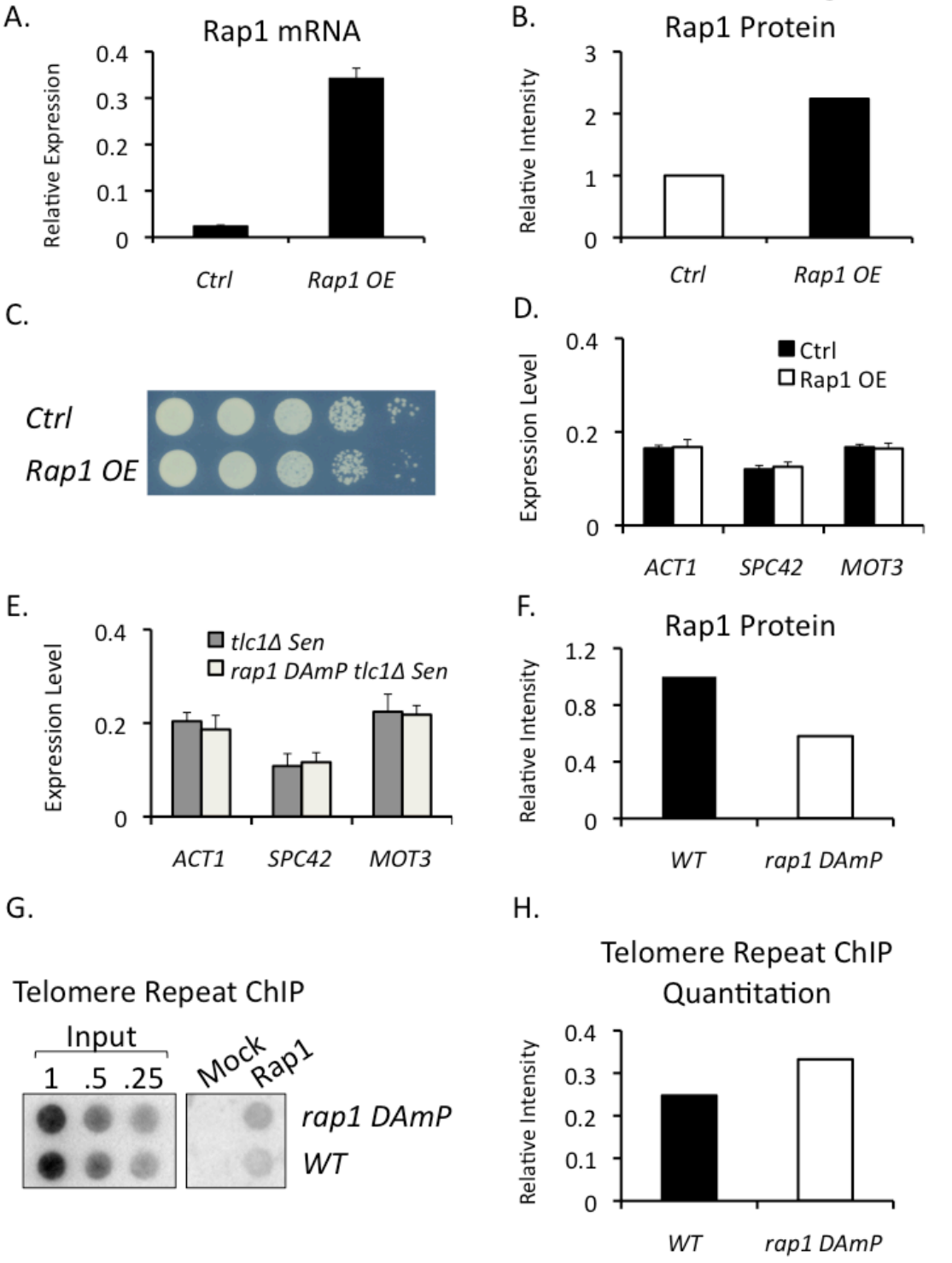
A.
Rap1 mRNA
Relative Expression
0.4
0.3
0.2
0.1
0
Ctrl
Rap1 OE
B.
Rap1 Protein
Relative Intensity
3
2
1
0
Ctrl
Rap1 OE
C.
Ctrl
Rap1 OE
D.
Expression Level
0.4
0.2
0
Ctrl
Rap1 OE
ACT1
SPC42
MOT3
E.
Expression Level
0.4
0.2
0
tlc1Δ Sen
rap1 DAmP tlc1Δ Sen
ACT1
SPC42
MOT3
F.
Rap1 Protein
Relative Intensity
1.2
0.8
0.4
0
WT
rap1 DAmP
G.
Telomere Repeat ChIP
Input
1
.5
.25
Mock
Rap1
rap1 DAmP
WT
H.
Telomere Repeat ChIP
Quantitation
Relative Intensity
0.4
0.3
0.2
0.1
0
WT
rap1 DAmP

Figure S5.

(A) *RAP1* transcripts are elevated in cells overexpressing *RAP1*. qPCR values are for *RAP1* mRNA normalized to *ACT1* mRNA from exponentially growing cultures of cells carrying vector (n=3; *Ctrl*) or the *NOP1p-RAP1* plasmid (n=3; *Rap1 OE*). p–value was calculated using Student's *t*-test. **(B)** Quantification of Rap1 immunoblot in Fig 3B. Rap1 intensity was normalized to the tubulin intensity, and show ~2-fold elevation in cells carrying the *NOP1p-RAP1* plasmid. **(C)** Rap1 overexpression *via* the *NOP1p-RAP1* plasmid is not toxic. Spot assay was performed with 10-fold serial dilutions from left to right of cells carrying vector (*Ctrl*) or the *NOP1p-RAP1* plasmid (*Rap1 OE*). $4x10^5$ cells were spotted in the initial, leftmost spot. **(D-E)** The control loci *ACT1*, *MOT3*, and *SPC42,* which do not show significant changes in expression at senescence (Nautiyal et al, 2002), are not regulated by Rap1. In tests of equal quantities of total RNA, two-fold overexpression of Rap1 *via* the *NOP1p-RAP1* plasmid (D) or reduction in Rap1 levels *via* the *DAmP* allele at senescence (E) did not affect mRNA levels from these loci. **(F)** Quantification of Rap1 immunoblot in Fig 3E. Rap1 intensity was normalized to the tubulin intensity, and shows ~40% reduced levels of Rap1 in *rap1 DAmP* cells. **(G-H)** Rap1 levels at telomere repeats are normal in the *rap1 DAmP* strain. **(G)** Dot blot of telomere DNA ChIPed with anti-Rap1 antibody from *WT* and *rap1 DAmP* cells. Two-fold serial dilutions of DNA from input chromatin are shown. **(H)** Quantification of Rap1 ChIP telomere dot blot in

(G). Signal intensities were background corrected by subtraction of mock ChIP intensities and were then normalized to the 0.25X input intensities.

Figure 2-S6

A.

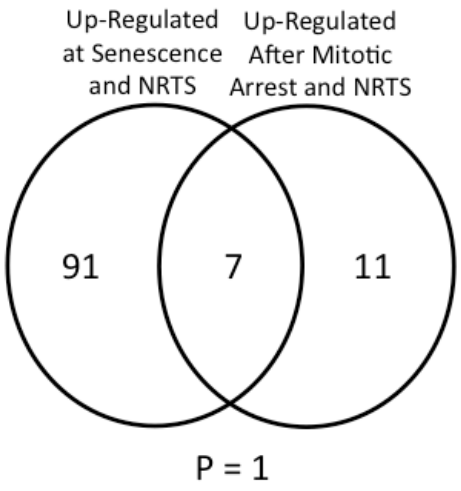

B.

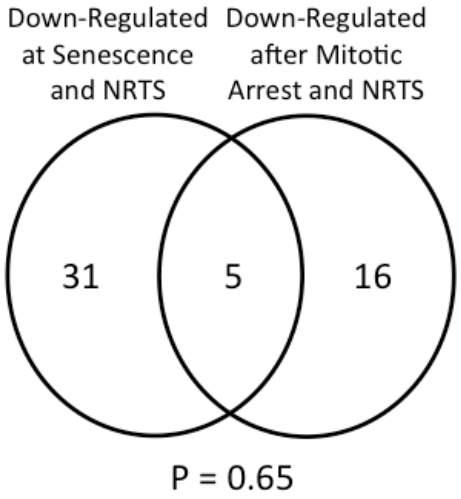

C.

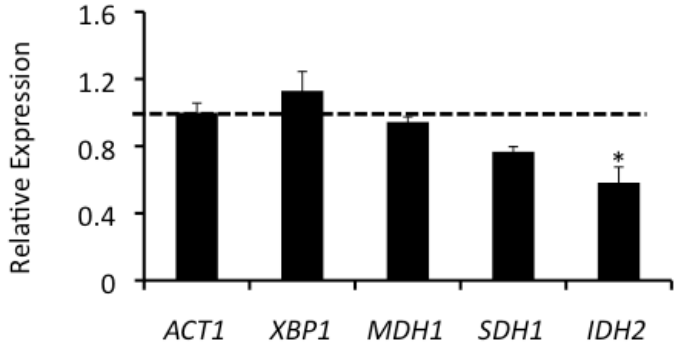

Figure S6.

The changes in NRTS expression at senescence are not a simple response to cell cycle arrest. **(A, B)** Venn diagrams comparing NRTS upregulated (A) or downregulated (B) at senescence to upregulated or downregulated, respectively, when cells are arrested in mitosis (*via cdc15-2* allele at 37°C). Intersections are of Fig 3A datasets and Spellman et al. datasets (Spellman et al. 1998) restricted to NRTS, and p-values were calculated using Fisher's exact test. There are 382 and 439 genes in remaining universes of Figures A and B respectively. **(C)** Upregulated NRTS are not activated by arrest with nocodazole. Data are plotted as fold change in mRNA expression in nocodazole arrested cells (n=3) relative to control cycling cells (n=3) and *ACT1* transcript (set at unity). Error bars are SEM, and p–values were calculated by Student's *t*-test (* $p < 0.05$).

Figure 2-S7

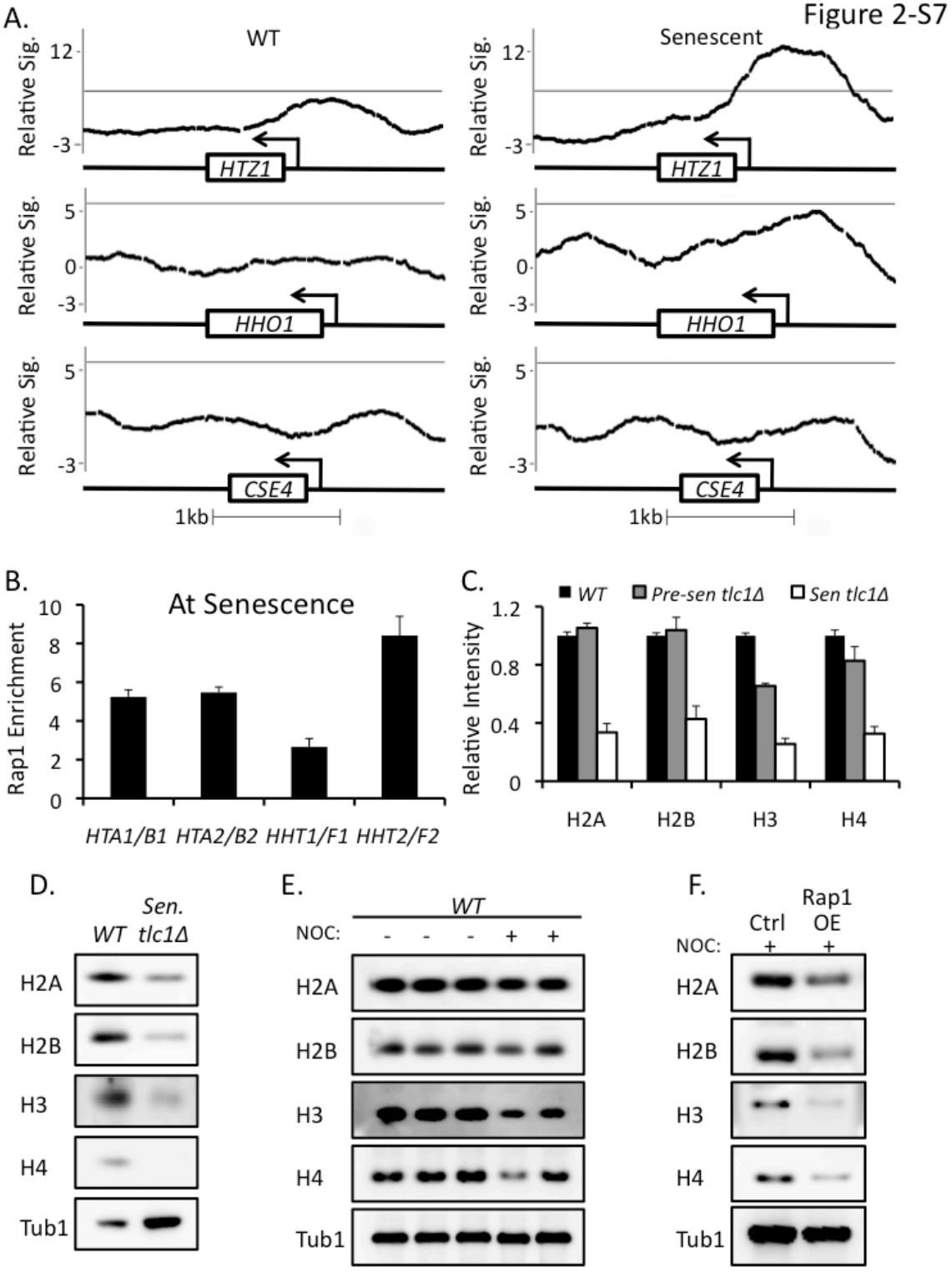
A.
WT
Senescent
Relative Sig.
12
-3
HTZ1
5
0
HHO1
CSE4
1kb
B.
At Senescence
Rap1 Enrichment
10
8
6
4
2
0
HTA1/B1
HTA2/B2
HHT1/F1
HHT2/F2
C.
WT
Pre-sen tlc1Δ
Sen tlc1Δ
Relative Intensity
1.2
0.8
0.4
0
H2A
H2B
H3
H4
D.
Sen.
WT
tlc1Δ
H2A
H2B
H3
H4
Tub1
E.
WT
NOC:
- - - + +
F.
Ctrl
Rap1 OE
NOC:
+ +

Figure S7.

(A) At senescence, Rap1 targets the *HTZ1* but not the *CSE4* promoter, and is moderately enriched at the *HHO1* promoter. Data are plotted as in Fig 1A. **(B**) Rap1 ChIP–qPCR confirmation of Rap1 targeting to core histone promoters at senescence. Data are plotted as fold change in Rap1 enrichment in senescent cells relative to wild type cells and the *ACT1* locus. Error bars are SEMs. **(C)** Quantification of immunoblot of core histones in Fig 4B. Shown are the ratios of H2A, H2B, H3, and H4 intensities to tubulin intensity and normalized to the ratio in wild type cells (WT levels are set at unity). **(D)** The decline in histone levels at senescence is also apparent when TCA extracts of equal numbers of cells are tested. Immunoblots of TCA extracts from equal numbers of wildtype and senescent *tlc1Δ* cultures were stained with anti-H2A, anti-H2B, anti-H3, anti-H4 or anti-tubulin antibodies. **(E)** Histone protein levels are largely unchanged in nocodazole-arrested cells. Immunoblots of TCA extracts from and equal number of the indicated cycling (n=3) and nocodazole arrested for 3hrs (n=2) wild type cells, stained as in (D). **(F)** Rap1 overexpression in nocodazole arrested wild type cells leads to downregulation of histone protein levels. Cells carrying pAG423-*NOP1-RAP1* or control vector were arrested for 2.5 hours in 1.5 μg/ml nocodazole, proteins were extracted with TCA, equal cell equivalents were loaded in each lane, and histone proteins were detected by immunoblotting.

Figure 2-S8

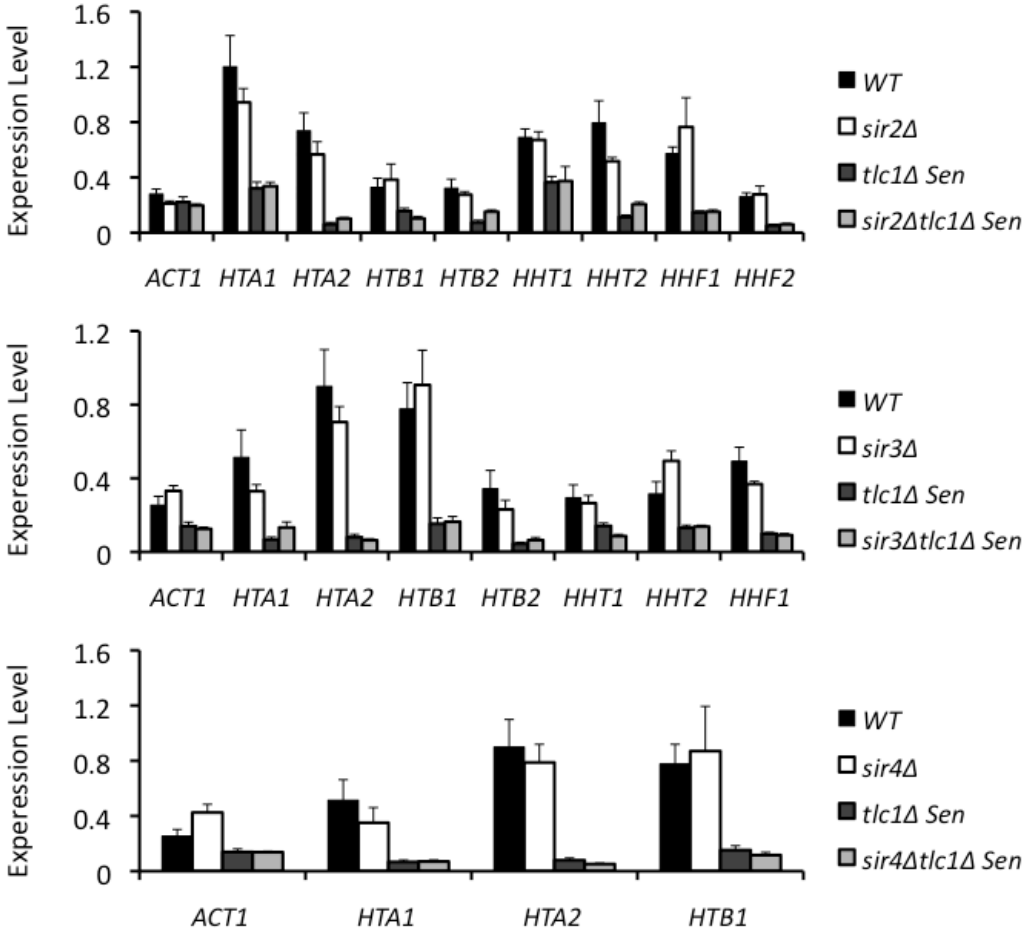
Experession Level
1.6
1.2
0.8
0.4
0
ACT1 HTA1 HTA2 HTB1 HTB2 HHT1 HHT2 HHF1 HHF2
WT
sir2Δ
tlc1Δ Sen
sir2Δtlc1Δ Sen
Experession Level
1.2
0.8
0.4
0
ACT1 HTA1 HTA2 HTB1 HTB2 HHT1 HHT2 HHF1
WT
sir3Δ
tlc1Δ Sen
sir3Δtlc1Δ Sen
Experession Level
1.6
1.2
0.8
0.4
0
ACT1 HTA1 HTA2 HTB1
WT
sir4Δ
tlc1Δ Sen
sir4Δtlc1Δ Sen

Figure S8.

Histone gene downregulation at senescence is Sir2/3/4-independent. mRNA levels were measured by qPCR for wild type (n=2), *sir2Δ* (n=2), *sir3Δ* (n=2), *sir4Δ* (n=2), senescent *tlc1Δ* (n=4), senescent *sir2Δ tlc1Δ* (n=4), senescent *sir3Δ tlc1Δ* (n=4), and senescent *sir4Δ tlc1Δ* (n=4) cultures.

Figure 2-S9

A.

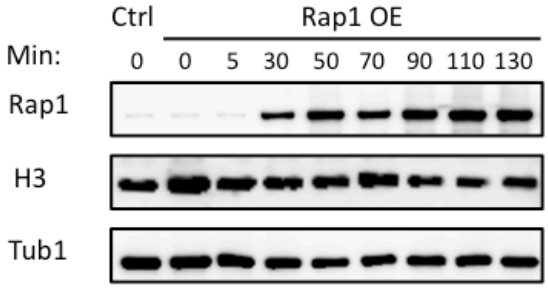

B.

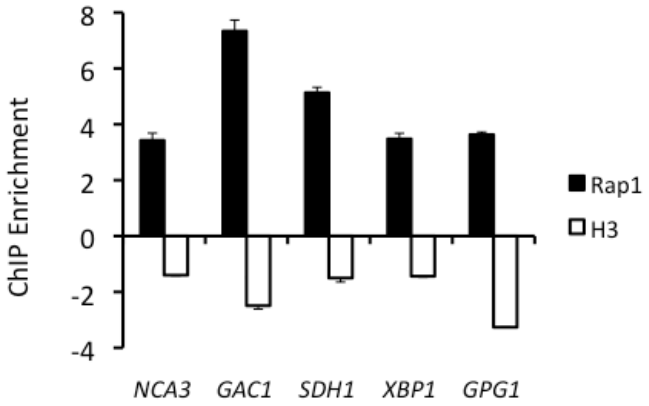

Figure S9.

Selective histone losses at activated NRTS are not simply a secondary consequence of Rap1-mediated repression of global histone levels. **(A)** Timecourse of total Rap1 and histone H3 levels following Rap1 overexpression in *WT* cells. Immunoblots of TCA extracts of *WT* cells possessing control vector or the *GAL1p-RAP1* plasmid following galactose induction are shown. 2% galactose was added to cells growing exponentially in SC-URA + 2% raffinose and at 1 x 10^6 cells/ml, and growth was continued for the times indicated. Lanes were loaded by equal cell number and stained with anti-Rap1, anti-H3, or anti-tubulin antibodies. **(B)** ChIP-qPCR analyses of Rap1 enrichment and H3 loss at NRTS upon Rap1 induction. Rap1 or H3 ChIP-qPCR data are plotted as fold changes in Rap1 and H3 enrichment in *GAL1p-RAP1* cells harvested at 130 min relative to vector control cells normalized to the non-Rap1-targeted *ACT1* locus. Error bars are SEMs. Note that histone levels at activated NRTS declined with Rap1 overexpression prior to global declines in histone levels, indicating that Rap1 is directly involved in reduced histone occupancy at activated NRTS rather than the reduced occupancy being only a secondary consequence of globally reduced levels of histones at senescence.

Figure 2-S10

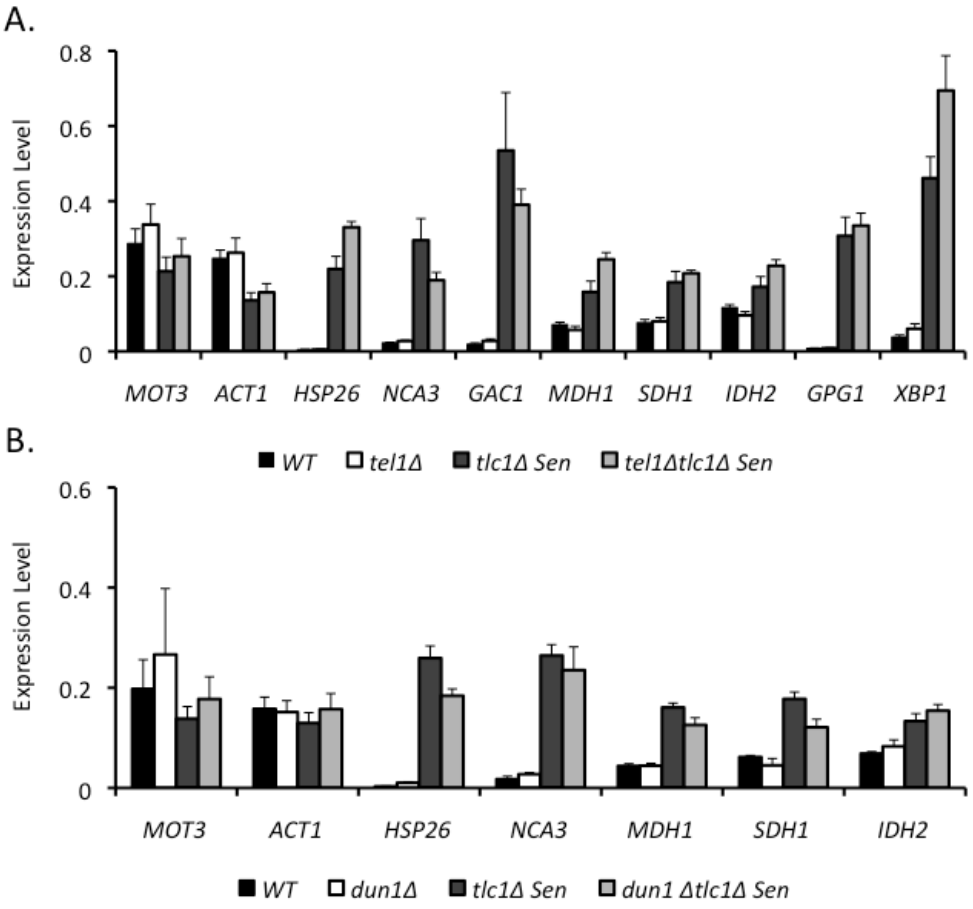
A.
Expression Level
0.8
0.6
0.4
0.2
0
MOT3
ACT1
HSP26
NCA3
GAC1
MDH1
SDH1
IDH2
GPG1
XBP1
B.
WT
tel1Δ
tlc1Δ Sen
tel1Δtlc1Δ Sen
Expression Level
0.6
0.4
0.2
0
MOT3
ACT1
HSP26
NCA3
MDH1
SDH1
IDH2
WT
dun1Δ
tlc1Δ Sen
dun1 Δtlc1Δ Sen

Figure S10.

Activation of NRTS at senescence is independent of *TEL1* and *DUN1*. **(A)** Upregulation of NRTS at senescence is independent of *TEL1*. RNA expression was measured by qPCR using RNA from wild type (n=2), *tel1Δ* (n=2), senescent *tlc1Δ* (n=4), and senescent *tel1Δ tlc1Δ* (n=4) cultures. **(B)** Activation of NRTS at senescence is independent of *DUN1*. RNA expression was measured by qPCR using RNA from wild type (n=2), *dun1Δ* (n=2), senescent *tlc1Δ* (n=4), and senescent *dun1Δtlc1Δ* (n=4) cultures.

Figure 2-S11

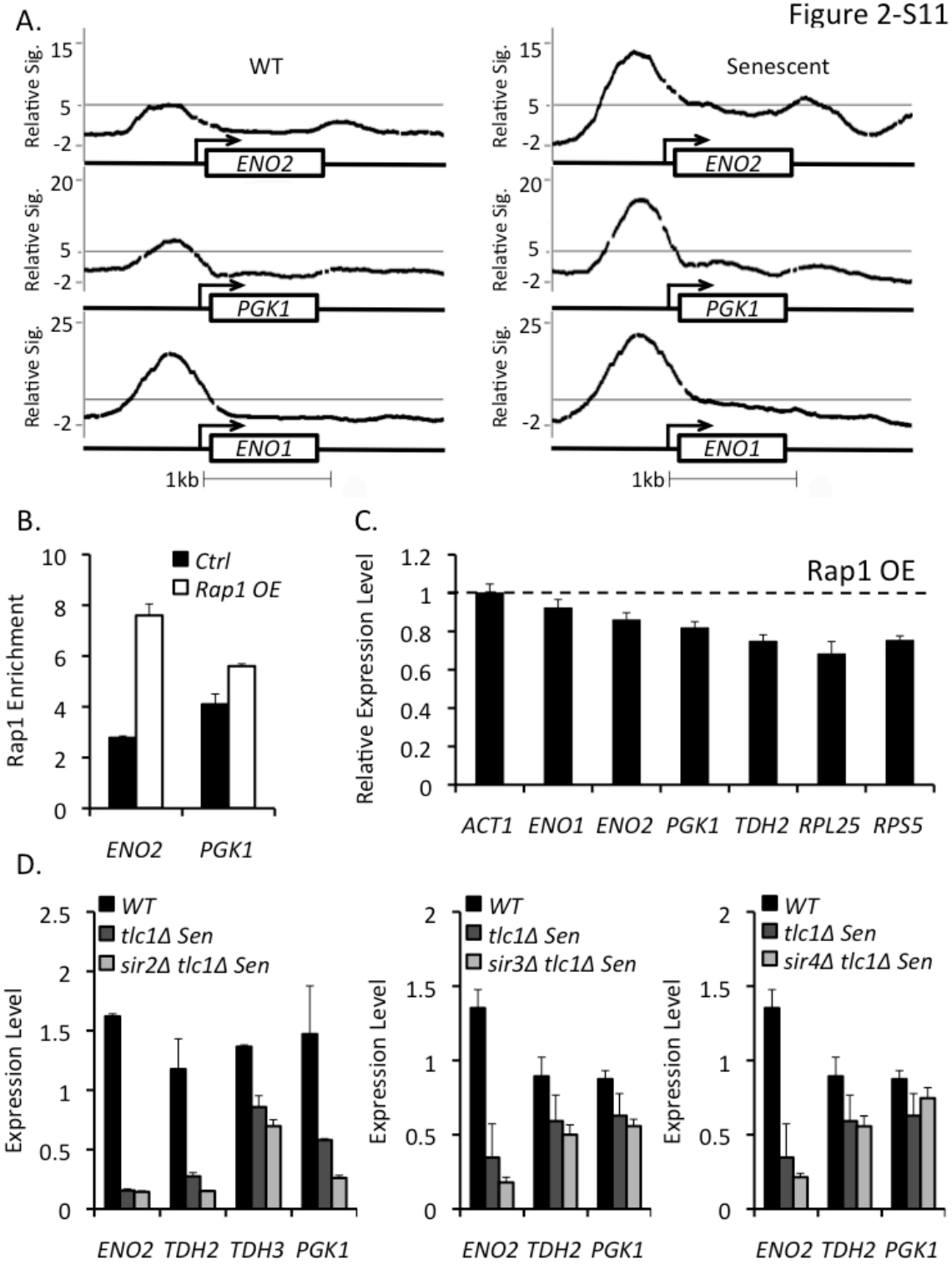
A.
WT
Senescent
Relative Sig.
ENO2
PGK1
ENO1
1kb
B.
Ctrl
Rap1 OE
Rap1 Enrichment
ENO2
PGK1
C.
Rap1 OE
Relative Expression Level
ACT1 ENO1 ENO2 PGK1 TDH2 RPL25 RPS5
D.
WT
tlc1Δ Sen
sir2Δ tlc1Δ Sen
sir3Δ tlc1Δ Sen
sir4Δ tlc1Δ Sen
Expression Level
ENO2 TDH2 TDH3 PGK1
ENO2 TDH2 PGK1
ENO2 TDH2 PGK1

Figure S11.

At senescence, Rap1 occupancy increases at its normal targets and contributes to their downregulation. **(A)** Rap1 ChIP-tiling array analyses of chromatin from wild type and senescent *tlc1Δ* cells for *ENO1, ENO2* and *PGK1*. Data are plotted as in Fig. 1A, i.e. they were normalized to control rabbit IgG ChIP data and plotted by relative significance using the MAT algorithm ($-\log_{10}$(p-value)). **(B)** Rap1 occupancy, as measured by qPCR and in comparison to input and *ACT1*, at the *ENO2* and *PGK1* promoters in cells with two-fold overexpression of Rap1 *via* the *NOP1p-RAP1* plasmid *vs.* vector control. **(C)** qPCR-measurements of mRNA levels from normal Rap1 target genes and *ACT1* in cells carrying the *NOP1p-RAP1* plasmid, in compared to vector control. **(D)** Normal Rap1 target gene downregulation at senescence is Sir2/3/4-independent. mRNA levels were measured by qPCR in the same fashion as for Fig S8.

Figure 2-S12

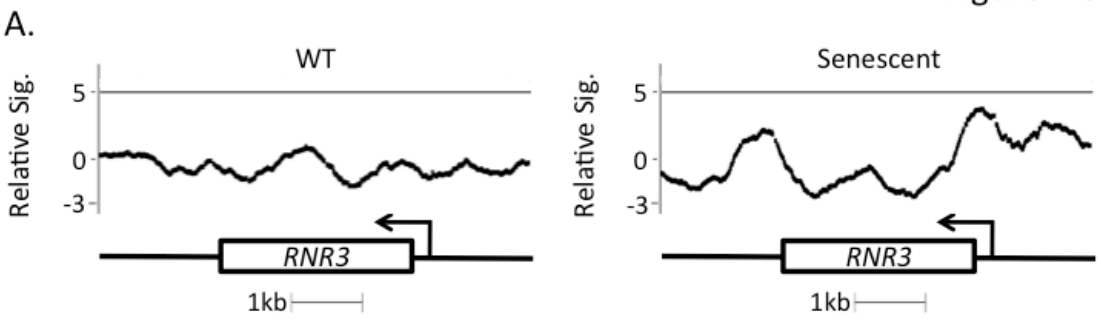
A.
WT
Relative Sig.
5
0
-3
RNR3
1kb
Senescent
Relative Sig.
5
0
-3
RNR3
1kb

Figure S12.

Rap1 occupancy at the *RNR3* promoter increases only modestly at senescence. Data are plotted as in Fig 1A.

Platt_Fig S13

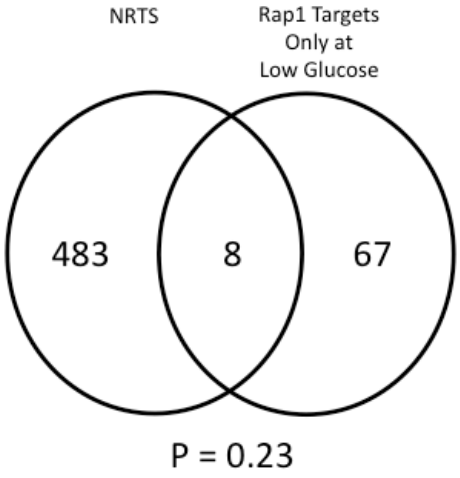

Figure S13.

Venn diagram comparing the intersection of NRTS and Rap1 targets in low glucose. The low glucose data is from Buck and Lieb, 2006 (Buck and Lieb 2006), and the p-value was calculated using Fischer's exact test. There are 5,722 genes in the remaining universe.

Platt_Table S1

P -Value	Intersection	NRTS Only	Rapid H3 Turnover Only	Remaining Universe
1.4×10^{-84}	289	202	1018	4842

Table S1.

Rap1 preferentially targets regions of the genome where histones turnover rapidly. Intersection of Fig 2A dataset and Dion et al. histone turnover dataset (Dion et al. 2007). P-values were calculated using Fisher's exact test.

ACACCCRT
ACACCCRY
ACAYCCRT
ACAYCCRY
CRTACATY
CRYACATY
CRTACAYM
CRYACAYM

Platt_Table S2B

Motif Number Requirement	P -Value	Intersection	NRTS Only	Rap1 Hemisite Linker Motif Only	Remaining Universe
1	2.7×10^{-4}	258	233	1982	2498
2	2.1×10^{-3}	204	287	1562	2918
3	9.2×10^{-4}	103	388	685	3795
4	5.6×10^{-3}	78	413	525	3955
5	2.3×10^{-4}	39	452	184	4296
6	0.034	22	469	127	4353
7	0.018	12	479	51	4429
8	0.026	9	482	35	4445
9	0.11	4	487	15	4465
10	7.9×10^{-3}	4	487	5	4475

Table S2.

NRTS promoters preferentially contain the Rap1 hemisite-linker motif. **(A)** The eight Rap1 hemisite-linker motifs that were used to in the analysis (hemisites are in black; linkers are in red). **(B)** Comparison of NRTS to regions of the genome that contain varying numbers of the Rap1 hemisite-linker motif (the *Motif Number Requirement* indicates the minimal number of hemisite-linker motifs present at a locus). We searched both Watson and Crick strands when searching for regions that contain the motif. Also, Rap1 hemisite-linker motifs that are already bound by Rap1 in WT cells were excluded from the number of unoccupied *Rap1 Hemisite Linker Motifs*. P-values were calculated using Fisher's exact test.

Cluster	Category	Term	Count	%	PValue	List Total	Pop Hits	Pop Total	Fold Enrichment	Bonferroni	Benjamini	FDR
15	INTERPRO	IPR007125~histone core	7	1.44	2.33E-05	395	9	4676	9.21	0.02	0.016	0.035
1	GOTERM_CC_FAT	GO:0001926~plasma membrane enriched fraction	19	3.90	2.11E-05	343	91	4595	2.98	0.02	0.006	0.035
15	GOTERM_BP_FAT	GO:0000788~nuclear nucleosome	6	1.23	4.81E-04	343	9	4870	9.53	0.47	0.105	0.796
10	GOTERM_BP_FAT	GO:0006633~fatty acid biosynthetic process	29	5.95	4.81E-04	413	172	4870	1.99	0.47	0.130	0.795
2	GOTERM_CC_FAT	GO:0005618~cell wall	39	8.01	6.50E-04	413	264	4595	1.74	0.48	0.041	0.958
2	GOTERM_CC_FAT	GO:0005576~cell wall, cellular region	17	3.49	9.33E-04	343	91	4595	2.50	0.78	0.072	1.844
10	GOTERM_BP_FAT	GO:0000122~negative regulation of transcription from RNA polymerase II promoter	16	3.29	1.45E-03	413	76	4870	2.48	0.85	0.214	2.351
8	GOTERM_BP_FAT	GO:0006084~acetyl-CoA metabolic process	10	2.05	1.57E-03	413	34	4870	3.47	0.88	0.189	2.544
8	GOTERM_BP_FAT	GO:0009109~coenzyme catabolic process	10	2.05	1.57E-03	413	34	4870	3.47	0.88	0.189	2.544
25	GOTERM_CC_FAT	GO:0031298~replication fork protection complex	8	1.64	1.77E-03	343	25	4595	4.29	0.97	0.068	2.397
9	PIR_SUPERFAMILY	PIRSF005376:conserved hypothetical protein YMR322c	4	0.82	1.98E-03	263	4	3234	12.30	0.42	0.423	2.581
2	GOTERM_CC_FAT	GO:0009277~fungal-type cell wall	19	3.90	2.10E-03	343	98	4595	2.32	0.53	0.072	2.844
9	INTERPRO	IPR002818:ThiJ/Pfpl	4	0.82	2.23E-03	395	4	4676	11.84	0.79	0.539	3.303
17	GOTERM_BP_FAT	GO:0000811~ion transport	31	6.37	2.53E-03	413	209	4870	1.75	0.97	0.228	4.060
12	GOTERM_MF_FAT	GO:0051540~metal cluster binding	9	1.85	2.57E-03	366	29	4190	3.55	0.80	0.554	3.751
8	GOTERM_BP_FAT	GO:0046356~acetyl-CoA catabolic process	9	1.85	2.71E-03	413	30	4870	3.54	0.97	0.227	4.349
22	GOTERM_BP_FAT	GO:0000096~glycolysis	9	1.85	2.71E-03	413	30	4870	3.54	0.97	0.227	4.349
10	GOTERM_MF_FAT	GO:0003704~specific RNA polymerase II transcription factor activity	13	2.67	3.05E-03	366	57	4190	2.61	0.85	0.473	4.444
7	GOTERM_BP_FAT	GO:0007568~aging	15	3.08	3.14E-03	413	74	4870	2.39	0.98	0.230	5.012
6	GOTERM_CC_FAT	GO:0000324~fungal-type vacuole	25	5.13	3.61E-03	343	181	4595	1.85	0.72	0.110	4.833
15	INTERPRO	IPR009072:Histone-fold	7	1.44	3.62E-03	395	19	4676	4.36	0.92	0.568	5.317
11	GOTERM_BP_FAT	GO:0046942~carboxylic acid transport	14	2.87	5.14E-03	413	70	4870	2.36	1.00	0.316	8.096
26	GOTERM_BP_FAT	GO:0033692~cellular polysaccharide biosynthetic process	9	1.85	7.50E-03	413	35	4870	3.03	1.00	0.365	11.597
3	GOTERM_BP_FAT	GO:0009309~amine biosynthetic process	22	4.52	7.69E-03	413	142	4870	1.83	1.00	0.360	11.871
3	GOTERM_BP_FAT	GO:0008652~cellular amino acid biosynthetic process	21	4.31	8.30E-03	413	134	4870	1.85	1.00	0.347	12.753
18	GOTERM_BP_FAT	GO:0009266~response to temperature stimulus	30	6.16	8.31E-03	413	217	4870	1.63	1.00	0.337	12.764
31	GOTERM_MF_FAT	GO:0016209~antioxidant activity	8	1.64	8.51E-03	366	28	4190	3.27	1.00	0.658	11.928
8	KEGG_PATHWAY	scer00020:Citrate cycle (TCA cycle)	9	1.85	0.010	139	33	1439	2.82	0.49	0.492	9.956
23	GOTERM_BP_FAT	GO:0016051~carbohydrate biosynthetic process	16	3.29	0.012	413	94	4870	2.01	1.00	0.394	17.434
10	GOTERM_MF_FAT	GO:0003700~transcription factor activity	21	4.31	0.012	366	135	4190	1.78	1.00	0.663	16.502
14	INTERPRO	IPR013087:Zinc finger, C2H2-type/integrase, DNA-binding	33	6.78	0.012	395	246	4676	1.54	1.00	0.627	17.015
25	GOTERM_CC_FAT	GO:0043596~nuclear replication fork	7	1.44	0.013	343	24	4595	3.45	1.00	0.826	17.297
10	GOTERM_BP_FAT	GO:0016481~negative regulation of transcription	9	1.85	0.013	413	43	4870	2.80	0.99	0.259	15.921
13	GOTERM_BP_FAT	GO:0006536~glutamate metabolic process	27	5.54	0.013	413	196	4870	1.62	1.00	0.416	19.665
25	GOTERM_CC_FAT	GO:0005657~replication fork	6	1.23	0.014	413	53	4870	3.93	1.00	0.423	21.094
21	GOTERM_BP_FAT	GO:0015749~monosaccharide transport	10	2.05	0.015	343	53	4595	2.53	1.00	0.286	18.727
16	GOTERM_MF_FAT	GO:0046914~transition metal ion binding	7	1.44	0.016	413	25	4870	3.30	1.00	0.441	22.751
3	GOTERM_BP_FAT	GO:0044271~nitrogen compound biosynthetic process	74	15.20	0.016	366	665	4190	1.27	1.00	0.436	23.522
6	GOTERM_CC_FAT	GO:0044437~vacuolar part	18	3.70	0.016	343	131	4595	1.84	1.00	0.292	20.206
7	GOTERM_BP_FAT	GO:0007569~cell aging	12	2.46	0.017	413	64	4870	2.21	1.00	0.437	24.626
5	GOTERM_BP_FAT	GO:0019320~hexose catabolic process	11	2.26	0.017	413	56	4870	2.32	1.00	0.436	25.089
25	GOTERM_CC_FAT	GO:0000790~nuclear chromatin	16	3.29	0.018	343	112	4595	1.91	1.00	0.301	21.958
16	GOTERM_MF_FAT	GO:0003497~chromatin assembly	8	1.64	0.018	413	33	4870	2.86	1.00	0.426	26.020
15	GOTERM_MF_FAT	GO:0043169~cation binding	91	18.69	0.019	413	850	4190	1.23	1.00	0.704	25.007
4	GOTERM_MF_FAT	GO:0008537~glutamate biosynthetic process	5	1.03	0.019	413	13	4870	4.54	1.00	0.434	27.552
4	GOTERM_MF_FAT	GO:0016566~specific transcriptional repressor activity	6	1.23	0.020	366	19	4190	3.62	1.00	0.630	26.366
28	GOTERM_BP_FAT	GO:0006091~generation of precursor metabolites and energy	33	6.78	0.022	413	264	4870	1.47	1.00	0.474	31.029
11	GOTERM_BP_FAT	GO:0006885~amino acid transport	10	2.05	0.022	413	50	4870	2.36	1.00	0.467	31.090
28	GOTERM_BP_FAT	GO:0015893~drug transport	6	1.23	0.023	413	20	4870	3.54	1.00	0.462	31.217
12	GOTERM_MF_FAT	GO:0051537~2 iron, 2 sulfur cluster binding	4	0.82	0.026	366	8	4190	5.72	1.00	0.673	32.766
23	GOTERM_BP_FAT	GO:0006304~DNA packaging	10	2.05	0.032	413	53	4870	2.22	1.00	0.549	41.092
20	GOTERM_BP_FAT	GO:0009083~glutamine family amino acid biosynthetic process	24	4.93	0.032	413	162	4870	1.75	1.00	0.545	41.317
28	GOTERM_BP_FAT	GO:0006637~cell wall chitin metabolic process	5	1.03	0.033	413	15	4870	3.93	1.00	0.537	41.803
47	GOTERM_CC_FAT	GO:0031670~cellular response to nutrient	4	0.82	0.033	343	10	4595	3.93	1.00	0.537	41.803
19	GOTERM_BP_FAT	GO:0030127~COPII vesicle coat	6	1.23	0.033	413	22	4870	3.22	1.00	0.535	42.640
19	PIR_SUPERFAMILY	PIRSF036260:Hexose biosynthetic process	6	1.23	0.034	263	22	3234	3.22	0.961	0.541	38.579
45	INTERPRO	IPR001411:Nucleobase-AA, transporter	4	0.82	0.034	395	9	4676	5.26	1.00	0.968	40.587
18	GOTERM_CC_FAT	GO:0005408~proton-dependent transporter	26	5.34	0.036	413	203	4870	1.51	1.00	0.546	43.691
2	GOTERM_CC_FAT	GO:0031225~anchored to membrane	11	2.26	0.036	343	71	4595	2.08	1.00	0.432	39.384
21	INTERPRO	IPR000961:Sugar/inositol transporter	7	1.44	0.036	395	30	4676	3.79	1.00	0.959	42.473
62	GOTERM_BP_FAT	GO:0007039~vacuolar protein catabolic process	17	3.49	0.036	413	117	4870	1.71	1.00	0.547	45.342
11	GOTERM_MF_FAT	GO:0015175~neutral amino acid transmembrane transporter activity	4	0.82	0.037	366	9	4190	5.09	1.00	0.773	42.926
44	GOTERM_BP_FAT	GO:0051253~negative regulation of RNA metabolic process	23	4.72	0.037	413	175	4870	1.55	1.00	0.552	46.381
24	GOTERM_BP_FAT	GO:0000296~spermine transport	3	0.62	0.038	413	4	4870	8.84	1.00	0.554	47.136
11	INTERPRO	IPR002293:Amino acid/polyamine transporter I	6	1.23	0.039	395	23	4676	3.09	0.964	45.246
24	GOTERM_MF_FAT	GO:0000297~spermine transmembrane transporter activity	3	0.62	0.040	366	4	4190	8.59	0.782	45.789
6	GOTERM_CC_FAT	GO:0005774~vacuolar membrane	16	3.29	0.041	343	124	4595	1.73	0.459	43.312
7	GOTERM_BP_FAT	GO:0001302~replicative cell aging	9	1.85	0.041	413	47	4870	2.26	0.577	49.824
21	GOTERM_MF_FAT	GO:0005353~fructose transmembrane transporter activity	5	1.03	0.044	366	16	4190	3.58	0.777	49.115

Table S3.

GO analysis of NRTS performed using The Database for Annotation, Visualization and Integrated Discovery v. 6.7 (DAVID) (Huang et al. 2009). *Pop Total* is all *S. cerevisiae* genes annotated in the system of classifying genes (i.e. *Category*). *Pop Hits* refers to all genes in *S. cerevisiae* that fall into the sub-category (i.e. *Term*). *List Total* is all NRTS that are annotated in the system of classifying genes. *Count* refers to all NRTS that fall into the sub-category. P-values were calculated using Fisher's-exact test. Bonferroni, Benjamini, and FDR are standard conservative adjustments to the p-value to control for effects of multiple comparisons.

Platt_Table S4A

Direction of Change	P -Value	Intersection	Senescence Regulated Only	H4 Depletion Regulated Only	Remaining Universe
Up	4.5×10^{-18}	171	671	524	4985
Down	1.7×10^{-49}	228	444	612	5067

Platt_Table S4B

Direction of Change	P -Value	Intersection	Senescence Regulated and NRTS Only	H4 Depletion Regulated and NRTS Only	Remaining Universe
Up	3.1×10^{-4}	28	70	51	342
Down	3.5×10^{-7}	15	21	37	418

Table S4.

Gene expression changes when histone H4 is depleted are very similar to the gene expression changes at senescence. **(A)** Intersection of Nautiyal et al. senescence dataset (Nautiyal et al. 2002) and Wyrick et al. H4-depletion dataset (Wyrick et al. 1999). **(B)** Comparison of NRTS that are differentially expressed at senescence to gene expression changes at NRTS when H4 is depleted. P-values were calculated using Fisher's exact test.

Platt_Table S5

Direction of Change	P -Value	Intersection	Senescence Regulated Only	Rapid H3 Turnover Only	Remaining Universe
Up	1.3×10^{-15}	264	578	1043	4466
Down	0.61	136	536	1171	4508

Table S5.

Genes upregulated at senescence have rapid histone turnover. Intersection of Nautiyal et al. senescence dataset (Nautiyal et al. 2002) and Dion et al. Histone Turnover dataset (Dion et al. 2007). P-values were calculated using Fisher's exact test.

Platt_Table S6A

min of MMS	P -Value	Intersection	Up-Regulated at Senescence and NRTS Only	Up-Regulated after MMS and NRTS Only	Remaining Universe
15	1.6×10^{-3}	15	83	15	372
30	2.0×10^{-5}	23	75	29	364
45	1.5×10^{-4}	25	73	40	353
60	6.6×10^{-5}	26	72	40	353
90	1.4×10^{-6}	32	66	45	348
120	1.7×10^{-7}	36	62	50	343

Platt_Table S6B

min of MMS	P -Value	Intersection	Down-Regulated at Senescence and NRTS Only	Down-Regulated after MMS and NRTS Only	Remaining Universe
15	0.059	4	32	17	438
30	1.1×10^{-3}	7	29	18	437
45	1.2×10^{-5}	11	25	25	430
60	9.6×10^{-7}	12	24	23	432
90	3.7×10^{-6}	12	24	27	428
120	5.3×10^{-9}	15	21	25	430

Table S6.

(A) Comparison of NRTS upregulated at senescence to genes activated with DNA damage. Intersection of Fig 3A dataset and Gasch et al. datasets (increasing amount of MMS treatment: Gasch et al. 2001). **(B)** Comparison of NRTS downregulated at senescence to genes repressed with DNA damage. Intersection of Fig 3A dataset and Gasch et al. datasets (increasing amount of MMS treatment: Gasch et al. 2001).

Platt_Table S7

Strain	Genotype	Reference (source)
YMK1	BY4743 *MAT a/a his3Δ1/his3Δ1 leu2Δ0/leu2Δ0 ura3Δ0/ura3Δ0 MET15/met15Δ0 LYS2/lys2Δ0*	Brachmann et al., 1998. (R. Davis)
JP46	YMK1 *TLC1/tlc1Δ::LEU2*	This Study
JP375	BY4741 *MAT a his3Δ1 leu2Δ0 met15Δ0 ura3Δ0*	Brachmann et al., 1998. (R. Davis)
JP377	JP375 + *pAG413-NOP1p::ccdB*	This Study
JP376	JP375 + *pAG413-NOP1p::Rap1*	This Study
JP208	BY4741 *rap1 DAmP::kanMX*	Breslow et al., 2008. (Thermo Sci.)
JP313	YMK1 *TLC1/tlc1Δ::HygB RAP1/rap1 DAmP::kanMX*	This Study
BKD223	BY4741 *ura3Δ0::pGAL HHT2 HHF2 URA3*	Feser et al., 2010. (J. Tyler)
BKD226	BY4741 *leu2Δ0/leu2Δ0::pGAL HTA1 HTB1 LEU2*	Feser et al., 2010. (J. Tyler)
JP435	YMK1 *leu2Δ0/leu2Δ0::pGAL HTA1 HTB1 LEU2 ura3Δ0/ura3Δ0::pGAL HHT2 HHF2 URA3 TLC1/tlc1Δ::HygB*	This Study
JP232	YMK1 *MEC1/mec1Δ::URA3 SML1/sml1Δ::KanMX TLC1/tlc1Δ::LEU2*	This Study
JP200	YMK1 *TEL1/tel1::KanMX TLC1/tlc1::LEU2*	This Study
JP203	YMK1 *DUN1/dun1::KanMX TLC1/tlc1::LEU2*	This Study
JP436	JP375 + *pAG426-GALp::ccdB*	This Study
JP437	JP375 + *pAG426-GALp::Rap1*	This Study
JP36	YMK1 *TLC1/tlc1Δ::Leu2, SAS2/sas2Δ::Hyg, SIR3/sir3Δ::G418*	Kozak et al., 2010. (F. B. Johnson)
JP37	YMK1 *TLC1/tlc1Δ::Leu2, SAS2/sas2Δ::Hyg, SIR2/sir2Δ::G418*	Kozak et al., 2010. (F. B. Johnson)
JP38	YMK1 *TLC1/tlc1Δ::Leu2, SAS2/sas2Δ::Hyg, SIR4/sir4Δ::G418*	Kozak et al., 2010. (F. B. Johnson)

Table S7.

Strains used in this study.

qPCR		
ACT1 F	AGAACCACCAATCCAGACGGAGT	This Study
ACT1 R	ATGCAAAAGGAAATCACCGCTTT	This Study
HSP26 F	CACACCCGCAAAGGATTCTACTG	This Study
HSP26 R	CAGGGACAAGTCATTGTCGAACC	This Study
NCA3 F	CCAACAGTAACCAAGCTGCCAAC	This Study
NCA3 R	AGAGCCATCTTCATACGCACAGC	This Study
GAC1 F	AACGCGGAGCCAAGTTCTATCTC	This Study
GAC1 R	TGTTGAAAAGCTGGACGTCATCA	This Study
XBP1 F	AACAAAACCAACGACCAGCTCAT	This Study
XBP1 R	GTTCAGTGAATTGTTCGCCCTTG	This Study
GPG1 F	GGCTGGGGCTGAACCAACTTAT	This Study
GPG1 R	AAGTGTGTGCAACTCTCCGACAA	This Study
MDH1 F	GCTGGCTCTGCTACGTTGTCAAT	This Study
MDH1 R	GATGACGTCTCTTTCGCCTTTGA	This Study
SDH1 F	CGCTCTCCAAGTTGACTTTGCTC	This Study
SDH1 R	GTTTACAGAGCCCTGCGTTTGG	This Study
IDH2 F	TAGTGCAGCAAACGTCCCCATAG	This Study
IDH2 R	TAGATTGTACGGCAGGGTCAGGA	This Study
SPC42 F	AAGAGCTGCAAAGCATGATGGAC	This Study
SPC42 R	GACTGGATTGGGAAGAATGACGA	This Study
MOT3 F	CGTCGTCCTTATTCAGTACACCAT	This Study
MOT3 R	CAGCAACAGCTCCCGAAAATG	This Study
RAP1 F	TATGAGCCATCACAGGCTGAAAAA	This Study
RAP1 R	GATCCCCGGATAAACACGTCAATA	This Study
HTA1 F	GGTTCTGGTGCTCCAGTCTAC	(Feser et al., 2010)
HTA1 R	TCTTCTTGTTATCCCTAGCAGCAT	(Feser et al., 2010)
HTA2 F	AGCTGGTTTAACATTCCCAGTT	(Feser et al., 2010)
HTA2 R	GCAGTTAGATAGACTGGAGCAC	(Feser et al., 2010)
HTB1 F	AGAGAAGCAAGGCTAGAAAGGA	(Feser et al., 2010)
HTB1 R	GGAAATACCAGTGTCAGGGTG	(Feser et al., 2010)
HTB2 F	GATTGATCTTACCTGGTGAATTGGCTAAA	(Feser et al., 2010)
HTB2 R	GGCTTGAGTAGAGGAGGAGTAT	(Feser et al., 2010)
HHT1 F	CTGCCATTCACGCCAAGC	(Feser et al., 2010)
HHT1 R	ATGATCTTTCACCTCTTAATCTTCTAGCC	(Feser et al., 2010)
HHT2 F	CCCCAAGAAAACAATTAGCCTCC	(Feser et al., 2010)
HHT2 R	AAGGCAACAGTACCTGGCTTAT	(Feser et al., 2010)
HHF1 F	AAGAGATAACATCCAAGGTATTACTAAGCC	(Feser et al., 2010)
HHF1 R	CAAACCAGAAATACGCTTGACAC	(Feser et al., 2010)
HHF2 F	ATCAGGGACTCTGTTACTTACACT	(Feser et al., 2010)
HHF2 R	GGTTCTACCTTGTCTCTTCAAAGCATAAA	(Feser et al., 2010)

Table S8.

DNA primers used for qPCR analyses of mRNA levels.

ChIP		
ENO1 F	GTCCAAATATGCAGGTGTTTG	This Study
ENO1 R	GCTTCTAGGCGGGTTATCTAC	This Study
PGK1 F	CTAGGACCTTGTTGTGTGACG	This Study
PGK1 R	GCTCGACTTCCTGTCTTCCTA	This Study
HSP26 F	TTTTCTTTTCATTTGGCAATTT	This Study
HSP26 R	GGCTTATGAGAGAGACCCATAG	This Study
NCA3 F	CCACTGACCCCATATTAAAAA	This Study
NCA3 R	AGCGACAATTAACCTAAAGAGG	This Study
GAC1 F	CCCATAACCCAGTGAGTATTTT	This Study
GAC1 R	TAACAGCCAAGCTAAAAGAACA	This Study
XBP1 F	GTATTAGGGGTGAGGGTGAATA	This Study
XBP1 R	CCTTGTACGAGTGCTATGAATG	This Study
GPG1 F	TTTTAAGGGAACTTCCTCACAC	This Study
GPG1 R	CACATCCTATATTCCCTTCGAG	This Study
SDH1 F	AAAGGTTAGAGTCGAGGATGC	This Study
SDH1 R	GCCTCTTCTATTGGTTGTTTGT	This Study
ACT1 F	TCGTTCCAATTTACGCTGGTT	(Kozak et al., 2010)
ACT1 R	CGGCCAAATCGATTCTCAA	(Kozak et al., 2010)
TEL6R-0.1-F	TGAGGCCATTTCCGTGTGTA	(Kozak et al., 2010)
TEL6R-0.1-R	CCCAGTCCTCATTTCCATCAA	(Kozak et al., 2010)
TEL6R-7.3kb-F	TGCGAAATAAGAACACGATCGT	(Kozak et al., 2010)
TEL6R-7.3kb-R	GTAGAAGGGCCGACATGTACTACA	(Kozak et al., 2010)
TEL6R-10kb-F	TCATCCGTACACACACAGAGACCA	(Kozak et al., 2010)
TEL6R-10kb-R	TCCAATTGTCAATGAGCAGGTTGA	(Kozak et al., 2010)
TEL6R-15kb-F	TCCCAAGGAAGTGAAACCGATTGC	This Study
TEL6R-15kb-R	CAACTGCTTCTGTTTCCTCCT	This Study
HHT1/HHF1 F	TTCGGTTTTTACCACTAACCA	This Study
HHT1/HHF1 R	GAAAACTTCGCATCTTCACATA	This Study
HHT2/HHF2 F	GCTGTTATCACGCAAACTATGT	This Study
HHT2/HHF2 R	AGTTGGTCATTTAGCGTTCATT	This Study
HTA1/HTB1 F	TCGTTACAAGATAACCAACCAA	This Study
HTA1/HTB1 R	AAAATCAAGAGAATTGGCCTTA	This Study
HTA2/HTB2 F	TACGTAACGAAAATGGTAGCAC	This Study
HTA2/HTB2 R	GCGAATTTCAGAGAACACATTA	This Study
RSP5 F	TGAGACTATTTTGGAGCAGGA	This Study
RSP5 R	AGAAACAAGCATTTTTGTCCTT	This Study
Subtel 4L F	GGAGTGGATGGTTGAGTGGGG	(Iglesias et al., 2011)
Subtel 4L R	CTAACACTACCCTATTCTAACCCTGATTTT	(Iglesias et al., 2011)
Subtel 13R F	ACGGTTATGGTGCACGATGGG	(Iglesias et al., 2011)
Subtel 13R R	TTACCCTCCATTACGCTACCTCC	(Iglesias et al., 2011)

Table S9.

DNA primers used for qPCR analyses of ChIP DNA samples.

CHAPTER 3: The effect of *BRE1/LGE1* on the rate of senescence and NRTS gene activation at senescence

INTRODUCTION

Though Rap1 is necessary to fully activate the NRTS at senescence, Rap1 is known to be a weak transcriptional activator by itself (Idrissi et al. 2001; 1998; Shore 1994). Instead, Rap1 is thought to behave more like a general regulatory factor (GRF; like *ABF1* and *REB1*) (Ganapathi et al. 2011; Venters et al. 2011). That is, Rap1 is thought to bind DNA in a sequences specific manner, open up the local chromatin, and recruit transcriptional co-activators or transcriptional co-repressors to perform specific functions at various sites throughout the genome. For example, Rap1 recruits Gcr1 and Gcr2 to glycolytic target genes and Fhl1, Ifh1, and TFIID to ribosomal protein genes and the Sir2/3/4 the silent mating type locus and telomeres (Moretti and Shore 2001; Zhao et al. 2006; Tornow et al. 1993; Schawalder et al. 2004). As a result, we wondered how Rap1 worked with other factors to activate the NRTS at senescence.

Because no known Rap1 co-activator consensus sequences were found in the promoter regions of the activated NRTS (including Gcr1, Fhl1, and Ifh1; data not shown), we considered the possibility that Rap1 was recruiting general transcriptional co-activators to the activated NRTS promoters at senescence. One

likely candidate was TFIID. Not only does Rap1 directly bind to TFIID and recruit it to the ribosomal protein genes where it acts as a transcriptional co-activator (Papai et al. 2010; Garbett et al. 2007), but also based on an unbiased whole genome analysis of 200 transcription related proteins during vegetative growth and acute heat shock Rap1 is both **1)** in the TFIID epistatsis group and is **2)** the main transcriptional 'orchestrator'/GRF of the TFIID pathway (Venters et al. 2011). However, there is one major problem with the idea that TFIID is the general transcriptional co-activator for the NRTS genes at senescence. In general, TFIID regulates the transcription of most housekeeping/'pro-growth' genes (i.e. genes involved biomass production including ribosomal protein genes, rRNA processing enzymes, and glycolytic enzymes) a category that would not include the NRTS genes, which are stress-response genes (Basehoar et al. 2004; Venters et al. 2011; Rando and Winston 2012; Zanton and Pugh 2006; Huisinga and Pugh 2004). Thus, even though Rap1 has TFIID-dependent functions and is the major orchestrator of TFIID pathway, its new functions at senescence at the activated NRTS are likely to be TFIID-independent.

Instead, the upregulation of activated NRTS genes at senescence likely depends on a SAGA-dependent pathway (Spt–Ada–Gcn5 acetyltransferase), which regulates the expression of most stress-response genes (Basehoar et al. 2004; Rando and Winston 2012; Huisinga and Pugh 2004). SAGA is a large, modular 20 protein complex whose functions are regulated by many loosely associated proteins,

which makeup the SAGA-pathway (Koutelou et al. 2010; Venters et al. 2011). On top of its physical complexity, SAGA has an equally intricate list of activities it performs to activate transcription, which include: localizing gene's upstream promoter regions with the help of Tra1, decompacting the local chromatin via its histone-acetyltransferase (HAT) activity, assembling the pre-initiation complex (PIC), and activating transcriptional elongation (Koutelou et al. 2010). In addition to the core members of the SAGA complex there are several key regulators of the SAGA-pathway that if disrupted prevent transcriptional activation. One such factor is Bre1, an E3 ubiquitin ligase that together with Lge1 and Rad6, its E2 ubiquitin ligase, leads to the ubiquitylation of H2B (H2BUb), which in turn is important for transcriptional initiation and elongation (Wood et al. 2003; Hwang et al. 2003; Henry et al. 2003; Weake and Workman 2008; Kao et al. 2004; Xiao et al. 2005). H2BUb is a key histone modification that regulates histone crosstalk and is necessary for di- and trimethylation of H3K4 (via Set1 and the COMPASS complex) and methylation of H3K79 (by Dot1) (Wood et al. 2003; Hwang et al. 2003).

An unbiased genome-wide screen found that there is a positive synthetic-genetic interaction between the hypomorphic *rap1-DAmP* allele and deletions in the genes encoding the H2BUb ubiquitylating enzymes (*BRE1* and *LGE1*) and the COMPASS complex members (*SWD1*, *SWD3*, *BRE2*, *SDC1*, and *SPP1*; Supplemental Figure 3-1) (Collins et al. 2007). Interactions discovered through synthetic genetic array (SGA) analysis are frequently found between members of multi-protein

complexes (Tong 2001; Boone et al. 2007), and thus these data suggest that Rap1 might be part of a larger Bre1-dependent COMPASS complex. Though these data are consistent with many models, one possibility is that *RAP1*, *BRE1*, and members of the COMPASS complex up-regulate the expression of stress-response genes that restrict vegetative growth. Because these modules can be more active under various stress conditions, for example during telomere dysfunction and senescence, we wondered if *BRE1* and the COMPASS complex affect the Rap1-dependent activation of up-regulated NRTS at senescence.

RESULTS and DISCUSSION

BRE1 and *LGE1* accelerate the pace of senescence

We had previously shown that *RAP1* drives the rate of senescence and because we speculated that some of the affects of *RAP1* at senescence were *BRE1*/*LGE1* dependent, we tested how *BRE1* and *LGE1* affect the pace of senescence. Similar to the *rap1-DAmP* allele, *BRE1* or *LGE1* deletion slow the pace of senescence, which suggest that the normal function of *BRE1* and *LGE1* (in wild-type cells) is to drive the rate of senescence (Figure 3-1).

Though *BRE1* and *LGE1* both accelerate the rate of senescence, the absolute affects of the two genes are different: according to the nadir of the curves, *BRE1*

deletions slows the rate of senescence by ~20PD (p = 0.0022), whereas *LGE1* deletion slows the pace of senescence by ~7PD (p = 0.0001). However, this difference is consistent with the biological activity of *BRE1* and *LGE1*. Though Lge1 forms a complex with Bre1 and stimulates its E3 ubiquitin ligase activity, Bre1 is still active without *LGE1* and downstream histone crosstalk to H3K4me3 and H3K79me3 is only partially reduced (Hwang et al. 2003). In comparison to a complete *BRE1* knockout, *lge1Δ* behaves like a hypomorphic *bre1* allele and thus its effects on the rate of senescence should be reduced as compared to *bre1Δ.*

***BRE1* is necessary to activate NRTS at senescence**

Though there is a positive genetic interaction between loss of function mutations in *RAP1* and H2B ubiquitylating enzymes (Supplemental Figure 3-1), it is unclear if *BRE1/LGE1* is active at the *RAP1*-dependent activated NRTS at senescence. Because H2BUb is a transient histone modification (Henry et al. 2003), we analyzed H3K4me3, which is a downstream readout of *BRE1/LGE1* activity, and measured how its occupancy changes at the NRTS promoters at senescence by ChIP-RTPCR. Even though H3 is preferentially lost at the upstream promoter regions of the activated NRTS (see Chapter 2), we find that the levels of H3K4me3 go up at these promoters at senescence (Figure 3-2A). These data suggest that *BRE1/LGE1* activity preferentially increases at the activated NRTS genes at senescence.

In addition to functioning at the NRTS promoters, *BRE1* is necessary to activate the upregulated NRTS at senescence (Figure 3-2B,C). Because *BRE1* deletion slows the pace of senescence, we compared both population doubling (PD) matched and senescence matched *bre1Δtlc1Δ* samples to senescent *tlc1Δ* samples (the latter being a more stringent test of necessity). Whereas the expression of *ACT1* a housekeeping gene is unaffected by *BRE1* deletion, the activation of NRTS at senescence is blunted in both PD matched and senescence matched *bre1Δtlc1Δ* cells. These data suggest that *BRE1* is necessary to activate the NRTS genes even when the cells are deeply senescent.

Altogether our data suggest that *BRE1*/*LGE1* preferentially targets the NRTS promoters and is necessary to activate the upregulated NRTS at senescence. However, further work is necessary to understand how Bre1 and Rap1 activate the NRTS genes at senescence. First, it will be important understand how Bre1 and Rap1 affect the other's localization at the NRTS promoters at senescence. Second, does *BRE1* affect the rate of senescence and the upregulation of NRTS genes at senescence through its ability to ubiquitylate H2BK123? Similarly, we should also determine which domains of Bre1 are important for NRTS upregulation at senescence (for example we should test point mutants that abolish its RING E3 ligase activity). Finally, we should assess if the affect of *BRE1* on the rate of senescence depends on *MEC1* and the DNA damage response.

UBP10 and *UBP8* slow the rate of senescence

Based on our finding that *BRE1/LGE1* accelerate the pace of senescence, we wondered if the ubiquitin proteases that de-ubiquitinate H2BK123Ub *UBP10* and *UBP8* slow rate of senescence. *UBP10* is preferentially localized at heterochromatin and subtelomeres and is important for telomere silencing (Kahana and Gottschling 1999; Gardner et al. 2005), whereas *UBP8* is a member of the SAGA complex and is involved in the initiation of transcription (Henry et al. 2003; Wyce et al. 2007). Even though *UBP8* and *UBP10* appear to have distinct roles, characterization of the double mutant suggests they have partially overlapping functions and synergize to alter gene expression (Gardner et al. 2005).

UBP10 and *UBP8* both slow the pace of senescence, and thus deleting either gene causes premature senescence: 15PD early ($p = 0.0039$) in the case of *UBP10* and ~5PD early ($p = 0.032$) for *UBP8*. It is interesting that the H2BUb ubiquitin proteases *UBP8* and *UBP10* slow the rate of senescence, whereas the H2BUb E3 ubiquitin ligases *BRE1* and *LGE1* accelerate the pace of senescence. Though it is currently just a correlation, these data are consistent with the idea the level of H2BUb drives the pace of senescence. However, more work needs to be done to fully understand how *UBP8/10* slow the pace of senescence. Not only is it important to assess if *UBP8/10* affects the rate of senescence are through de-ubiquitylating

H2BUb (by performing epistasis analyses with mutants of H2B that cannot be ubiquitylated – including H2BK123R), but also we should determine how *UBP8* and *UBP10* affect NRTS expression at senescence. Finally, because *UBP10* has already been linked to stabilizing the Rap1/Sir2/3/4 complex at subtelomeres (Emre et al. 2005), it will also be interesting to determine how *UBP10* affects Rap1 relocalization from subtelomeres at senescence.

SWD3 drives the rate of senescence

We were interested how the COMPASS complex affects the pace of senescence for two reasons. First, H3K4me3 occupancy – a readout of COMPASS complex activity – preferentially increases at the upstream promoters of activated NRTS. Second, the affect of *BRE1* on the rate of senescence (20PD extension) is only partially explained by the H3K79 methyltransferase *DOT1* (10PD extension), which suggests that the remaining affect might be due to the COMPASS complex.

To determine how the COMPASS complex affects the rate of senescence, we looked at *SWD3*, which not only has a positive genetic interaction with Rap1 (Supplemental Figure 3-1), but also is a core member of the COMPASS complex that is essential for both complex formation and methyltransferase activity (Shilatifard 2012). *SWD3* accelerates the rate of senescence and when deleted the cells senesce ~7PD ($p = 0.029$) later than wildtype. Taken together with *BRE1/LGE1* and *DOT1*,

these findings suggest that each node of histone cross-talk accelerates the rate of senescence. However, more work needs to be done to understand how *SWD3* drives the rate of senescence. It will be important to perform epistasis experiments to determine if *SWD3* and *BRE1* accelerate the rate of senescence in the same pathway. In addition, we should determine if *SWD3* accelerates the rate of senescence through H3K4me3.

References

Basehoar AD, Zanton SJ, Pugh BF. 2004. Identification and distinct regulation of yeast TATA box-containing genes. *Cell* **116**: 699–709.

Boone C, Bussey H, Andrews BJ. 2007. Exploring genetic interactions and networks with yeast. *Nat Rev Genet* **8**: 437–449.

Collins SR, Miller KM, Maas NL, Roguev A, Fillingham J, Chu CS, Schuldiner M, Gebbia M, Recht J, Shales M, et al. 2007. Functional dissection of protein complexes involved in yeast chromosome biology using a genetic interaction map. *Nature* **446**: 806–810.

Emre NCT, Ingvarsdottir K, Wyce A, Wood A, Krogan NJ, Henry KW, Li K, Marmorstein R, Greenblatt JF, Shilatifard A, et al. 2005. Maintenance of low histone ubiquitylation by Ubp10 correlates with telomere-proximal Sir2 association and gene silencing. *Mol Cell* **17**: 585–594.

Ganapathi M, Palumbo MJ, Ansari SA, He Q, Tsui K, Nislow C, Morse RH. 2011. Extensive role of the general regulatory factors, Abf1 and Rap1, in determining genome-wide chromatin structure in budding yeast. *Nucleic Acids Res* **39**: 2032–2044.

Garbett KA, Tripathi MK, Cencki B, Layer JH, Weil PA. 2007. Yeast TFIID serves as a coactivator for Rap1p by direct protein-protein interaction. *Mol Cell Biol* **27**:

297–311.

Gardner RG, Nelson ZW, Gottschling DE. 2005. Ubp10/Dot4p regulates the persistence of ubiquitinated histone H2B: distinct roles in telomeric silencing and general chromatin. *Mol Cell Biol* **25**: 6123–6139.

Henry KW, Wyce A, Lo W-S, Duggan LJ, Emre NCT, Kao C-F, Pillus L, Shilatifard A, Osley MA, Berger SL. 2003. Transcriptional activation via sequential histone H2B ubiquitylation and deubiquitylation, mediated by SAGA-associated Ubp8. *Genes Dev* **17**: 2648–2663.

Huisinga KL, Pugh BF. 2004. A genome-wide housekeeping role for TFIID and a highly regulated stress-related role for SAGA in Saccharomyces cerevisiae. *Mol Cell* **13**: 573–585.

Hwang WW, Venkatasubrahmanyam S, Ianculescu AG, Tong A, Boone C, Madhani HD. 2003. A conserved RING finger protein required for histone H2B monoubiquitination and cell size control. *Mol Cell* **11**: 261–266.

Idrissi F-Z, Fernandez-Larrea JB, Piña B. 1998. Structural and functional heterogeneity of Rap1p complexes with telomeric and UASrpg-like DNA sequences. *Journal of Molecular Biology* **284**: 925–935.

Idrissi F-Z, García-Reyero N, Fernandez-Larrea JB, Piña B. 2001. Alternative

mechanisms of transcriptional activation by Rap1p. *J Biol Chem* **276**: 26090–26098.

Kahana A, Gottschling DE. 1999. DOT4 links silencing and cell growth in Saccharomyces cerevisiae. *Mol Cell Biol* **19**: 6608–6620.

Kao C-F, Hillyer C, Tsukuda T, Henry K, Berger S, Osley MA. 2004. Rad6 plays a role in transcriptional activation through ubiquitylation of histone H2B. *Genes Dev* **18**: 184–195.

Koutelou E, Hirsch CL, Dent SYR. 2010. Multiple faces of the SAGA complex. *Current Opinion in Cell Biology* **22**: 374–382.

Kozak ML, Chavez A, Dang W, Berger SL, Ashok A, Guo X, Johnson FB. 2010. Inactivation of the Sas2 histone acetyltransferase delays senescence driven by telomere dysfunction. *EMBO J* **29**: 158–170.

Moretti P, Shore D. 2001. Multiple Interactions in Sir Protein Recruitment by Rap1p at Silencers and Telomeres in Yeast. *Mol Cell Biol* **21**: 8082–8094.

Papai G, Tripathi MK, Ruhlmann C, Layer JH, Weil PA, Schultz P. 2010. TFIIA and the transactivator Rap1 cooperate to commit TFIID for transcription initiation. *Nature* **465**: 956–960.

Rando OJ, Winston F. 2012. Chromatin and transcription in yeast. *Genetics* **190**:

351–387.

Schawalder SB, Kabani M, Howald I, Choudhury U, Werner M, Shore D. 2004. Growth-regulated recruitment of the essential yeast ribosomal protein gene activator Ifh1. *Nature* **432**: 1058.

Shilatifard A. 2012. The COMPASS Family of Histone H3K4 Methylases: Mechanisms of Regulation in Development and Disease Pathogenesis. *Annu Rev Biochem* **81**: 65–95.

Shore D. 1994. RAP1: a protean regulator in yeast. *Trends Genet* **10**: 408–412.

Tong AHY. 2001. Systematic Genetic Analysis with Ordered Arrays of Yeast Deletion Mutants. *Science* **294**: 2364–2368.

Tornow J, Zeng X, Gao W, Santangelo GM. 1993. GCR1, a transcriptional activator in Saccharomyces cerevisiae, complexes with RAP1 and can function without its DNA binding domain. *EMBO J* **12**: 2431–2437.

Venters BJ, Wachi S, Mavrich TN, Andersen BE, Jena P, Sinnamon AJ, Jain P, Rolleri NS, Jiang C, Hemeryck-Walsh C, et al. 2011. A comprehensive genomic binding map of gene and chromatin regulatory proteins in Saccharomyces. *Mol Cell* **41**: 480–492.

Weake VM, Workman JL. 2008. Histone ubiquitination: triggering gene activity. *Mol*

Cell **29**: 653–663.

Wood A, Krogan NJ, Dover J, Schneider J, Heidt J, Boateng MA, Dean K, Golshani A, Zhang Y, Greenblatt JF, et al. 2003. Bre1, an E3 ubiquitin ligase required for recruitment and substrate selection of Rad6 at a promoter. *Mol Cell* **11**: 267–274.

Wyce A, Xiao T, Whelan KA, Kosman C, Walter W, Eick D, Hughes TR, Krogan NJ, Strahl BD, Berger SL. 2007. H2B ubiquitylation acts as a barrier to Ctk1 nucleosomal recruitment prior to removal by Ubp8 within a SAGA-related complex. *Mol Cell* **27**: 275–288.

Xiao T, Kao C-F, Krogan NJ, Sun Z-W, Greenblatt JF, Osley MA, Strahl BD. 2005. Histone H2B ubiquitylation is associated with elongating RNA polymerase II. *Mol Cell Biol* **25**: 637–651.

Zanton SJ, Pugh BF. 2006. Full and partial genome-wide assembly and disassembly of the yeast transcription machinery in response to heat shock. *Genes Dev* **20**: 2250–2265.

Zhao Y, McIntosh KB, Rudra D, Schawalder S, Shore D, Warner JR. 2006. Fine-structure analysis of ribosomal protein gene transcription. *Mol Cell Biol* **26**: 4853–4862.

Materials and Methods

Senescence assays

Senescence assays were performed in YPAD using fresh spore products from dissection plates, with growth in liquid starting approximately 25 PD after loss of telomerase. All comparisons between different genotypes were performed using spore products obtained from the same *TLC1/tlc1Δ* diploid possessing any other heterozygous genetic changes of interest (e.g. *BRE1/bre1Δ*) to ensure that the haploid cells being compared had inherited telomeres of similar length and from the same epigenetic environment. Spore products (N=4 per genotype unless otherwise specified) were passaged serially in fresh liquid media. 10^6 cells were inoculated into 5 mL of media, were grown for 22 hours, counted using a Coulter counter and then re-inoculated at 10^6 cells/5 ml media. Cell counts were used to determine elapsed PDs (PD = $\log_2$(final/starting concentration)). *P*-values for differences between rates of senescence were calculated using the PD at the nadir of the curves for individual cultures and using a Student's *t*-test. Samples for mRNA expression and ChIP assays of senescent cells were obtained ~5 PDs prior to the nadir to avoid contributions from survivors of senescence, and cells were harvested under optimal growth conditions (i.e. at < 2 x 10^7 cells/ml after 12-16 hours of growth for senescent cultures after an initial inoculation at ≤ 2 x 10^6 cells/ml in fresh medium, while carefully following their growth and doubling times).

Chromatin immunoprecipitation and analysis

ChIP was performed as previously described (Kozak et al. 2010). Briefly, $2x10^8$ cells were harvested during exponential growth, crosslinked with formaldehyde and sonicated to an average 100-200 bp DNA fragment size. Chromatin (750 μg total protein, measured using the BCA method) was immunoprecipitated using rabbit H3K4me3 (Active Motif), rabbit anti-total H3 (ab1791, Abcam), or rabbit IgG (31207, Pierce). Purified DNA was quantified using qPCR and standard curves, and the enrichment for specific ChIP signals (H3K4me3) at specific target loci were calculated by normalization to histone H3 ChIP, input (obtained from 50 μg total protein), rabbit IgG controls, and an unaffected reference locus (*MDP1*), as follows: Enrichment for Rap1 at target locus = $[(H3K4me3_{target} - IgG_{target})/((H3_{target} - IgG_{target})(Input_{target}))] / [(H3K4me3_{reference} - IgG_{reference})/((H3_{reference} - IgG_{reference})(Input_{reference}))]$. Overall ChIP patterns were similar when the IgG control and reference locus normalization were omitted from calculations.

Quantitation of mRNA expression

Cells were harvested during exponential growth and frozen in liquid N_2 and stored at -80^0 C. RNA was extracted using the RNeasy Mini protocol (Qiagen), including the on column DNaseI digestion. 0.5 μg of RNA was reverse transcribed using the TaqMan Reverse Transcription Kit (ABI) at 25°C for 10', 42°C for 30', and 48°C for

20’. cDNA was analyzed using qPCR analysis on a Roche Applied Sciences Light Cycler 480 using SYBR Green Jumpstart *Taq* ReadyMix (Sigma) according to kit directions. Samples were run in triplicate in a 384-well format. A standard curve was run for each PCR reaction, using 4–fold serial dilutions of pooled cDNA samples. In most cases, the following qPCR program was run: 95°C 10’, followed by 50 cycles of [95°C 15”, 60°C 59”, 60°C 1” with signal acquisition], followed by signal acquisition during melting up to 95°C to ensure single species amplification.

Figure 3-1

A.

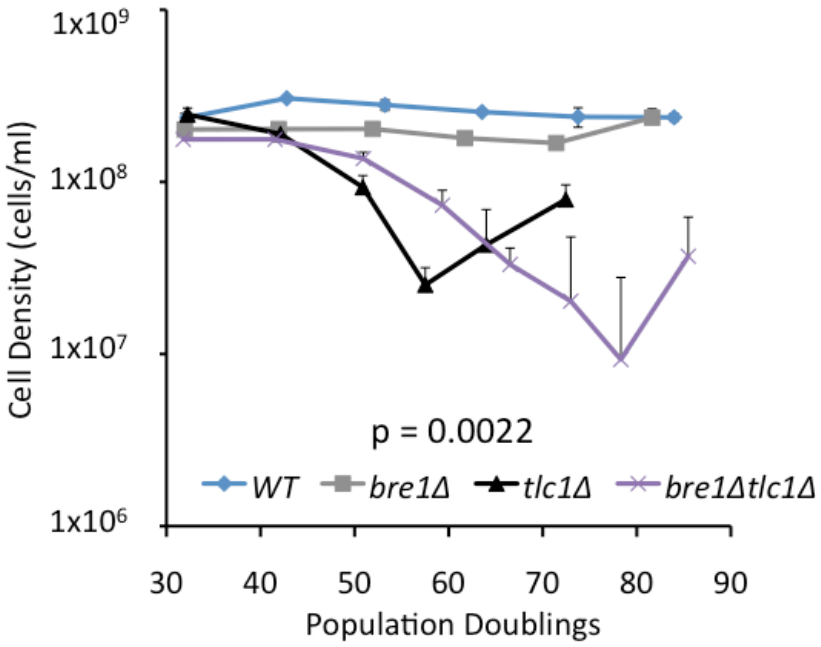
1x10⁹
1x10⁸
1x10⁷
1x10⁶
Cell Density (cells/ml)
p = 0.0022
WT
bre1Δ
tlc1Δ
bre1Δtlc1Δ
30
40
50
60
70
80
90
Population Doublings

B.

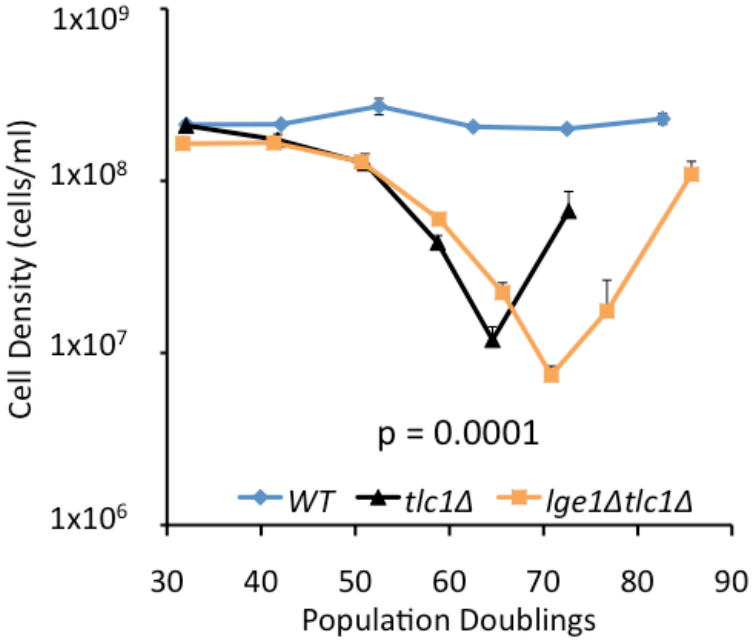
1x10⁹
1x10⁸
1x10⁷
1x10⁶
Cell Density (cells/ml)
p = 0.0001
WT
tlc1Δ
lge1Δtlc1Δ
30
40
50
60
70
80
90
Population Doublings

Figure 3-1. *BRE1/LGE1* the H2BK123 E3 ubiquitin ligase complex drives the rate of senescence.

(A) *BRE1* accelerates the pace of senescence. Senescence assay comparing wild-type (*n* = 2), *bre1Δ* (n = 2), *tlc1Δ* (*n* = 5), and *bre1Δtlc1Δ* cells (*n* = 5). *P* = 0.0022 for delayed senescence by deleting *BRE1*. (B) *LGE1* accelerates the pace of senescence. Senescence assay comparing wild-type (*n* = 2), *tlc1Δ* (*n* = 5), and *lge1Δtlc1Δ* cells (*n* = 5). *P* = 0.0001 for delayed senescence by deleting *LGE1*. P-values were calculated using a one-tailed student's t-test.

Figure 3-2

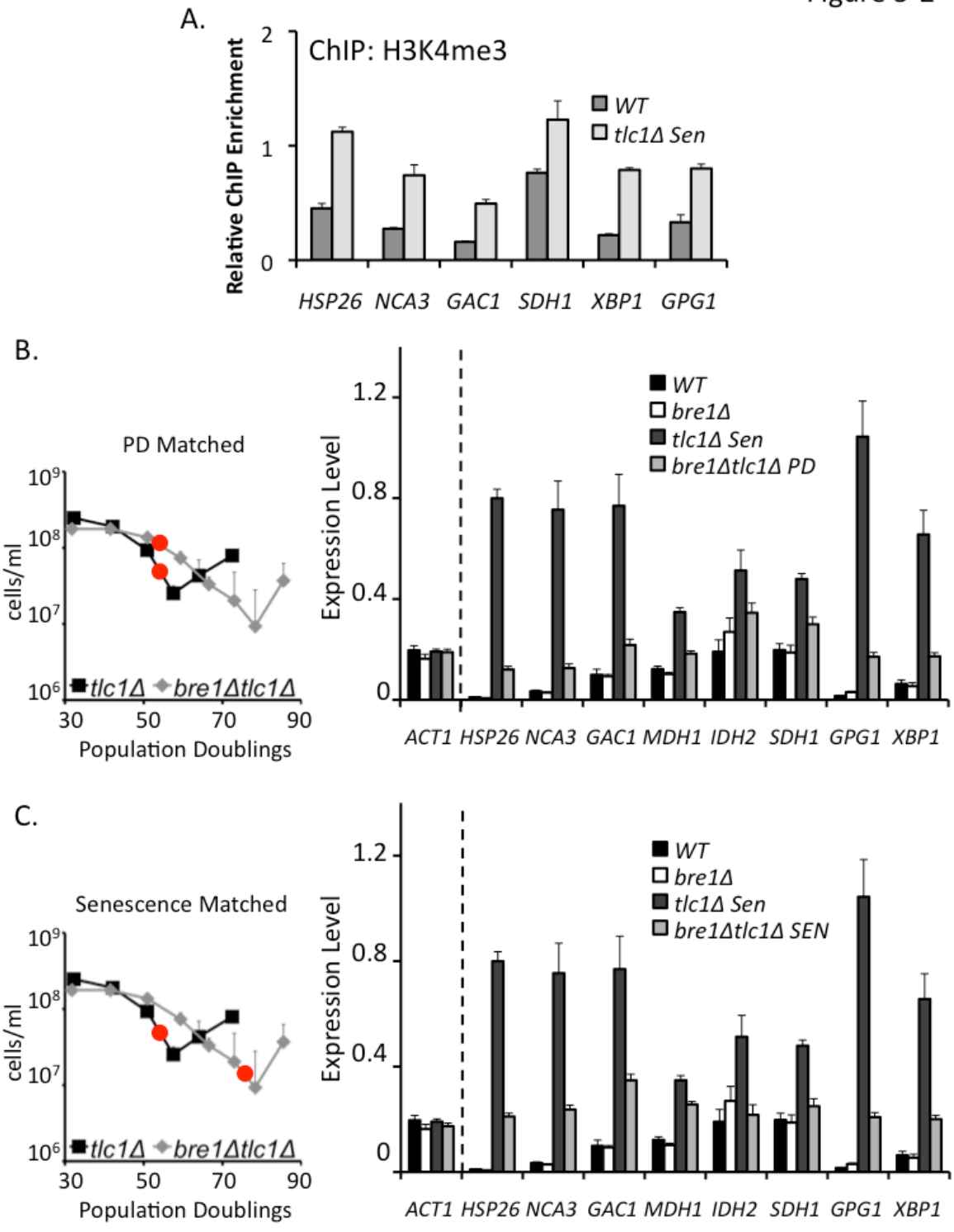
A.
ChIP: H3K4me3
Relative ChIP Enrichment
WT
tlc1Δ Sen
HSP26 NCA3 GAC1 SDH1 XBP1 GPG1
B.
PD Matched
cells/ml
tlc1Δ
bre1Δtlc1Δ
Population Doublings
Expression Level
WT
bre1Δ
tlc1Δ Sen
bre1Δtlc1Δ PD
ACT1 HSP26 NCA3 GAC1 MDH1 IDH2 SDH1 GPG1 XBP1
C.
Senescence Matched
cells/ml
tlc1Δ
bre1Δtlc1Δ
Population Doublings
Expression Level
WT
bre1Δ
tlc1Δ Sen
bre1Δtlc1Δ SEN
ACT1 HSP26 NCA3 GAC1 MDH1 IDH2 SDH1 GPG1 XBP1

Figure 3-2. BRE1 is necessary to activate NRTS at senescence.

(A) At senescence, the level of H3K4me3 goes up at the upstream promoter regions of activated NRTS genes. H3K4me3 ChIP enrichment is the ratio of the H3K4me3 level at each targeted locus compared with *MDP1* (a gene that is neither targeted by Rap1 nor differentially expressed at senescence), normalized to nonspecific IgG and input controls. All qPCR data are means (N = 3). (B-C) Activation of NRTS at senescence depend on *BRE1*. qPCR measurements of mRNA from wild-type (WT) (n = 2), *bre1Δ* (n = 2), senescent *tlc1Δ* (n = 4), senescent *bre1Δtlc1Δ* PD matched (n = 4) cultures (Figure 3-2B), and senescent *bre1Δtlc1Δ* senescence matched (n = 4) cultures (Figure 3-2C). Graphical representation of the distinction between PD and senescence matched samples; red dots correspond to approximately when the samples were harvested.

Figure 3-3

A.

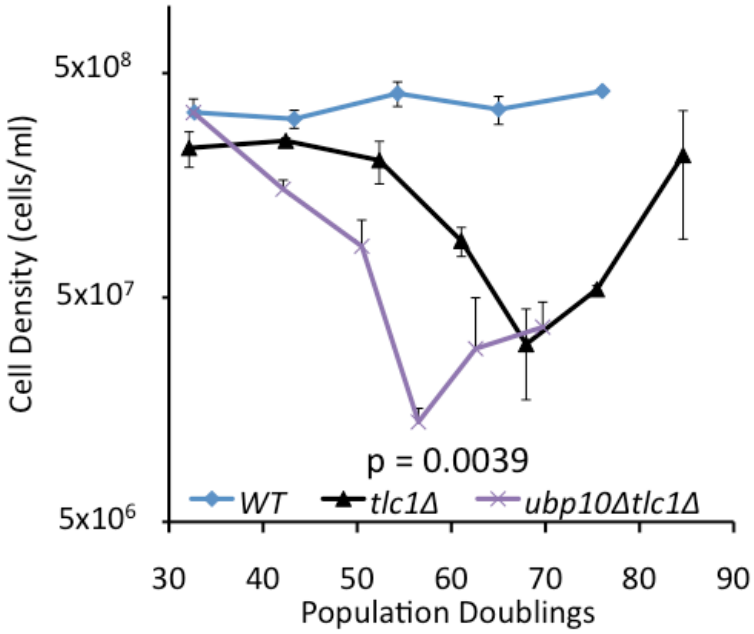
5x10^8
5x10^7
5x10^6
Cell Density (cells/ml)
p = 0.0039
WT
tlc1Δ
ubp10Δtlc1Δ
30
40
50
60
70
80
90
Population Doublings

B.

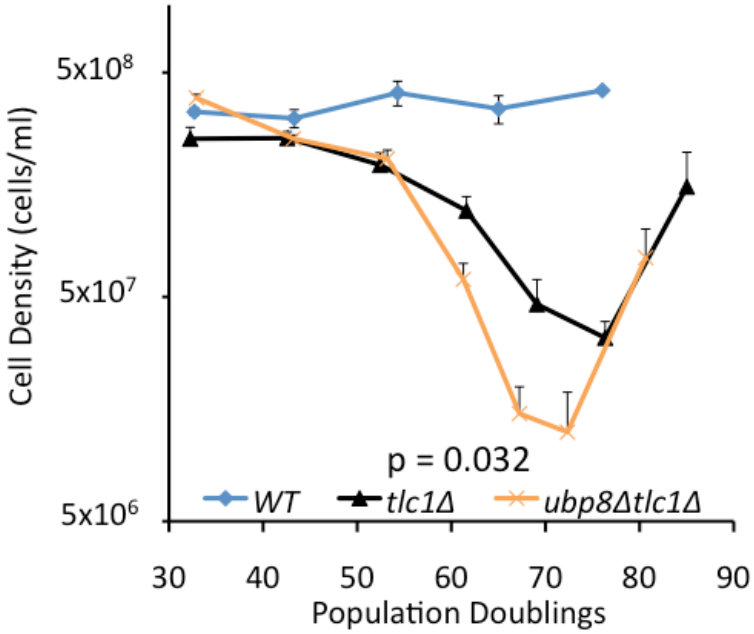
5x10^8
5x10^7
5x10^6
Cell Density (cells/ml)
p = 0.032
WT
tlc1Δ
ubp8Δtlc1Δ
30
40
50
60
70
80
90
Population Doublings

Figure 3-3. *UBP10* and *UBP8* H2BK123 deubiquitinases slow the rate of senescence.

(A) *UBP10* slows the pace of senescence. Senescence assay comparing wild-type (*n* = 2), *tlc1Δ* (*n* = 5), and *ubp10Δtlc1Δ* cells (*n* = 5). *P* = 0.0039 for accelerated senescence by deleting *UBP10*. (B) *UBP8* slows the pace of senescence. Senescence assay comparing wild-type (*n* = 2), *tlc1Δ* (*n* = 5), and *ubp8Δtlc1Δ* cells (*n* = 5). *P* = 0.032 for accelerated senescence by deleting *UBP8*. P-values were calculated using a one-tailed student's t-test.

Figure 3-4

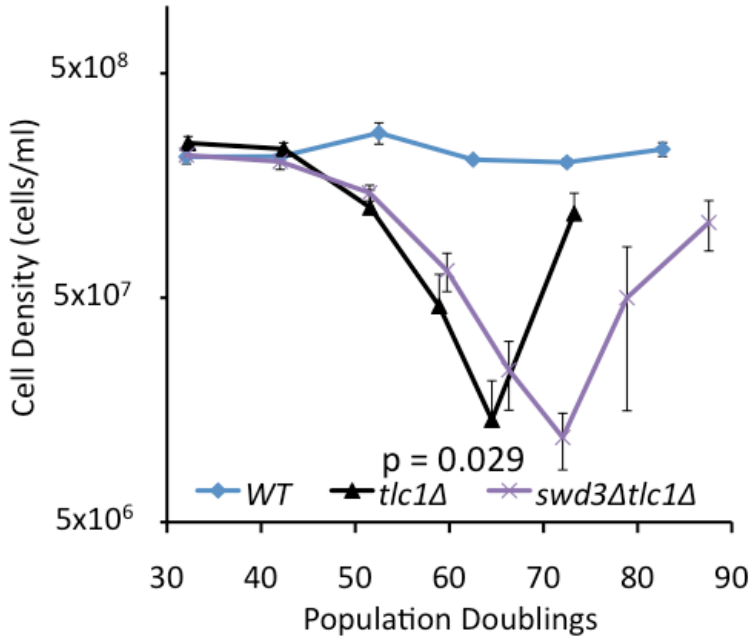
5x10^8
5x10^7
5x10^6
Cell Density (cells/ml)
p = 0.029
WT
tlc1Δ
swd3Δtlc1Δ
30
40
50
60
70
80
90
Population Doublings

Figure 3-4. *SWD3* an essential member of the COMPASS complex drives the rate of senescence.

Senescence assay comparing wild-type (*n* = 2), *swd3Δ* (n = 2), *tlc1Δ* (*n* = 5), and *swd3Δtlc1Δ* cells (*n* = 5). *P* = 0.029 for delayed senescence by deleting *SWD3*. P-value was calculated using a one-tailed student's t-test.

Supplemental Figure 3-1

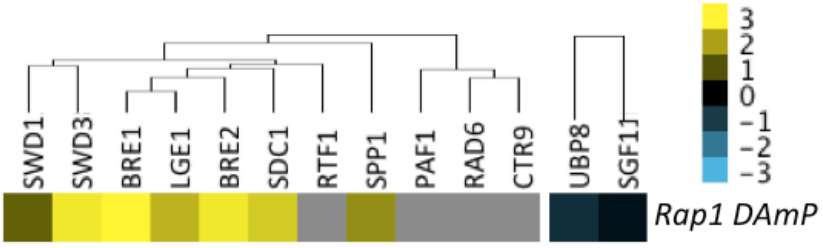

Supplemental Figure 3-1. Deleting *BRE1*, *LGE1*, or members of the downstream COMPASS complex give a growth advantage the hypomoric *rap1 DAmP* strain.

The figure is adapted from Collins et al. (Collins et al. 2007). These data were acquired from an SGA (synthetic genetic analysis) screen, which involves comparing the vegetative growth of single mutants to double mutants and then uses those data to calculate if there is a significant positive or negative genetic interaction between various mutants and alleles. Yellow and blue represent positive and negative genetic interactions respectively.

CHAPTER 4: Factors that affect the slower-mobility Rap1 species at senescence

Several slower-mobility Rap1 species appear at senescence (Chapter 2). It is possible that these reflect Rap1 post-translational modifications that might influence Rap1 activities at senescence. We wanted to better characterize these Rap1 species, and so we screened various factors that affect protein post-tranlsational modification. Because the senescence-associated Rap1 species are substantially heavier than full length Rap1 (some are 40kd and >100kd heavier than full-length Rap1) and they are fairly labile (Chapter 2), we considered that the Rap1 species might be modified by SUMOylation, ubiquitylation, or NEDDylation.

RESULTS and DISCUSSION

Slower-mobility Rap1 species present at senescence depend on *MEC1* but are phosphatase resistant

As discussed in Chapter 2, several slower-mobility Rap1 species are enriched and become quite prominent at senescence (Figure 4-1A). These species appear as four discrete bands of varying intensities that range in size from ~125kD to >200kD (Figure 4-1A,B) and are detected by three different Rap1 antibodies (santa cruz

antibodies yC-19, y-300, and yN-18; data not shown). Though they are efficiently extracted under denaturing TCA conditions, we do not see these Rap1 species when senescent cells are extracted using less harsh protocols (for example whole cell extracts (WCE), Chapter 2). Because other nuclear proteins are efficiently extracted with WCE, these findings suggest that the slower-mobility Rap1 species are fairly labile. Either the Rap1 species are being degraded or the post-translational modifications are being removed. It is also important to note that the level of tubulin per cell increases at senescence (Figure 4-1A). This is consistent with previous reports in the literature that cell size increases dramatically at senescence (Johnson et al. 2001; IJpma and Greider 2003; Matsui and Matsuura 2010).

In the course of studying Rap1 relocalization, we determined that *MEC1* is necessary to both remove Rap1 from subtelomeres and to activate NRTS at senescence (Chapter 2). *MEC1* is the *S. cerevisiae* homologue of human ATR and is also a checkpoint kinase that modulates the DNA damage response (Morrow et al. 1995). At senescence, *MEC1* is part of the pathway that senses dysfunctional telomeres as DNA double strand breaks and signals a cell cycle arrest (Abdallah et al. 2009; IJpma and Greider 2003; Enomoto et al. 2002).

While characterizing how *MEC1* and the DDR act on Rap1 at senescence, we noticed that the slower mobility Rap1 species depend *MEC1* (Figure 4-1B). Because *MEC1* affects the entire *RAP1* pathway at senescence (including Rap1 relocalization

and NRTS upregulation), these data further strengthen the connection between the slower-mobility Rap1 species and the Rap1-dependent changes at senescence. However, these findings do not establish a causal link. Another interesting aspect about these data is that they suggest that *MEC1* orchestrates post-translational modification of Rap1 at senescence, either directly or indirectly. There are three likely scenarios. First, it is possible that Mec1 directly phosphorylates Rap1 at senescence. Second, *MEC1* might have an indirect role in this process and instead act upstream, regulating the factors that post-translationally modify Rap1. Finally, to 'muddy the waters,' both scenarios might be true. Because there are several slower-mobility Rap1 species, *MEC1*'s role might be direct for some and indirect for others.

We were excited by the possibility that Mec1 might directly phosphorylate Rap1 at senescence. Rap1 is known to be phosphorylated in vivo (Smolka et al. 2007). As a result, we tested the possibility that the slower-mobility Rap1 species are phosphorylated forms of Rap1 by treating the neutralized extracts with increasing amounts of phosphatase (Figure 4-1C). The slower-mobility Rap1 species are phosphatase resistant, which suggests that the slow mobility species are not due to phosphorylation. This is consistent with work from Zhou and colleagues who show that when cells are treated with the DNA damaging agent methyl methanesulfonate (MMS) Mec1 does not directly phosphorylate Rap1 (Smolka et al. 2007; however it is important to note that this genome wide screen may not have

been that sensitive). Instead, our data suggest that *MEC1* indirectly regulates the post-translational modification of Rap1 at senescence.

To determine how Rap1 is modified at senescence and better characterize its slow-mobility species, we performed a targeted screen of enzymes that catalyze the addition of large post-translational modifications – including SUMO, ubiquitin, and NEDD.

SIZ1 and *SIZ2*

We considered the possibility that some of the slow-mobility Rap1 species present at senescence were Rap1 proteins that had been modified by SUMO (small ubiquitin-like modifier protein). There were several reasons we were interested in SUMO and compelled to test if the slow mobility Rap1 species were dependent on SUMOylation (the addition of SUMO to a target protein). On the surface, SUMO is a large protein modification (~11kD) and so poly-SUMOylation could account for the large shifts of Rap1. However, on a deeper biological level, SUMOylation is important in regulating the DNA damage response and the rate of senescence (Chavez et al. 2010; Jackson and Durocher 2013; Psakhye and Jentsch 2012). Furthermore the absolute levels of protein SUMOylation go up dramatically at senescence, which increase the likelihood that the slow-mobility Rap1 species are

SUMOylation products (Chavez et al. 2010). We were also intrigued by SUMO because Rap1 was previously shown to be SUMOylated under various stress conditions – including heat shock and DNA damage (Hang et al. 2011). Several years later, these SUMOlyated Rap1 species were shown to promote via NHEJ telomere fusions, which also go up dramatically at senescence (Lescasse et al. 2013; Hackett and Greider 2003). We were further intrigued by Rap1 SUMOylation because it is conserved throughout evolution (from yeast to humans). Human Rap1 (hRap1) is SUMOylated and contributes to telomere recombination and maintenance in ALT cells (alternative lengthening of telomeres) (Potts and Yu 2007). Although the functions of yeast and human SUMOylated Rap1 have diverged over evolutionary time, the conservation of this mark throughout evolution highlights its importance. Based on the importance of SUMOylation in regulating the DNA damage response and previous data on Rap1 SUMOylation, we tested if Rap1 was SUMOylated at senescence.

To test if Rap1 was SUMOylated at senescence we deleted *SIZ1* and *SIZ2*. *SIZ1* and *SIZ2* are SUMO E3 ligases that catalyze the final step in the process of adding SUMO to a target protein. There are several reasons why we chose to look at *SIZ1* and *SIZ2*. First, *SIZ1* and *SIZ2* catalyze the majority of protein SUMOylation in vegatatively growing cells (Chavez et al. 2010). Second, unlike the other major SUMO E3 ligase *MMS21*, neither gene slows the rate of senescence (*SIZ2* accelerates the rate of senescence, whereas *SIZ1* has no affect on the rate of senescence), which

is consistent with our hypothesis that the slow-mobility Rap1 species have acquired new functions and accelerate the rate of senescence (Chavez et al. 2010).

Whereas *SIZ1* does not affect Rap1 post-translational modification (Figure 4-2A), *SIZ2* is necessary for several (two of the four species, including the ~140kD and >200kD species) of the modified Rap1 species present at senescence (Figure 4-2B). On one hand, assuming that the slow mobility species drive the rate of senescence, our findings are consistent with the way *SIZ1* and *SIZ2* affect the pace of senescence (Chavez et al. 2010). However, on the other hand, the role of *SIZ1* and *SIZ2* appear to have swapped at senescence as compared to stationary yeast cells (Lescasse et al. 2013). Unlike our findings, Marcand and colleagues find that *SIZ1* – as compared to *SIZ2* – plays a more prominent role in poly-SUMOylating Rap1 in stationary yeast cells (Lescasse et al. 2013). The significance of these differences is not entirely clear and might simply represent a biological difference between stationary and senescent yeast.

Altogether, our data suggest that *SIZ2* orchestrates the post-translational modification of several slow-mobility Rap1 species present at senescence. However, we do not know how *SIZ2* post-translationally modifies Rap1 at senescence and what role it plays in this process. Similar to *MEC1*, one possibility is that *SIZ2* directly SUMOylates Rap1 at senescence. Alternatively, *SIZ2* might just be an upstream effector in a pathway that leads to Rap1 post-translational modification at

senescence. To get at this question, we tried immuno-precipitating (IP) Rap1 from cycling and senescent cultures. Although we were able to IP Rap1 in both conditions, we were unable to purify the slow-mobility Rap1 species (data not shown). Most likely the labile modifications were cleaved off once the samples were neutralized. To get around these problems, we will IP tagged Smt3 (*S. cerevisiae* SUMO) at senescence under denaturing conditions as previously described (using TCA and His tagged proteins), which will hopefully allow us to further characterize these species with mass-spectrometry (Lescasse et al. 2013).

Another interesting point is that the same Rap1 species that are dependent on *SIZ2* are also dependent on *MEC1* (Figure 4-1A, 4-2A, 4-3C). There are several interpretation of these findings: 1) Mec1 is upstream of Siz2, which directly SUMOylates Rap1; 2) Siz2 is upstream of Mec1 or 3) Mec1 and Siz2 are both upstream of another unknown factor that modifies Rap1 at senescence. Although epistasis experiments will be necessary to work out this pathway, we should first characterize these slow-mobility Rap1 species with IP-mass spec and determine their identities.

Thus far, our data suggests that Rap1 might be SUMOylated at senescence, however we do not know if these species actually affect the pace of senescence or they are just co-occurring biomarkers that are not functionally important. To address this question we focused on *ULS1* a SUMO-targeted ubiquitin ligase (STUbL)

whose only known target is Rap1. Uls1 is thought to ubiquitylate SUMOylated Rap1 and direct these species for degradation (Lescasse et al. 2013). Thus when *ULS1* is deleted poly-SUMOylated Rap1 species accumulate along with telomere fusions. When we deleted *ULS1* the cells rapidly senesced as compared to the wild-type controls ($p = 0.0129$; Figure 4-2C). These data suggest that *ULS1* slows the rate of senescence and are consistent with the idea that SUMOylated Rap1 species accelerate the pace of senescence. However, at the moment it is not clear how *ULS1* slows the pace of senescence and more work needs to be done to characterize its affects. On one hand, it is possible that the benefit of *ULS1* is completely though targeting SUMOylated Rap1 species for degradation. Alternatively, it all could be through Rap1-independent functions of *ULS1*. To get at these questions epistasis experiments with various *rap1* alleles – including *rap1 DAmP*, *rap1 Tet-off*, and *rap1-2R* (a Rap1 allele that reduces Rap1 poly-SUMOylation) – will help us determine if the benefit of *ULS1* at senescence is through Rap1 and its SUMOylation.

UBI4

We also wondered if some of the slow-mobility Rap1 species present at senescence were ubiquitylated (the addition of ubiquitin to a target protein) forms of Rap1. Our justification to test ubiquitination was similar to our rationale to test SUMOylation. That is, we were attracted to ubiquitination because the modification

is large (ubiquitin is a ~8.4kD protein) and important in regulating the DNA damage response (Jackson and Durocher 2013).

Ubiquitin is frequently linked to proteins via an isopeptide linkage between the carboxyl terminus of ubiquitin and the ε–amino group of the target lysine residue in the modified protein (Finley et al. 2012). Similar to higher eukaryotes, ubiquitylation in *S. cerevisiae* is carried out by an E1-E2-E3 enzymatic cascade, which involves one E1 enzymes (*UBA1*), eleven E2 enzymes, and 60-100 E3 enzymes (Finley et al. 2012). The complexity of the ubiquitin system does not stop there; 4 different genes encode for ubiquitin in yeast – *UBI1*, *UBI2*, *UBI3*, and *UBI4* (Ozkaynak et al. 1987). Interestingly, *UBI1, UBI2,* and *UBI3* encode for ribosomal protein-ubiquitin fusions (the alternative names of these genes are *RPL40A*, *RPL40B*, and *RPS31*) that are processed and ultimately cleaved apart (Finley et al. 1989). On the other hand, *UBI4* encodes five head-to-tail copies of ubiquitin that are processed into ubiquitin monomers (Ozkaynak et al. 1984; 1987; Finley et al. 1987). Under various stress conditions – including heat shock, starvation, and amino acid analogs – *UBI4* is upregulated and essential to respond to the stresses (Finley et al. 1987).

We tested the possibility that Rap1 was ubiquitylated at senescence by deleting *UBI4* and senescing the cells. One slow-mobility Rap1 species (~125kD) is dependent on *UBI4*, whereas another species is partially dependent (~140kD; Figure 4-3A). Once again, these data open a lot of questions about the role that

ubiquitylation plays in modifying Rap1 and how direct it is at senescence. On one hand, these Rap1 species might be ubiquitylated forms of Rap1, or alternatively ubiquitylation might simply regulate the Rap1 modification pathway at senescence. To get at this question, we should use Rap1 IP-mass spec, non-ubiquitylatable mutants of Rap1, and various alleles of *UBA1* to completely shut down/dampen ubiquitylation at senescence.

RUB1

We also considered the possibility that some Rap1 species at senescence were NEDDylated (the addition of NEDD8 to a target protein). In *S. cerevisiae*, the NEDD8 homologue is *RUB1*, which encodes for a ~9kD protein. Activated Rub1 is first conjugated to an E1 heterodimer (Ula1/Uba3), which then transfers it to an E2 enzyme (Ubc12), which in turn conjugates it to its target protein (Liakopoulos et al. 1998). We tested the possibility that Rap1 was NEDDylated at senescence by deleting *RUB1* and senescing the cells. However, it appears that none of the slower-mobility Rap1 species present at senescence depend on *RUB1* (Figure 4-3B), which suggests that none of these modified Rap1 species are NEDDylation products.

REFERENCES

Abdallah P, Luciano P, Runge KW, Lisby M, Géli V, Gilson E, Teixeira MT. 2009. A two-step model for senescence triggered by a single critically short telomere. *Nature Cell Biology* **11**: 988–993.

Chavez A, George V, Agrawal V, Johnson FB. 2010. Sumoylation and the structural maintenance of chromosomes (Smc) 5/6 complex slow senescence through recombination intermediate resolution. *J Biol Chem* **285**: 11922–11930.

Enomoto S, Glowczewski L, Berman J. 2002. MEC3, MEC1, and DDC2 are essential components of a telomere checkpoint pathway required for cell cycle arrest during senescence in Saccharomyces cerevisiae. *Mol Biol Cell* **13**: 2626–2638.

Finley D, Bartel B, Varshavsky A. 1989. The tails of ubiquitin precursors are ribosomal proteins whose fusion to ubiquitin facilitates ribosome biogenesis. *Nature* **338**: 394–401.

Finley D, Ozkaynak E, Varshavsky A. 1987. The yeast polyubiquitin gene is essential for resistance to high temperatures, starvation, and other stresses. *Cell* **48**: 1035–1046.

Finley D, Ulrich HD, Sommer T, Kaiser P. 2012. The ubiquitin-proteasome system of Saccharomyces cerevisiae. *Genetics* **192**: 319–360.

Hang LE, Liu X, Cheung I, Yang Y, Zhao X. 2011. SUMOylation regulates telomere length homeostasis by targeting Cdc13. *Nat Struct Mol Biol* **18**: 920–926.

IJpma AS, Greider CW. 2003. Short telomeres induce a DNA damage response in Saccharomyces cerevisiae. *Mol Biol Cell* **14**: 987–1001.

Jackson SP, Durocher D. 2013. Regulation of DNA damage responses by ubiquitin and SUMO. *Mol Cell* **49**: 795–807.

Johnson FB, Marciniak RA, McVey M, Stewart SA, Hahn WC, Guarente L. 2001. The Saccharomyces cerevisiae WRN homolog Sgs1p participates in telomere maintenance in cells lacking telomerase. *EMBO J* **20**: 905–913.

Lescasse R, Pobiega S, Callebaut I, Marcand S. 2013. End-joining inhibition at telomeres requires the translocase and polySUMO-dependent ubiquitin ligase Uls1. *EMBO J* **32**: 805–815.

Liakopoulos D, Doenges G, Matuschewski K, Jentsch S. 1998. A novel protein modification pathway related to the ubiquitin system. *EMBO J* **17**: 2208–2214.

Matsui A, Matsuura A. 2010. Cell size regulation during telomere-directed senescence in Saccharomyces cerevisiae. *Biosci Biotechnol Biochem* **74**: 195–198.

Morrow DM, Tagle DA, Shiloh Y, Collins FS, Hieter P. 1995. TEL1, an S. cerevisiae

homolog of the human gene mutated in ataxia telangiectasia, is functionally related to the yeast checkpoint gene MEC1. *Cell* **82**: 831–840.

Ozkaynak E, Finley D, Solomon MJ, Varshavsky A. 1987. The yeast ubiquitin genes: a family of natural gene fusions. *EMBO J* **6**: 1429–1439.

Ozkaynak E, Finley D, Varshavsky A. 1984. The yeast ubiquitin gene: head-to-tail repeats encoding a polyubiquitin precursor protein. *Nature* **312**: 663–666.

Potts PR, Yu H. 2007. The SMC5/6 complex maintains telomere length in ALT cancer cells through SUMOylation of telomere-binding proteins. *Nat Struct Mol Biol* **14**: 581–590.

Psakhye I, Jentsch S. 2012. Protein group modification and synergy in the SUMO pathway as exemplified in DNA repair. *Cell* **151**: 807–820.

Smolka MB, Albuquerque CP, Chen S-H, Zhou H. 2007. Proteome-wide identification of in vivo targets of DNA damage checkpoint kinases. *Proc Natl Acad Sci USA* **104**: 10364–10369.

MATERIALS and METHODS

Senescence assays

Senescence assays were performed in YPAD using fresh spore products from dissection plates. All comparisons between different genotypes were performed using spore products obtained from the same *TLC1/tlc1Δ* diploid possessing any other heterozygous genetic changes of interest (e.g. *SIZ2/siz2Δ*) to ensure that the haploid cells being compared had inherited telomeres of similar length and from the same epigenetic environment. For liquid senescence assays, cells were grown in liquid starting approximately 25 PD after loss of telomerase. Spore products (N=4 per genotype unless otherwise specified) were passaged serially in fresh liquid media. 10^6 cells were inoculated into 5 mL of media, were grown for 22 hours, counted using a Coulter counter and then re-inoculated at 10^6 cells/5 ml media. Cell counts were used to determine elapsed PDs (PD = $\log_2$(final/starting concentration)). P-values for differences between rates of senescence were calculated using the PD at the nadir of the curves for individual cultures and using a Student's t-test. For restreak senescence assays, cells were streaked out for single colonies on YPAD plates starting from spore products (N=3 per genotype unless otherwise specified). All the relevant genotypes (e.g. *WT*, *siz2Δ*, *tlc1Δ*, *siz2Δtlc1Δ*) were streaked on the same plate. Cells were allowed to grow for 2 days, imaged on a scanner, and then multiple single colonies (at least 5 of the averaged sized colonies

– i.e. neither the largest nor the smallest) from an individual genotype were restreaked onto another YPAD plate.

Samples for immunoblotting of senescent cells were obtained ~5 PDs prior to the nadir (for liquid senescence assays) and close to the nadir (for restreak senescence assays) to avoid contributions from survivors of senescence, and cells were harvested under optimal growth conditions (i.e. at < 2 x 10^7 cells/ml after between 12-16 hours of growth in fresh medium after an initial inoculation at ≤ 2 x 10^6 cells/ml, while carefully following their growth and doubling times). For restreak assays, in order to get enough cells for the initial inoculation, as many cells as possible from each genotype were inoculated overnight in 5mL of YPAD from the second to last restreak plate.

Cell extract preparation and immunoblotting

Cells were counted using a Coulter counter, harvested during exponential growth by centrifugation and pellets containing ~ 1-2x10^8 cells were frozen in liquid N_2 and then stored at -80˚C. Cell pellets were resuspended in 200 µl of 20% TCA along with 400 µl acid-washed glass beads (soda lime; BioSpec), disrupted with a mini–beadbeater for 3 x 90 sec at 4°C, and extracts were centrifuged at 14,000 rpm for 10 min. Pellets were resuspended in 100 µl Laemmli buffer and ~50 µl 2 M

Tris base to neutralize pH. Samples were recentrifuged at 14,000 rpm for 10 min, boiled, and loaded by equal cell number.

Extracts were run on 4–12% Bis-Tris gels (NuPAGE, Invitrogen) and transferred to nitrocellulose membranes. Membranes were blotted with anti-Rap1 antibody (Y-300, Santa Cruz), anti-tubulin antibody (ab6160, Abcam). Membranes were blocked with TBS-T (0.1% Tween-20) with 5% milk and all wash steps were performed with TBS–T.

Figure 4-1

A.

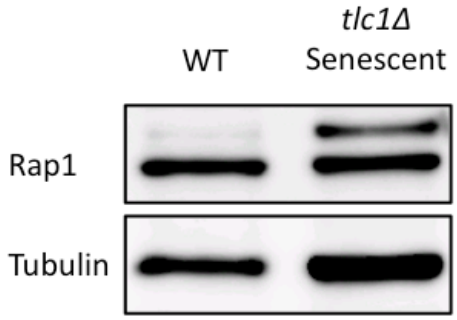

B.

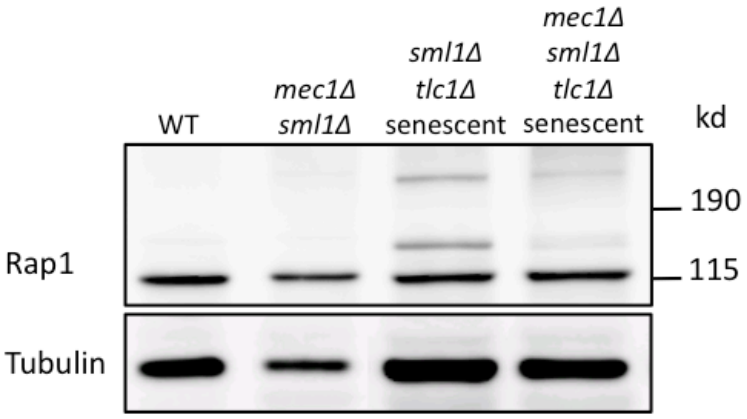

C.

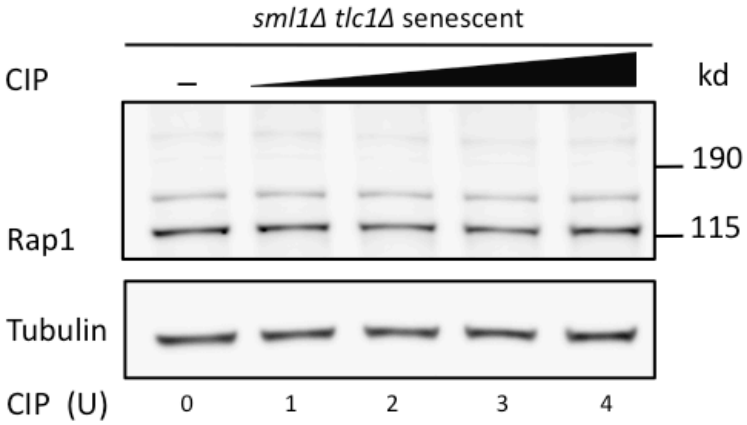

Figure 4-1. Slower-mobility species of Rap1 present at senescence depend on MEC1.

(A) The levels of several slower-mobility Rap1 species go up at senescence. (B) Senescence-associated slower-mobility Rap1 species depend on *MEC1*. (C) The slower-mobility Rap1 species present at senescence are phosphatase resistant. Immunoblots of TCA extracts, loaded by equal cell number and stained with anti-Rap1 or anti-tubulin antibodies. For phosphatase treatment, TCA extracts were neutralized and then incubated with increasing amount of calf intestinal phosphatase (*CIP*). For all experiments, senescent cultures were harvested five PDs prior to the growth nadir, which for sml1Δ tlc1Δ was ~70 PDs and for mec1Δ sml1Δ tlc1Δ was ~80 PDs.

Figure 4-2

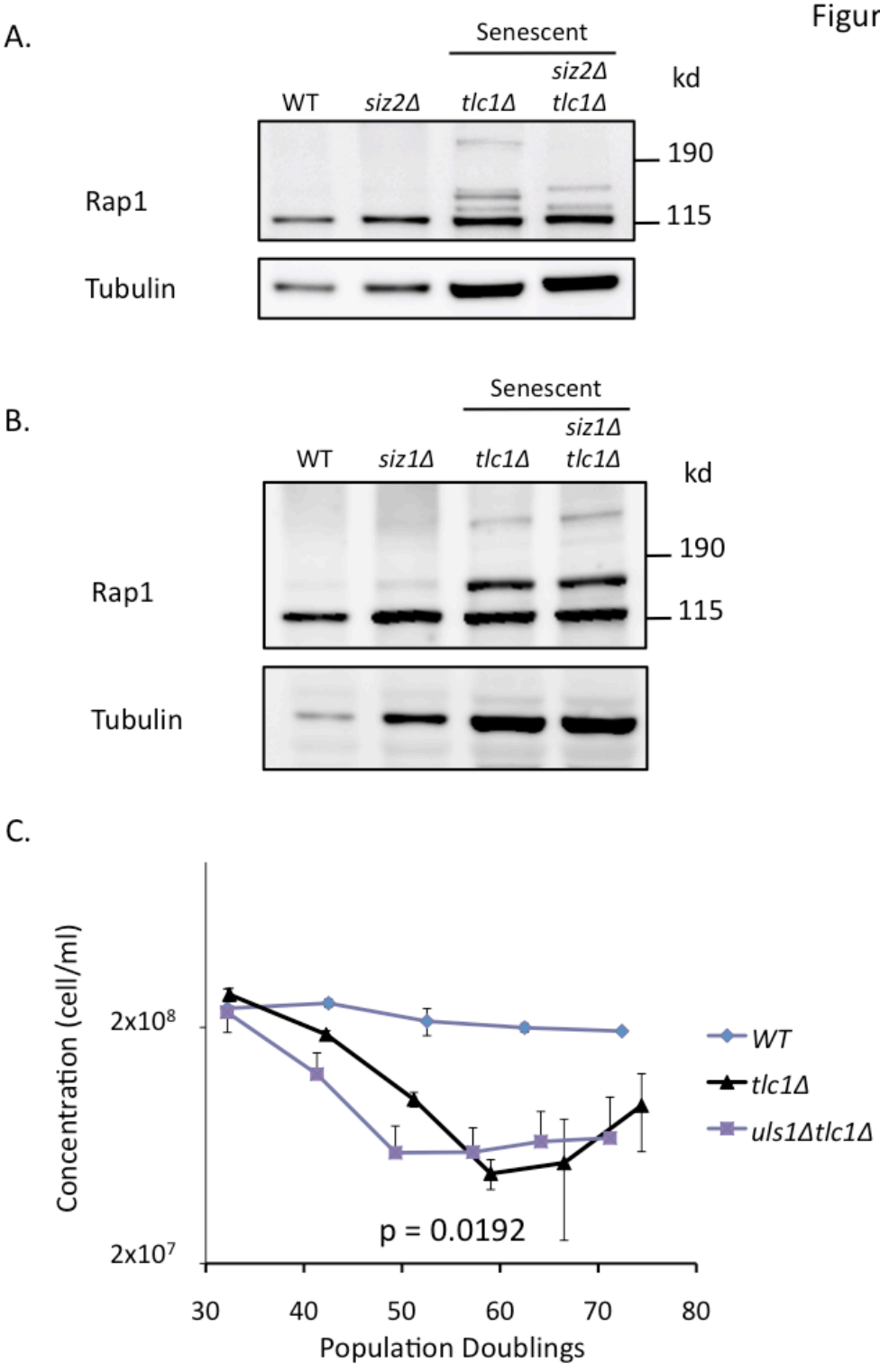
A.
Senescent
WT
siz2Δ
tlc1Δ
siz2Δ tlc1Δ
kd
190
115
Rap1
Tubulin
B.
Senescent
WT
siz1Δ
tlc1Δ
siz1Δ tlc1Δ
kd
190
115
Rap1
Tubulin
C.
Concentration (cell/ml)
2x10^8
2x10^7
p = 0.0192
30
40
50
60
70
80
Population Doublings
WT
tlc1Δ
uls1Δtlc1Δ

Figure 4-2. Slower-mobility species of Rap1 present at senescence depend on (A) *SIZ2* but not (B) *SIZ1*.

Immunoblots of TCA extracts, loaded by equal cell number and stained with anti-Rap1 or anti-tubulin antibodies. For all experiments, cells were senesced by restreaking and senescent cultures were harvested close to the growth nadir. (C) *ULS1* slows the rate of senescence. Senescence assay comparing wild-type (n = 2), *tlc1Δ* (n = 5), and *uls1Δtlc1Δ* cells (n = 5). P = 0.0192 for accelerated senescence by deleting *ULS1*. P-value was calculated using a one-tailed student's t-test.

Figure 4-3

A.

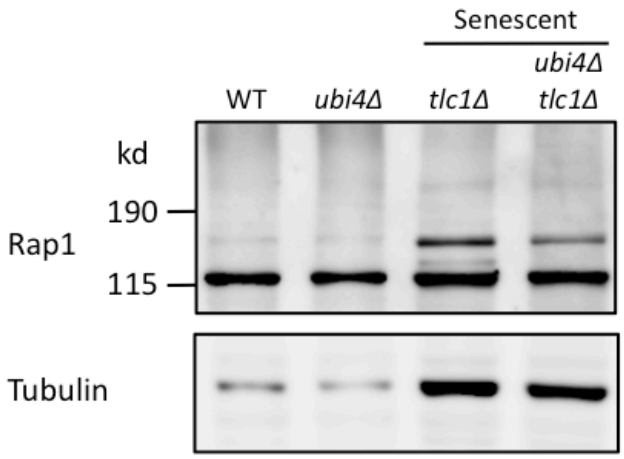

B.

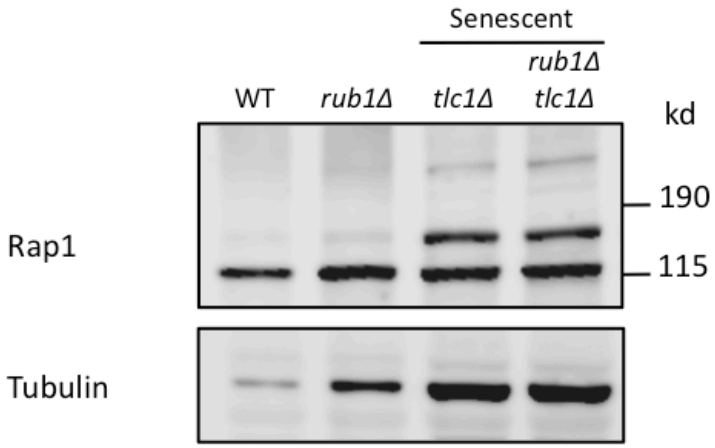

C.

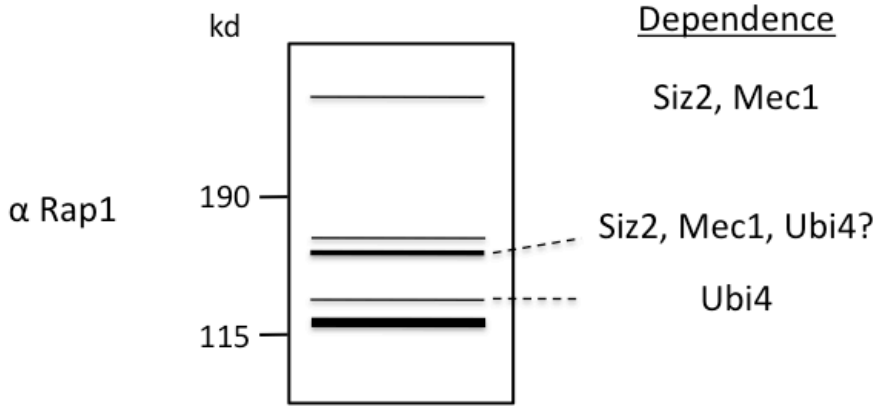

Figure 4-3. Some Slower-mobility species of Rap1 present at senescence depend on (A) *UBI4* but not (B) *RUB1*.

Immunoblots of TCA extracts, loaded by equal cell number and stained with anti-Rap1 or anti-tubulin antibodies. For all experiments, cells were senesced by restreaking and senescent cultures were harvested close to the growth nadir. (C) Summary of the screen. This picture shows how the different slower-mobility Rap1 species depend on various factors at senescence.

CHAPTER 5: N-terminal residues of Rap1 are important to bind G-quadruplex DNA

INTRODUCTION

In addition to binding duplex DNA, Rap1 binds G-quadruplex DNA (G4DNA) with high affinity (Kd ~10^{-8}M) (Giraldo and Rhodes 1994; Giraldo et al. 1994). G4DNAs are a family of DNA secondary structures that certain guanine (G) rich sequences adopt by stacking sets of planar G-tetrads (Burge et al. 2006; Lane et al. 2008). Most telomere sequences, including yeast and human telomeres, are capable of forming G4DNA – i.e. they have high G4DNA forming potential (QFP). In fact, they form *in vitro* at physiologic conditions and exist *in vivo* at telomeres of the protist *S. lemnae* and yeast *S. cerevisiae* (Venczel and Sen 1993; Parkinson et al. 2002; Schaffitzel et al. 2001; Paeschke et al. 2005; Zhang et al. 2010). These secondary structures are stabilized by Hoogsteen-hydrogen bonding, π-π interactions, and a central monovalent cation – such as Na^+ or K^+ (Williamson et al. 1989; Sundquist and Klug 1989). The diverse family of G4DNAs can either be intramolecular (within one DNA strand) or intermolecular (between several DNA strands): including bi-, tri-, and tetra-molecular quadruplexes (Neidle and Parkinson 2008). Stable intramolecular G4DNAs require four runs of at least two G's that are each separated by 1-7 nucleotides – the "spacer" (though spacers of more than 25 nt have been

observed). Stability increases with longer runs of G's and shorter spacers (Risitano and Fox 2004; 2003).

In yeast, Rap1 has many functions, including telomere capping, telomere length maintenance, and transcriptional activation/repression. In addition to its many functions and binding duplex DNA, Rap1 also binds G-quadruplex DNA. We wondered what is the biological role of Rap1's G4DNA-binding activity and how does it affect Rap1 function? To address this question, we wanted to map Rap1's G4DNA binding domain so that we could study the activities of mutant Rap1 proteins that selectively lack G4DNA binding activity. Previous work from Giraldo and Rhodes had showed that full length Rap1 binds G4DNA whereas its minimal duplex DNA binding domain (DBD) cannot, which suggests that Rap1 uses residues outside of its DBD to bind G4DNA (Giraldo and Rhodes 1994). As a result, we characterized how the N- and C-termini of Rap1 affect G4DNA binding.

RESULTS and DISCUSSION

The N-terminal residues of Rap1 are important to bind G-quadruplex DNA

Previous work suggests that Rap1 stabilizes and binds G-quadruplex DNA (Giraldo et al. 1994; Giraldo and Rhodes 1994). We used the same oligonucleotides that were used by Giraldo and Rhodes, including the duplex *dDNA* probe that

contains two strong Rap1 binding sties and the single stranded *G4DNA* probe (that was previously called 4G3; Figure 5-1A), which readily adopts a G-quadruplex conformation (Giraldo et al. 1994; Giraldo and Rhodes 1994; Lieb et al. 2001).

Similar to previous reports, we find that Rap1 forms a slow-mobility complex with both probes, which suggests that Rap1 binds both the duplex *dDNA* and single stranded *G4DNA* probes (Figure 5-1B). Furthermore, we also find that Rap1 only binds the *G4DNA* probe in its G-quadruplex conformation, which is consistent with work from Giraldo and Rhodes (Giraldo and Rhodes 1994). Specifically, we find that methylating the *G4DNA* oligonucleotide with dimethyl sulfide – which preferentially methylates nitrogen-7, destabilizes Hoogsteen base pairing, and thus disrupts G-quadruplexes – prevents Rap1 binding (data not shown) (Giraldo and Rhodes 1994; Williamson et al. 1989).

Whereas full-length Rap1 binds both duplex and G-quadruplex DNA, its minimal duplex DNA binding domain (DBD) preferentially interacts with duplex DNA (Giraldo and Rhodes 1994). Because the Rap1 DNA binding domain is not sufficient to bind G-quadruplex DNA, these data suggest that other residues of the protein are necessary to interact with G-quadruplexes. To map which residues outside of the DNA binding domain of Rap1 are important for G-quadruplex binding, we deleted various regions of Rap1 (including the N-terminus and C-terminus) and assessed their ability to bind G-quadruplex DNA.

First, to control that the recombinant proteins were well folded and functional, we determined if the Rap1 constructs can bind duplex DNA (*dDNA* probe; Figure 5-1C). As expected, all the Rap1 constructs (full-length (*FL*) 1-827AA, Rap1-ΔN (*ΔN*) 1,353-827AA, Rap1-ΔC (*ΔC*) 1-598AA, and Rap1-DBD (*DBD*) 1,353-598AA – all of which contain the Rap1 DBD) form a slow-mobility complex with the *dDNA* probe and thus bind duplex DNA, which suggests that they all are well folded and functional.

We then assessed if the Rap1 constructs can bind G-quadruplex DNA (Figure 5-1C). As expected, full-length Rap1 binds the *G4DNA* probe, whereas in the setting of the Rap1 DNA binding domain (DBD) this interaction is *largely* lost (reduced fourfold, quantified with ImageJ). Surprisingly, though this interaction is abrogated for the most part, a faint slow-mobility band is apparent in the presence of the Rap1 DBD, which suggests that the Rap1 DBD forms a weak complex with the *G4DNA* probe. Though in later experiments this pattern is lost (including the slow-mobility band and probe retardation; Figure 5-2A,B), the Rap1 DBD construct also has reduced activity toward duplex DNA (it binds the dDNA probe less well; Figure 5-2A), which suggests that it is less functional. Most likely this reduction in Rap1 DBD activity is due to the effects of freezing and thawing. Ultimately, the question comes up: why does the Rap1 DBD construct *slightly* interact with the *G4DNA* probe, which is different from what Giraldo and Rhodes found (they found that the Rap1 DBD:G4DNA is not stable in an EMSA, but the construct does stimulate parallel

G4DNA formation in solution)? One possibility is that this is because we used slightly different constructs. Whereas Giraldo and Rhodes used an untagged Rap1 DBD, we purified a poly-histidine tagged Rap1 DBD construct. These extra residues that were added to the N-terminus of the Rap1 DBD might account for the difference in binding activity of our constructs. The other possibility is that this difference in G-quadruplex binding is due to the differences in our purification schemes. Whereas our Rap1 DBD construct was well folded following nickel column purification, Giraldo and Rhodes had to refold theirs from inclusion bodies (Giraldo and Rhodes 1994). To address this question we can purify various Rap1 DBD constructs (i.e. without a tag or with a different tag) and assess their ability to bind G-quadruplex DNA.

We next mapped which region of Rap1 outside of its DBD (i.e. the N- or C-terminus) is important for G-quadruplex binding. We find that the Rap1 ΔC construct (that lacks its C-terminus) behaves like full-length Rap1 and tightly binds the *G4DNA* probe, which suggests that the C-terminus of Rap1 is truly expendable and not necessary to bind G-quadruplex DNA (Figure 5-1C). The C-terminus of Rap1 contains most of its functional domains (including its toxicity, silencing, activation, and Rap1 C-terminus (RCT) domains; Figure 5-1C) and is necessary for viability (Graham et al. 1999). On the other hand, the Rap1 ΔN construct (that lacks its N-terminus) behaves like the Rap1 DBD and its interaction with the *G4DNA* oligonucleotide is reduced twofold (quantified with ImageJ; Figure 5-1C). Though

the effect of the Rap1 ΔN construct is in line with the Rap1 DBD, it interacts with the *G4DNA* probe more tightly than the Rap1 DBD. In the presence of Rap1 ΔN there is a prominent slow-mobility band, which suggests that Rap1 ΔN forms a complex with the *G4DNA* probe. However, 73.8% of the probe either is either completely unshifted or partially shifted, which indicates that the Rap1 ΔN:*G4DNA* complex is weak and falls apart while running the gel. Altogether our data demonstrate that the Rap1 ΔN construct has a twofold reduced affinity toward G-quadruplex DNA and suggest that the N-terminus of Rap1 contains residues that are important for G-quadruplex binding.

We wanted to further map which residues of Rap1 outside of its DNA binding domain are important for G-quadruplex binding. Though the N-terminus of Rap1 (1-352AA) contains residues that are important for G-quadruplex binding, Rap1 ΔN still binds G-quadruplexs with a reduced affinity. When designing our Rap1 ΔN construct, we used Giraldo and Rhodes definition of the Rap1 N-terminus (1-352AA) that was itself based on work from Gasser and colleagues (Giraldo and Rhodes 1994; Gilson et al. 1993). However, previous work shows that the minimal DNA binding domain of Rap1 is 361-596AA (Henry et al. 1990), which is slightly smaller than Giraldo and Rhodes' definition of the DBD. This suggest that the eight N-terminal residues of the DBD (353-360AA - that have theoretical pI of 8.76) can be removed and not affect duplex DNA binding. We further truncated the Rap1 ΔN construct, making Rap1 ΔN^{short} (1-361-827AA). Though Rap1 ΔN^{short} is functional and binds

the duplex *dDNA* probe, it behaves like Rap1 DBD (see Figure 5-1C[1]) and its interaction with the G-quadruplex *G4DNA* oligonucleotide is reduced threefold (quantified with ImageJ; Figure 5-2A,B). Some G4DNA probe is partially retarded, which suggests (as previously discussed) that Rap1 ΔN^{short} *weakly* binds G4DNA and the complex falls apart while running the gel. Altogether, our data indicate that residues 353-360 of Rap1 are quite important for G-quadruplex binding.

The Rap1 N-terminus weakly binds G-quadruplex DNA without its central DNA binding domain (DBD)

Based on our finding that the N-terminus of Rap1 (1-352AA and especially 1-360AA) is necessary to bind G-quadruplexes, we wondered if the N-terminus of Rap1 binds G-quadruplex DNA by itself (i.e. without its DNA binding domain). We made a minimal N-terminal Rap1 Construct (Rap1 N-term; 1-352AA) and as expected it does not bind the duplex *dDNA* probe (Figure 5-2A). However, Rap1 N-term weakly interacts with the G-quadruplex *G4DNA* probe and forms two faint slow-mobility complexes. This suggests that a Rap1 N-terminal fragment is sufficient to *weakly* bind G-quadruplex DNA (only shifting 3% of the signal,

[1] As previously mentioned, Rap1 DBD is less functional in Figure 5-2A,B as compared to Figure 5-1C (some fraction has reduced affinity or is unable to bind to the *dDNA* probe). This is potentially due to freezing and thawing.

quanitified with ImageJ), though it does not completely recapitulate the interaction seen with full-length Rap1.

This finding is quite interesting and raises several questions. First, can we improve the ability of Rap1 N-term to bind to G-quadruplex DNA? Because our data suggests that residues 353-360AA are important for G-quadruplex binding, it might be interesting to make a modified Rap1-N-term (slightly extending it eight residues – i.e. make 1-360AA) and test its ability to bind G-quadruplex DNA. It is also likely that some Rap1 DBD residues are more critical for G-quadruplex binding in the context of a minimal N-terminal Rap1 fragment. For example, we could fuse various Rap1 DBD domains to Rap1 N-term (with or without a flexible linker) and test their ability to bind G-quadruplex DNA. Another question that comes up is: which portion of the Rap1 N-terminus is important for G-quadruplex binding? Over the years, the Rap1 N-terminus has been ascribed very few functions and only contains two domains: a DNA bending domain (44-274AA) and within that domain a BRCA1 C-terminal domain (BRCT domain, 125-209AA) (Gilson et al. 1993; Callebaut and Mornon 1997). Though the N-terminus of Rap1 is predicted to have a relatively low pI of 4.19, the BRCT domain has a bit higher predicted pI of 5.52 and its crystal structure shows several patches of positive charge. Assuming that these patches of positive charge are surface exposed in full length Rap1, we should selectively mutate these residues (potentially in conjunction with residues 353-360) and determine how they affect G-quadruplex binding.

The Rap1 N-terminus promotes the appearance of a faster-mobility G-quadruplex species

While characterizing how Rap1 binds G-quadruplex DNA, we noticed that full-length Rap1 forms a faster-mobility DNA species specifically in the presence of the *G4DNA* probe (Figures 5-1C, 5-2A,B). We did not know what this species was. On one hand, it could be just the result of a co-purifying nuclease. This seems unlikely; not only would we expect more smearing and signal loss, but also we performed our binding reactions in the presence of a high concentrations of EDTA (1mM), which prevents DNase activity. On the other hand, it could be a faster-mobility, alternate conformation of the *G4DNA* probe.

We mapped which residues of Rap1 are required for its formation. Whereas Rap1 ΔC behaves like full-length Rap1 and stabilizes this faster-mobility *G4DNA* conformation, increasing amounts of the Rap1 DBD and Rap1 ΔN have no affect and do not form this DNA species (Figure 5-3, arrowheads). Furthermore, the N-terminus or Rap1 (1-352AA) by itself is sufficient to form this faster-mobility *G4DNA* species (Figure 5-2B, arrowhead). Altogether, these data suggest that the N-terminus of Rap1 is both necessary and sufficient to form this faster-mobility species of *G4DNA*.

Though we know that the N-terminus of Rap1 is important to form this faster-mobility *G4DNA* conformation, we need to further characterize this species and how it affects Rap1 G-quadruplex binding. We should purify this species, analyze it with circular dichroism (CD) spectroscopy, and determine how annealing affects its mobility on a native PAGE gel. In addition, we need to determine the role that this species plays in the Rap1 G-quadruplex binding reaction. On one hand, because Rap1 is known to promote G-quadruplex formation (Giraldo and Rhodes 1994; Giraldo et al. 1994), this species might be an intermediate (depicted as *G4DNA*$^{\perp}$) in the Rap1 *G4DNA* binding reaction (see below).

$$Rap1 + G4DNA \xleftrightarrow{1} Rap1 + G4DNA^{\perp} \xleftrightarrow{2} Rap1 : G4DNA^{\perp}$$

If this model were true, one prediction is that reaction 1 is much faster than reaction 2, thus creating a 'bottleneck' and allowing us to observe the intermediate *G4DNA*$^{\perp}$. We can test this hypothesis by performing kinetic studies with full-length Rap1 and determining the rate of appearance of the faster-mobility *G4DNA* species and the Rap1:*G4DNA* complex. On the other hand, this species (*G4DNA*$^{\perp}$) might be a byproduct of a 'side' reaction of Rap1 (i.e. reaction 1; see below) and is actually 'un-shiftable' in regards to reaction 2 (see below).

$$Rap1 + G4DNA^{\perp} \xleftarrow{1} Rap1 + G4DNA \xrightarrow{2} Rap1 : G4DNA$$

We should purify the faster-mobility *G4DNA* species and determine if Rap1 can bind it via an EMSA.

The N-terminal residues of Rap1 are important to bind RNA with high G-quadruplex forming potential (QFP)

Though Rap1 is well characterized to be a duplex and G-quadruplex DNA binding protein, little is know about its ability to bind RNA. Recently, Rap1 was shown to affect the stability of mRNA transcripts that happened to have high G-quadruplex forming potential (QFP) (Bregman et al. 2011) and we wondered if Rap1 might bind RNA G-quadruplexes. We assessed the ability of full-length Rap1 to bind an RNA oligonucleotide that has high QFP, *TERRA*, via EMSA. Surprisingly, full-length Rap1 forms two slow-mobility complexes (that might represent a monomeric and dimeric complex), which suggests that Rap1 readily binds the *TERRA* probe (Figure 5-4). This is the first time someone has observed that Rap1 binds an RNA species.

To further characterize how Rap1 binds RNA G-quadruplexes, we mapped which residues of Rap1 are required to complex with the *TERRA* oligonucleotide. Though each of the Rap1 constructs bind duplex DNA (which suggests that they are functional proteins), only Rap1 ΔC binds the *TERRA* oligonuleotide (Figure 5-4). On the other hand, the affinity of Rap1 ΔN and Rap1 DBD to *TERRA* is dramatically

reduced (onefold and twofold respectively, quantified with ImageJ); Rap1 ΔN partially binds the probe, whereas Rap1 DBD has *almost* completely lost the ability to interact with *TERRA* (the weak complex likely falls apart while running the gel). These data suggest that the N-terminus of Rap1 contains residues that are important to bind both DNA and RNA G-quadruplexes.

Our observations are very exciting and many questions remain to be address. For example: 1. How specific is this interaction? 2. What RNA species does Rap1 prefer to bind *in vitro* and *in vivo*? 3. Which specific residues of Rap1 are important for RNA binding?

Future Directions

In order to understand the biological role of Rap1's G4DNA-binding activity and how it affects Rap1 function we will need to finely map which residues of Rap1's N-terminus are most important for G-quadruplex binding. To do so, we will use phage display to engineer a Rap construct that cannot bind G-quadruplexes but still binds duplex DNA. We will use these alleles in a battery of experiments to understand the role of Rap1's G-quadruplex binding activity – in particular telomere capping, telomere length maintenance, the rate of senescence, and transcriptional activation/repression.

REFERENCES

Arnoult N, Shin-Ya K, Londoño-Vallejo JA. 2008. Studying telomere replication by Q-CO-FISH: the effect of telomestatin, a potent G-quadruplex ligand. *Cytogenet Genome Res* **122**: 229–236.

Bregman A, Avraham-Kelbert M, Barkai O, Duek L, Guterman A, Choder M. 2011. Promoter Elements Regulate Cytoplasmic mRNA Decay. *Cell* **147**: 1473–1483.

Burge S, Parkinson GN, Hazel P, Todd AK, Neidle S. 2006. Quadruplex DNA: sequence, topology and structure. *Nucleic Acids Res* **34**: 5402–5415.

Callebaut I, Mornon JP. 1997. From BRCA1 to RAP1: a widespread BRCT module closely associated with DNA repair. *FEBS Lett* **400**: 25–30.

Gilson E, Roberge M, Giraldo R, Rhodes D, Gasser SM. 1993. Distortion of the DNA double helix by RAP1 at silencers and multiple telomeric binding sites. *Journal of Molecular Biology* **231**: 293–310.

Giraldo R, Rhodes D. 1994. The yeast telomere-binding protein RAP1 binds to and promotes the formation of DNA quadruplexes in telomeric DNA. *EMBO J* **13**: 2411–2420.

Giraldo R, Suzuki M, Chapman L, Rhodes D. 1994. Promotion of parallel DNA quadruplexes by a yeast telomere binding protein: a circular dichroism study.

Proc Natl Acad Sci USA **91**: 7658–7662.

Graham IR, Haw RA, Spink KG, Halden KA, Chambers A. 1999. In vivo analysis of functional regions within yeast Rap1p. *Mol Cell Biol* **19**: 7481–7490.

Henry YA, Chambers A, Tsang JS, Kingsman AJ, Kingsman SM. 1990. Characterisation of the DNA binding domain of the yeast RAP1 protein. *Nucleic Acids Res* **18**: 2617–2623.

Lane AN, Chaires JB, Gray RD, Trent JO. 2008. Stability and kinetics of G-quadruplex structures. *Nucleic Acids Res* **36**: 5482–5515.

Lieb JD, Liu X, Botstein D, Brown PO. 2001. Promoter-specific binding of Rap1 revealed by genome-wide maps of protein-DNA association. *Nat Genet* **28**: 327–334.

Neidle S, Parkinson GN. 2008. Quadruplex DNA crystal structures and drug design. *Biochimie* **90**: 1184–1196.

Oganesian L, Graham ME, Robinson PJ, Bryan TM. 2007. Telomerase recognizes G-quadruplex and linear DNA as distinct substrates. *Biochemistry* **46**: 11279–11290.

Paeschke K, Simonsson T, Postberg J, Rhodes D, Lipps HJ. 2005. Telomere end-binding proteins control the formation of G-quadruplex DNA structures in vivo.

Nat Struct Mol Biol **12**: 847–854.

Parkinson GN, Lee MPH, Neidle S. 2002. Crystal structure of parallel quadruplexes from human telomeric DNA. *Nature* **417**: 876–880.

Phatak P, Cookson JC, Dai F, Smith V, Gartenhaus RB, Stevens MFG, Burger AM. 2007. Telomere uncapping by the G-quadruplex ligand RHPS4 inhibits clonogenic tumour cell growth in vitro and in vivo consistent with a cancer stem cell targeting mechanism. *Br J Cancer* **96**: 1223–1233.

Risitano A, Fox KR. 2004. Influence of loop size on the stability of intramolecular DNA quadruplexes. *Nucleic Acids Res* **32**: 2598–2606.

Risitano A, Fox KR. 2003. Stability of intramolecular DNA quadruplexes: comparison with DNA duplexes. *Biochemistry* **42**: 6507–6513.

Rizzo A, Salvati E, Porru M, D'Angelo C, Stevens MF, D'Incalci M, Leonetti C, Gilson E, Zupi G, Biroccio A. 2009. Stabilization of quadruplex DNA perturbs telomere replication leading to the activation of an ATR-dependent ATM signaling pathway. *Nucleic Acids Res* **37**: 5353–5364.

Schaffitzel C, Berger I, Postberg J, Hanes J, Lipps HJ, Plückthun A. 2001. In vitro generated antibodies specific for telomeric guanine-quadruplex DNA react with Stylonychia lemnae macronuclei. *Proc Natl Acad Sci USA* **98**: 8572–8577.

Smith JS, Chen Q, Yatsunyk LA, Nicoludis JM, Garcia MS, Kranaster R, Balasubramanian S, Monchaud D, Teulade-Fichou M-P, Abramowitz L, et al. 2011. Rudimentary G-quadruplex–based telomere capping in Saccharomyces cerevisiae. *Nat Struct Mol Biol* **18**: 478–485.

Sundquist WI, Klug A. 1989. Telomeric DNA dimerizes by formation of guanine tetrads between hairpin loops. *Nature* **342**: 825–829.

Venczel EA, Sen D. 1993. Parallel and antiparallel G-DNA structures from a complex telomeric sequence. *Biochemistry* **32**: 6220–6228.

Williamson JR, Raghuraman MK, Cech TR. 1989. Monovalent cation-induced structure of telomeric DNA: the G-quartet model. *Cell* **59**: 871–880.

Zahler AM, Williamson JR, Cech TR, Prescott DM. 1991. Inhibition of telomerase by G-quartet DNA structures. *Nature* **350**: 718–720.

Zhang M-L, Tong X-J, Fu X-H, Zhou BO, Wang J, Liao X-H, Li Q-J, Shen N, Ding J, Zhou J-Q. 2010. Yeast telomerase subunit Est1p has guanine quadruplex-promoting activity that is required for telomere elongation. *Nat Struct Mol Biol* **17**: 202–209.

MATERIALS and METHODS

^{32}P-End Labeling and Annealing of Oligonucleotides

15pmol of each oligonucleotide was end-labeled with 105μCi of [γ–^{32}P] ATP (3000 Ci/mmol) and 15U of T4 polynucleotide kinase (New England Biolabs) in a final reaction volume of 15μl. The reaction was incubated at 37°C for 45min. Afterwards, the unincorporated [γ–^{32}P] ATP was separated from the labeled substrate by centrifuging the reaction for 2min at 750g through a Centri·Spin 20 (Princeton Separations, Inc) spin column that had been pre-equilibrated for 30min with 650μl of TE. Single stranded labeled oligonucleotides (*G4DNA* and *TERRA*) were annealed by running the following protocol on a thermocycler in the presence of 100mM KCl: 95°C 10', 90°C 5', 85°C 5', 80°C 5', 75°C 5', 70°C 5', 65°C 5', 60°C 5', 55°C 5', 50°C 5', 45°C 5', 40°C 5', 35°C 5', 30°C 5', 25°C 5'. Likewise, we made duplex DNA (dDNA) by annealing labeled *G4DNA* to its complementary unlabeled oligonucleotide (3'-CCACACCCACACACCCACACACCCACACACCCAGAATT-5') by running the same thermocycler protocol in the presence of 100mM $MgCl_2$.

Electrophoretic Mobility Shift Assay (EMSA)

Our EMSA experiments were performed essentially as described earlier (Giraldo and Rhodes 1994). All binding reactions were performed in a final volume of 20μl, incubating 100fmol of different labeled oligonucleotides (*dDNA*, *G4DNA*, and

TERRA) with varying amount of Rap1 constructs (*FL* 1-827AA, *DBD* 1,353-598AA, *ΔC* 1-598AA, *ΔN* 1,353-827AA, ΔN^{short} 1-362-827AA, and *N-term* 1-352AA) in a binding buffer: 20mM Tris-HCl pH 7.5, 1mM EDTA, 1mM DTT, 6% glycerol, 100μg/ml BSA, 10μg/ml poly(dI-dC), KCl 100mM (adjusting for the solutes provided in the purified protein). The binding reactions were incubated on ice for 5min and then at room temperature for 60min. 5μl of 5x loading buffer (20% glycerol, 0.1% bromophenol blue) was added to the 20μl binding reaction and then immediately run at 4 V/cm for 10hr, at 4°C on a 6% or 4-20% polyacrylamide (acrylamide:bisacrylamide = 19:1) non-denaturing gel that was pre-run for 30min at 4 V/cm. The gels were dried for 75min at 65°C on Whatman paper, exposed to a phosphorimager screen, and then imaged on a Storm phosphorimager (Molecular Dynamics).

A.

Figure 5-1

Oligo Name	Sequence
dDNA	5′AATTCTGGGTGTGTGGGTGTGTGGGTGTGTGGGTGTGG 3′TTAAGACCCACACACCCACACACCCACACACCCACACC
G4DNA	5′AATTCT**GGG**TGTGT**GGG**TGTGT**GGG**TGTGT**GGG**TGTGG
TERRA	5′AAUUCU**GGG**UGUGU**GGG**UGUGU**GGG**UGUGU**GGG**UGUGG

B.

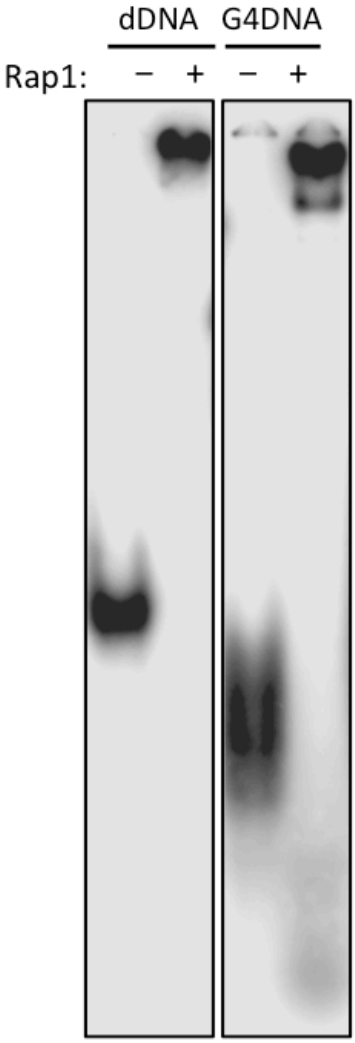

C.

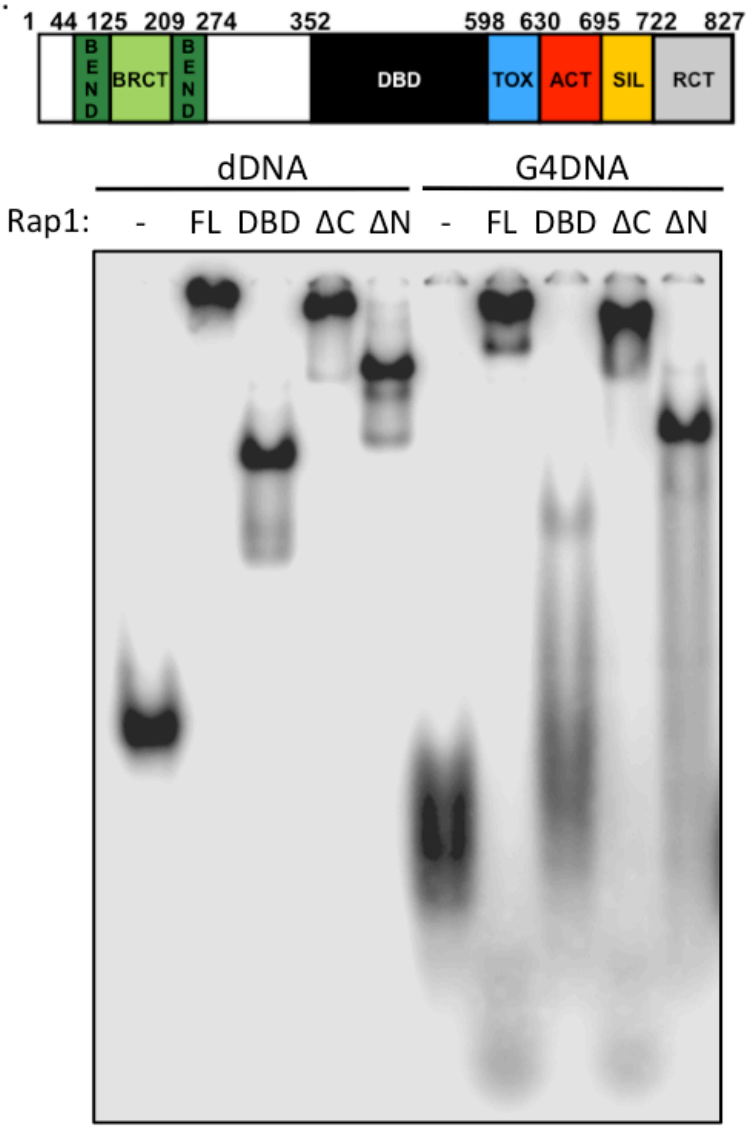

Figure 5-1. The N-terminal residues of Rap1 are important to bind G-quadruplex DNA.

(A) Oligonucleotide sequences for the probes that were used in the various studies. Note that *dDNA* is duplex DNA that was pre-annealed. (B) Rap1 binds G4DNA. His tagged Rap1 protein was expressed and purified from *E. coli*. (C) The N-terminal residues of Rap1 are important for binding G4DNA. We have included a schematic of Rap1 that shows its domains. The Rap1 construct abbreviations correspond to the following proteins: *FL* 1-827AA, *DBD* 1,353-598AA, *ΔC* 1-598AA, and *ΔN* 1,353-827AA. The *G4DNA* probe was pre-annealed prior to incubation. His tagged Rap1 protein was expressed and purified from *E. coli*. For both studies, ^{32}P-labeled *G4DNA* or *dDNA* probe (final concentration 5nM) was incubated with various purified Rap1 proteins (final concentration 1.25μM) in the following binding buffer: 20mM Tris-HCl pH 7.5, 1mM EDTA, 1mM DTT, 6% glycerol, 100μg/ml BSA, 10μg/ml poly(dI-dC), KCl 100mM (adjusting for the solutes provided in the purified protein). The binding reactions were incubated on ice for 5min and then at room temperature for 60min and then run out on a 6% non-denaturing polyacrylamide gel.

Figure 5-2

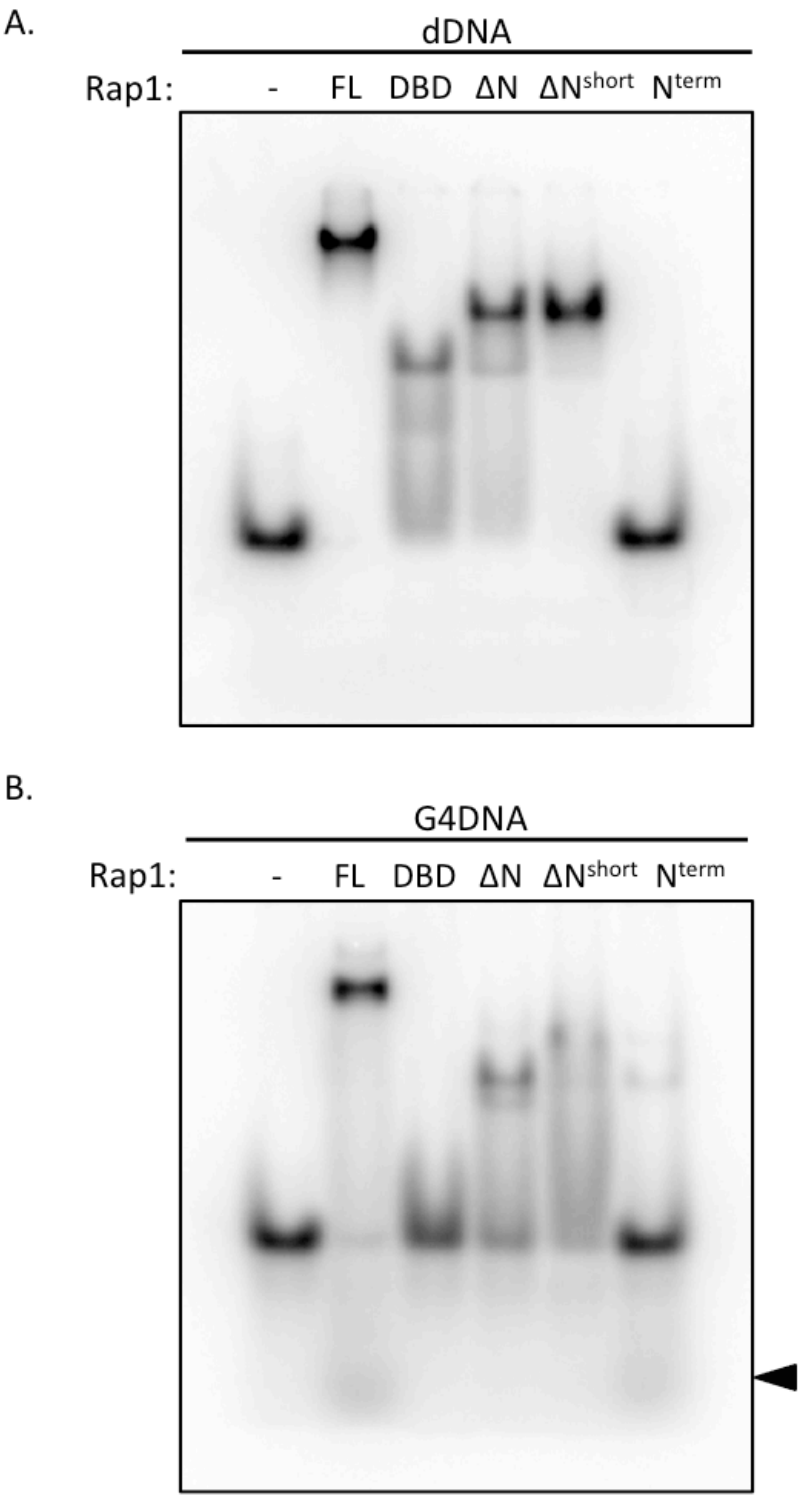
A.
dDNA
Rap1:
-
FL
DBD
ΔN
ΔNshort
Nterm
B.
G4DNA
Rap1:
-
FL
DBD
ΔN
ΔNshort
Nterm

Figure 5-2. An N-terminal fragment of Rap1, which lacks its central DNA binding domain (DBD), weakly binds G-quadruplex DNA.

^{32}P-labeled (A) *dDNA* or (B) *G4DNA* probe (final concentration 5nM) was incubated with various purified Rap1 constructs (final concentration 1.25μM) and then run out on a 4-20% non-denaturing polyacrylamide gel. The Rap1 construct abbreviations correspond to the following proteins: *FL* 1-827AA, *DBD* 1,353-598AA, *ΔN* 1,353-827AA, ΔN^{short} 1-361-827AA, and *N-term* 1-352AA. The *G4DNA* probe was pre-annealed prior to incubation. The arrowhead marks a faster-mobility DNA species. His tagged Rap1 protein was expressed and purified from *E. coli*.

Figure 5-3

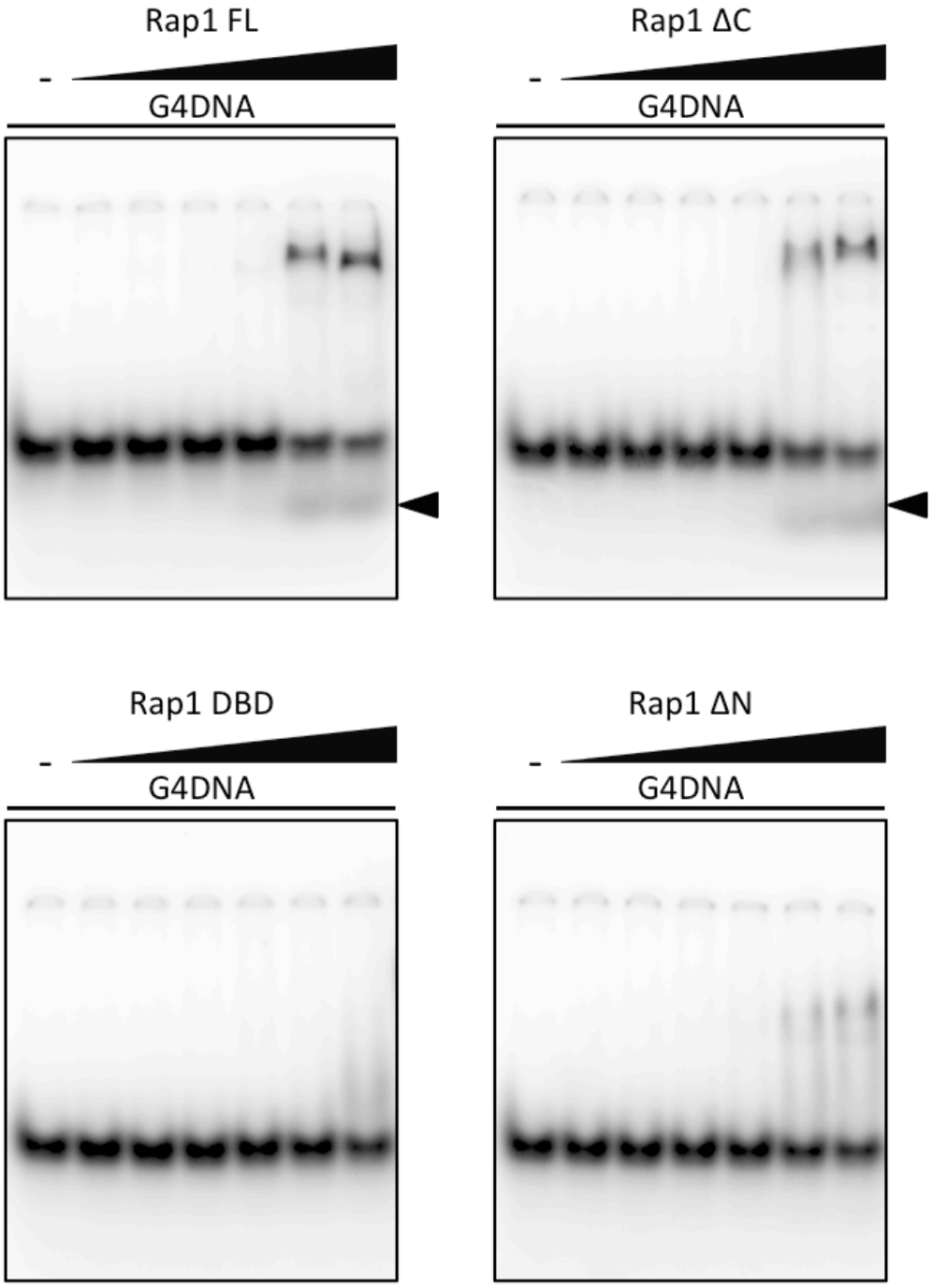

Figure 5-3. The N-terminus of Rap1 promotes the appearance of a faster-mobility G-quadruplex species.

In each of the panels, ^{32}P-labeled *G4DNA* probe (at a final concentration of 5nM) was incubated with an increasing amount of the various Rap1 constructs (final concentration of the constructs in lanes 1 to 7: 0nM, 0.125nM, 1.25nM, 12.5nM, 125nM, 1.25μM, and 2.20μM) and then run out on a 4-20% non-denaturing polyacrylamide gel. The Rap1 construct abbreviations correspond to the following proteins: *FL* 1-827AA, *DBD* 1,353-598AA, *ΔC* 1-598AA, and *ΔN* 1,353-827AA. The *G4DNA* probe was pre-annealed prior to incubation. His tagged Rap1 protein was expressed and purified from *E. coli*.

Figure 5-4

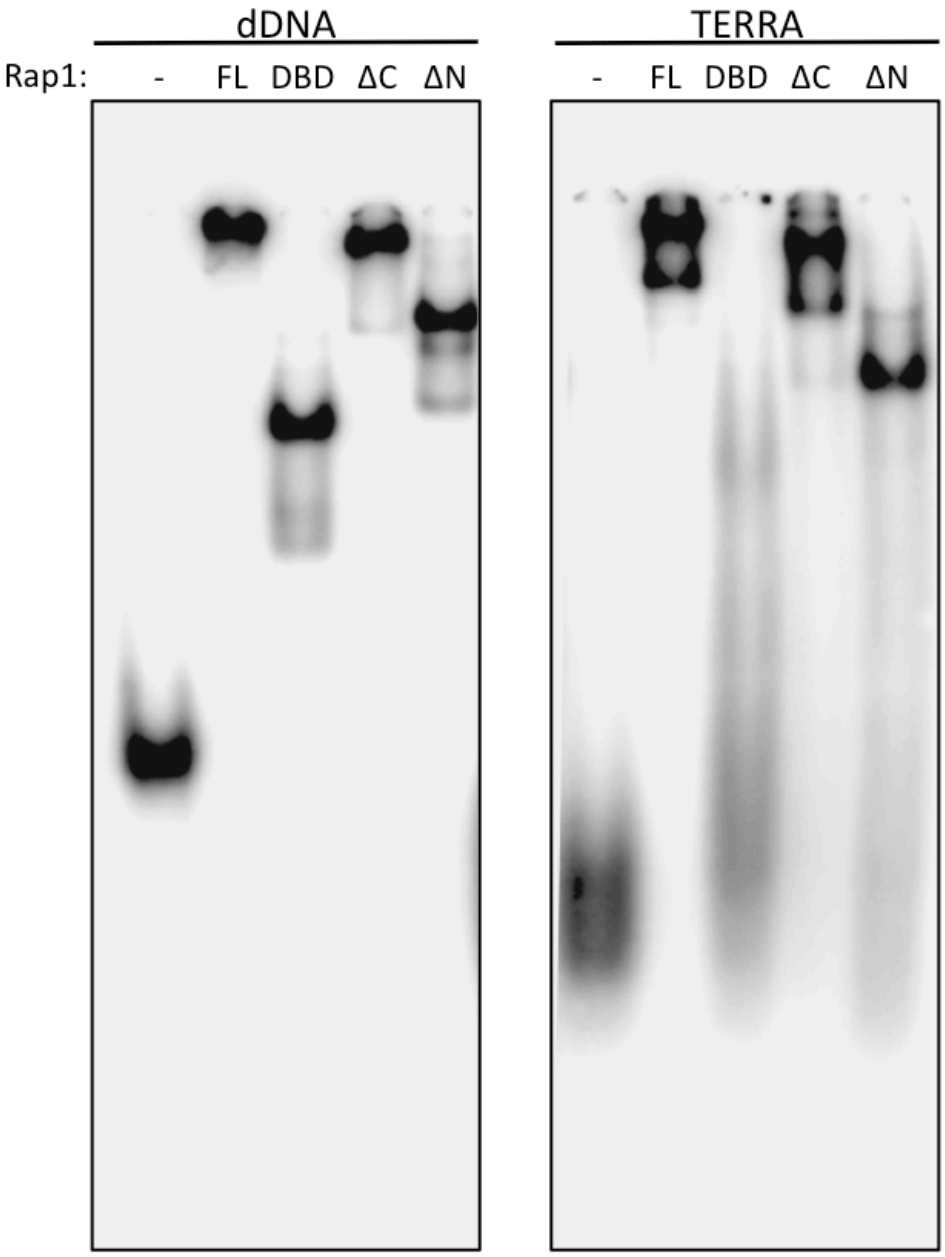

Figure 5-4. The N-terminal residues of Rap1 are important to bind RNA species that have high G-quadruplex forming potential (QFP).

Pre-annealed ^{32}P-labeled *dDNA* or *TERRA* probe (at a final concentration of 5nM) was incubated with an increasing amount of the various Rap1 constructs (final concentration 1.25μM) and then run out on a 6% non-denaturing polyacrylamide gel. The Rap1 construct abbreviations correspond to the following proteins: *FL* 1-827AA, *DBD* 1,353-598AA, *ΔC* 1-598AA, and *ΔN* 1,353-827AA. His tagged Rap1 protein was expressed and purified from *E. coli*.

CHAPTER 6: Characterization of hRap1 at senescence

Based on our work on yeast Rap1 (yRap1) at senescence, we wondered if the pathway was evolutionarily conserved and if human Rap1 (hRap1) leaves shortened telomeres and binds new sites throughout the genome when cells senesce due to telomeric dysfunction. To address this question, we compared hRap1 localization in proliferating cells to senescent cells.

RESULTS and DISCUSSION

Though many stimuli drive cellular senescence (including oncogene over-expression, ionizing radiation (IR), and various drugs), we chose replicative senescence because it is largely driven by telomeric shortening and dysfunction (Rubio et al. 2002). We harvested senescent cells by passaging primary human fibroblasts (IMR90 cells) until they stopped proliferating. At this stage the cells were grossly senescent (the cells were enlarged, splayed out, and did not pack tightly together), highly (60-70%) SA β-Gal (senescence-associated β-galactosidase positive) positive, and highly SAHF (senescence-associated heterochromatic foci) positive (Supplementary Figure 6-1, Figure 6-2) (Dimri et al. 1995; Narita et al. 2003).

Similar to yRap1, hRap1 occupancy increases at many of its normal sites at senescence

We assessed hRap1's localization in proliferating (PD 29.5) and senescent (PD 75.5) cells by performing hRap1 ChIP RTPCR (Figure 6-1; hRap1 was completely immuno-depleted from the lysates, Supplemental Figure 6-1; the Bethyl A300-306A αRap1 antibody was used previously for ChIP-seq by Yang et al., 2011). As a confirmation, we compared hRap1's occupancy at previously characterized sites that were found via hRap1 ChIP-seq in a fibrosarcoma cell line (HTC75) (Yang et al. 2011). At senescence, we found that hRap1 occupancy increases at many sites (6 out of 11, Figure 6-1A) and decreases at a few loci (Figure 6-1C). However, there were three sites that hRap1 occupancy did not seem to change (Figure 6-1B). Overall at senescence, hRap1 occupancy goes up at many of its normal, proliferating targets. This finding is strikingly similar to what we found in *S. cerevisiae* – i.e. at senescence, yRap1 occupancy goes up dramatically at its normal, WT targets (including *ENO1* and *PGK1*; chapter 2). Altogether, this interesting parallel between yeast and human Rap1 occupancy at senescence might be a hint that the pathway we discovered in yeast is also active in senescent human cells. However, our preliminary results are just *suggestive* and further experiments are warranted – including hRap1 ChIP-seq in proliferating and senescent cells – to determine if hRap1 indeed targets new sites throughout the genome.

hRap1 is preferentially excluded from SAHF's at senescence

In addition to hRap1 ChIP RTPCR, we compared the localization of hRap1 in proliferating (PD 29.5) and senescent cells (PD 75.5) via immuno-fluorescence microscopy (IF; Figure 6-2). We found several senescence-associated changes in hRap1 localization. First, hRap1 levels appear to go up dramatically at senescence (Figure 6-2). This finding is consistent with our preliminary data that hRap1 levels go up per cell via Rap1 immunoblot (data not shown). However, the changes observed by microscopy might be an indirect result of the altered chromatin in senescent cells (O'Sullivan et al. 2010; Ivanov et al. 2013) – i.e. the chromatin changes might make hRap1 less diffuse, more locally concentrated, and more accessible to anti-Rap1 antibodies. Second, whereas hRap1 foci mostly co-localize with Trf2 foci in proliferating cells, at senescence the hRap1 IF pattern appears less punctate, more diffuse, and co-localizes less with Trf2 foci (Figure 6-2). Even though hRap1 was thought to require Trf2 to bind DNA, hRap1 IF foci do not perfectly co-localize with Trf2 foci in cycling cells (Li et al. 2000). At best, 70-80% of hRap1 foci co-localize with Trf2 foci in HeLaI.2.11 cells (Li et al. 2000), which is consistent with what we see in proliferating cells (Figure 6-2). Instead at senescence, only 10-20% of hRap1 foci (that are frequently the brightest foci) co-localize with Trf2 foci. Because Trf2 is an excellent marker of telomeres, these data suggest that hRap1 has increased Trf2-independent and telomere-independent

functions at senescence. All together, these findings are consistent with both what we found in senescent *S. cerevisiae* – i.e. that yRap1 has increased non-telomeric functions at senescence – and recent data that suggest that hRap1 can bind DNA independently of Trf2 to non-telomeric chromatin sites (Arat and Griffith 2012; Yang et al. 2011). In fact, murine Rap1 is found even found to affect the expression of histone genes (Yeung et al. 2013).

Our third finding is that even though hRap1 adopts a more diffuse staining pattern at senescence, hRap1 foci are largely excluded from the SAHF's (Figure 6-2). SAHF's are large blocks of heterochromatin (that are marked with HP1, MacroH2A, H3K9me3, H3K27me3, and H3K36me3) that regulate RNA polymerase II (RNAP II) localization and gene repression at senescence (Funayama et al. 2006; Narita et al. 2006; 2003; Zhang et al. 2005; 2007). This is one of our most exciting and striking findings and place hRap1 in the right location to upregulate gene expression at senescence. These data warrant further investigation to determine if hRap1 foci co-localize with other factors involved with active transcription – including RNAP II, general transcription factors, and histone marks associated with transcriptional activation i.e. H3K4me3.

Finally, we see that hRap1 foci are also found in the recently characterized senescence-associated cytoplasmic chromatin fragments (CCF's) (Ivanov et al. 2013). Intrigued by the finding that histone proteins are lost at senescence

(O'Sullivan et al. 2010), Adams and colleagues recently discovered an autophagy-dependent pathway that leads to nuclear budding, CCF formation, and ultimately histone degradation (Ivanov et al. 2013). Not only is it fascinating that hRap1 is present in CCFs (which are present in ~10% of the cells) but also it raises the possibility that hRap1 is involved in their formation (ie. budding) and/or their degradation. It would be interesting to repeat these experiments in hRap1 knockout cells to determine if hRap1 affects CCF formation/degradation – as well as the rate of senescence and gene expression changes at senescence.

Though our results hint that hRap1 might be relocalizing at human cellular senescence, it is important to point out that hRap1 may not be binding new sites throughout the genome. Our data are very preliminary and we do not know yet where hRap1 binds in the genome at senescence and if it indeed targets new sites. In the chance that hRap1 does bind new sites throughout the genome at senescence, it will be important to determine mechanistically how this process occurs. For example, is it an active process (as it is in *S. cerevisiae*)? Or is it a passive process that is completely driven by the number of telomere repeats that are lost (ie. simply mass action)? Ultimately, we will try to determine which pathways act on hRap1 at senescence; post-translational modification of hRap1 might also play a role (as they seem to do in *S. cerevisiae*).

REFERENCES

Arat NÖ, Griffith JD. 2012. Human Rap1 Interacts Directly with Telomeric DNA and Regulates TRF2 Localization at the Telomere. *J Biol Chem* **287**: 41583–41594.

Dimri GP, Lee X, Basile G, Acosta M, Scott G, Roskelley C, Medrano EE, Linskens M, Rubelj I, Pereira-Smith O. 1995. A biomarker that identifies senescent human cells in culture and in aging skin in vivo. *Proc Natl Acad Sci USA* **92**: 9363–9367.

Funayama R, Saito M, Tanobe H, Ishikawa F. 2006. Loss of linker histone H1 in cellular senescence. *J Cell Biol* **175**: 869–880.

Ivanov A, Pawlikowski J, Manoharan I, van Tuyn J, Nelson DM, Rai TS, Shah PP, Hewitt G, Korolchuk VI, Passos JF, et al. 2013. Lysosome-mediated processing of chromatin in senescence. *J Cell Biol* **202**: 129–143.

Li B, Oestreich S, de Lange T. 2000. Identification of human Rap1: implications for telomere evolution. *Cell* **101**: 471–483.

Narita M, Narita M, Krizhanovsky V, Nuñez S, Chicas A, Hearn SA, Myers MP, Lowe SW. 2006. A novel role for high-mobility group a proteins in cellular senescence and heterochromatin formation. *Cell* **126**: 503–514.

Narita M, Nuñez S, Heard E, Narita M, Lin AW, Hearn SA, Spector DL, Hannon GJ, Lowe SW. 2003. Rb-mediated heterochromatin formation and silencing of E2F

target genes during cellular senescence. *Cell* **113**: 703–716.

O'Sullivan RJ, Kubicek S, Schreiber SL, Karlseder J. 2010. Reduced histone biosynthesis and chromatin changes arising from a damage signal at telomeres. *Nat Struct Mol Biol* **17**: 1218–1225.

Rubio MA, Kim S-H, Campisi J. 2002. Reversible manipulation of telomerase expression and telomere length. Implications for the ionizing radiation response and replicative senescence of human cells. *J Biol Chem* **277**: 28609–28617.

Yang D, Xiong Y, Kim H, He Q, Li Y, Chen R, Songyang Z. 2011. Human telomeric proteins occupy selective interstitial sites. *Cell Res*.

Zhang R, Chen W, Adams PD. 2007. Molecular dissection of formation of senescence-associated heterochromatin foci. *Mol Cell Biol* **27**: 2343–2358.

Zhang R, Poustovoitov MV, Ye X, Santos HA, Chen W, Daganzo SM, Erzberger JP, Serebriiskii IG, Canutescu AA, Dunbrack RL, et al. 2005. Formation of MacroH2A-containing senescence-associated heterochromatin foci and senescence driven by ASF1a and HIRA. *Developmental Cell* **8**: 19–30.

MATERIALS and METHODS

Cell culture

Primary human diploid fibroblasts (IMR90) were passaged until senescence starting from a late population doubling (PD) stock (PD 64; gift of P. Shah). As cells approached senescence, cells were refed every 4 days. Early and late PD cells were grown in low oxygen conditions (3% O_2) in Dulbecco's Modified Eagle Medium supplemented with 10% non-heat inactivated FBS (Hyclone, Thermo, Lot#: AWG18846), 1% Penn-Strep (Lonza, BioWhittaker), and 0.5% fungizone (Gibco, Invitrogen).

Senescence-associated β-galactosidase staining

Cells were grown to ~70% confluency, washed with PBS and fixed at room temperature with 2% paraformaldehyde, 0.2% glutaraldehyde in 1X PBS. After washing twice with PBS, the cells were stained with X-gal (1mg/mL X-gal in 40mM citrate-phosphate buffer pH 6.0, 5mM K ferrocyanide, 5mM K ferricyanide, 150mM NaCl, 2mM $MgCl_2$) for 16-18 hours at 37°C.

Chromatin Immunoprecipitation (ChIP)

Early PD, proliferating cells (PD 29.5) were grown to 80-90% confluency and then crosslinked. Whereas highly senescent cells (PD 75.5), which took 7 days to become confluent following a 1:3 split, 'matured' on plates for an additional week and then were crosslinked (Ivanov et al. 2013). Cells were crosslinked at room

temperature for 5min by adding formaldehyde from a 37% stock to a final concentration of 1%. Crosslinking was quenched for 5min at room temperature by adding glycine to a final concentration of 125mM. Cells were then washed once with PBS and then frozen at -80°C.

10-30x10^6 Cells (one 15cm plate) were thawed and resuspended in 10mL of Lysis buffer (50 mM HEPES pH 7.9, 140 mM NaCl, 1 mM EDTA, 10% glycerol, 0.5% NP-40, 0.25% Triton X-100, 1x complete protease inhibitors (Roche)) and rotated at 4°C for 10min. The lysate was spun down at 4000 RPM at 4°C for 5min and the pellet was resuspended in 10mL of wash buffer (10 mM Tris-HCl pH 8.1, 200 mM NaCl, 1 mM EDTA pH 8.0, 0.5 mM EGTA pH 8.0, 1x complete protease inhibitors (Roche)) and rotated at 4°C for 10min. The lysate was spun down at 4000 RPM at 4°C for 5min and the pellet was twice resuspended in 1.5mL of shearing buffer (0.1% SDS, 1 mM EDTA, 10 mM Tris, pH 8.1). After a final spin at 4000 RPM at 4°C for 5min, the pellet was resuspended in 1ml of shearing buffer and transferred to a TC12x12mm tube with AFA fiber (Covaris) and filled to the top with shearing buffer. The lysate was sheared in the covaris S220 sonicator for 10min (30% duty cycle, 35W average intensity power, 145W peak incident power, 200 cycles per burst, 5-10˚C temperature, frequency sweeping power mode, continuous degassing, no intensifier). Afterwards, the buffer was adjusted to (150mM NaCl, 1% Triton X-100, 0.5% Na Deoxycholate, 0.1% SDS, 50mM Tris-HCl, pH 8) and the lysate was spun at 13,000RPM for 10min at 4°C. The protein concentration of the supernatant was

quantified via the Bradford assay. Equal cell equivalents of lysate (~500μg of chromatin for the less concentrated senescent lysate) was added to 30μl protein G dynabeads (dynal, invitrogen) that had previously been prepared by washing twice with 1ml block solution (0.5% BSA, 1X PBS), resuspending the beads in 250μl of block solution, incubating overnight at 4°C with 4μg of either αhRap1 antibody (A300-306A, Bethyl Labs) or rabbit IgG (31207, Pierce), and then washing three times with 1ml block solution. The chromatin:bead mixture rotated overnight at 4°C. The following day, the beads were washed five times with RIPA buffer (50mM Tris-HCl, pH 8.0, 150mM NaCl, 1% Triton X-100, 0.5% Na deoxycholate, 0.1% SDS, 1x complete protease inhibitors (Roche)). The protein:DNA complexes were eluted off the beads by adding 200μl of elution buffer (50mM Tris-HCl pH 8.0, 10mM EDTA, 1% SDS) and incubating the mixture at 65°C for 30min on a thermomixer (eppendroff). After separating the supernatant from the beads, the crosslinks were reversed by raising the concentration of NaCl to 200mM and incubating the mixture at 65°C overnight on a thermomixer. The following day the samples were treated with RNaseA (0.2mg/mL, 37°C, 2hr), proteinase K (0.2mg/mL, 55°C, 2hr), and the DNA was purified via a phenol:chloroform:isoamyl alcohol extraction followed by an ethanol precipitation. Purified DNA was quantified using qPCR and standard curves, and the enrichment for hRap1 ChIP signals at specific target loci were calculated by normalizing to a previously characterized negative control region (*neg.chr2*).

Immunofluorescence

Cells were spotted on slides and allowed to adhere overnight. The following day the cells were fixed for 10min at room temperature in 4% paraformaldehyde, 1x PBS and extracted for 1min at room temperature in 0.2% Triton X-100, 1x PBS. The cells were incubated at 37°C for 30min in BSA blocking buffer (1x PBS, 1% BSA, 0.2% tween-20, 0.02% azide) and then at 37°C for 1hr in primary antibody dilutions (see below). Afterwards, the slides were washed three times for 5min in wash buffer (1x PBS, 0.2% Tween-20). The cells were blocked again with BSA blocking buffer and incubated with secondary antibody dilutions (see below). The slides were washed in the following buffers for 5min 1) wash buffer 2) wash buffer + 0.3 ug/ml DAPI 3) wash buffer. The slides were mounted with vectashield (vector labs).

Figure 6-1

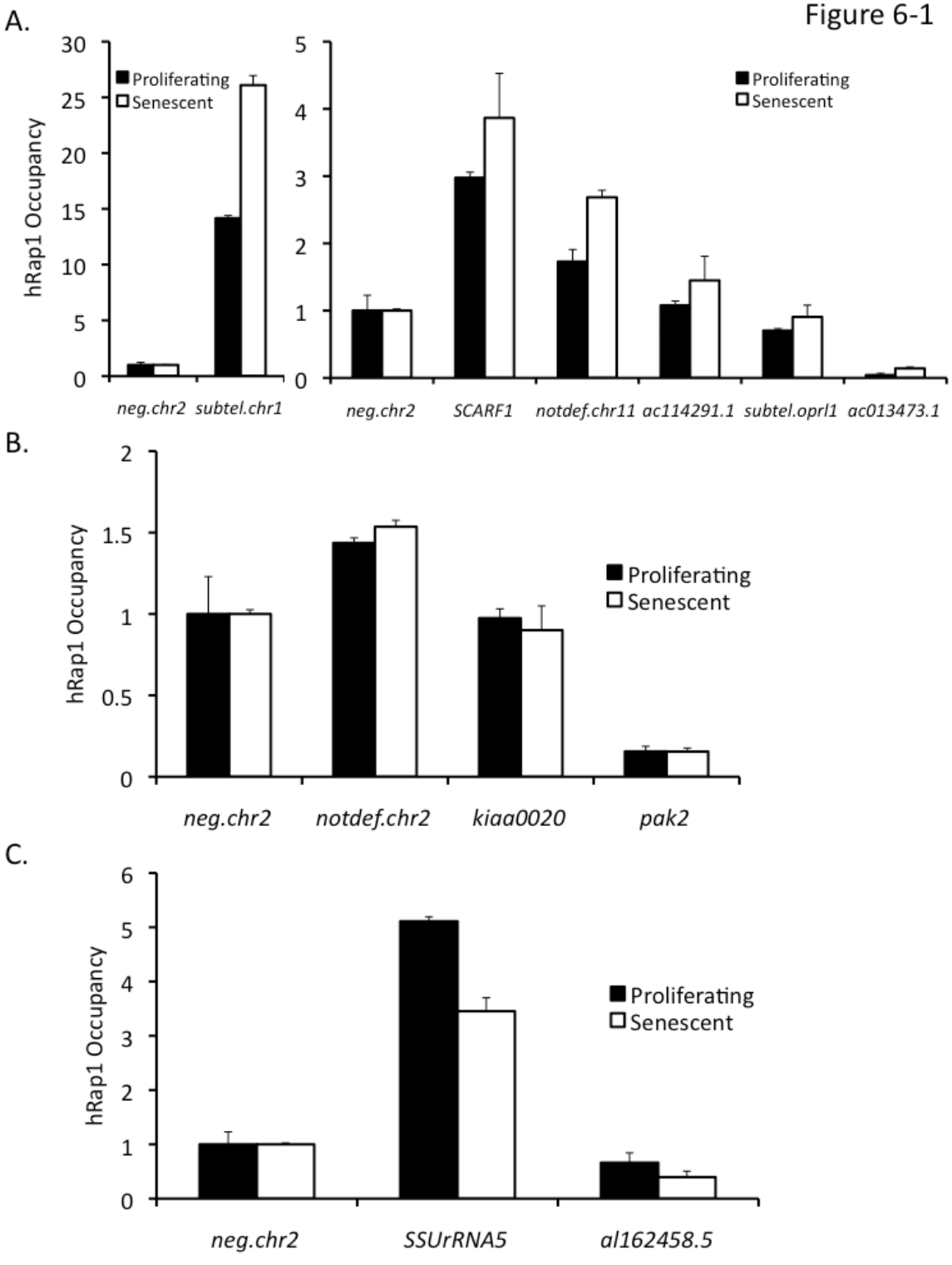
A.
hRap1 Occupancy
Proliferating
Senescent
neg.chr2
subtel.chr1
SCARF1
notdef.chr11
ac114291.1
subtel.oprl1
ac013473.1
B.
notdef.chr2
kiaa0020
pak2
C.
SSUrRNA5
al162458.5

Figure 6-1. hRap1 Occupancy in proliferating and senescent IMR90 cells.

At senescence, hRap1 occupancy increases (A), decreases (C), and is unchanged (B) at several sites throughout the genome. hRap1 occupancy was measured by hRap1 ChIP RT-PCR in proliferating (PD 29.5) and senescent (PD 75.5) IMR90 cells normalized to a previously characterized negative control region (*neg.chr2*) that hRap1 was shown not to bind in HTC75 cells (Yang et al. 2011). The means and SEM's are from three independent RT-PCR experiments.

Figure 6-2

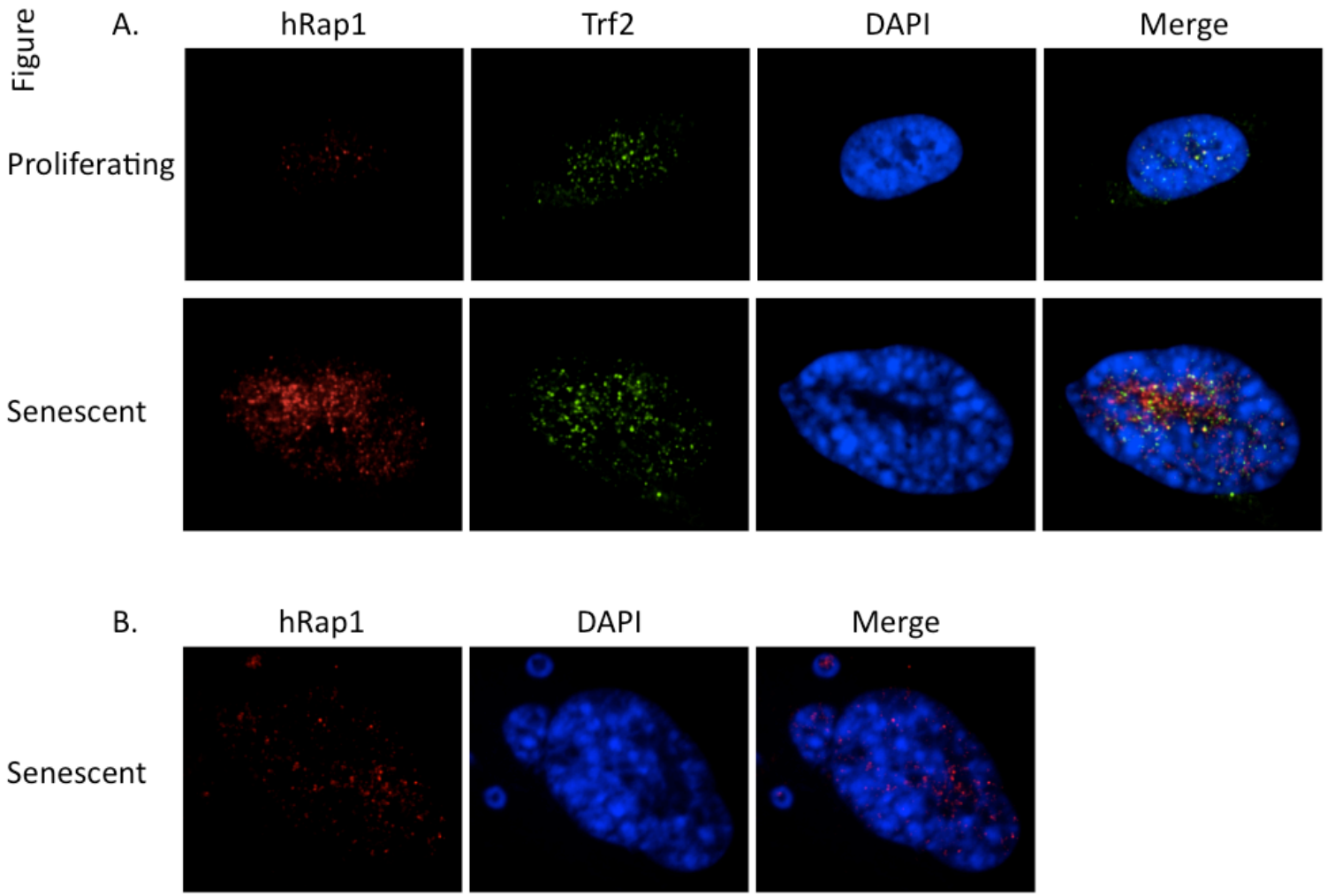
A.
hRap1
Trf2
DAPI
Merge
Proliferating
Senescent
B.
hRap1
DAPI
Merge
Senescent

Figure 6-2. At senescence, as hRap1 fluorescence levels increase, hRap1 is excluded from SAHFs and is located in CCFs.

(A-B) Proliferating (PD 29.5) and senescent (PD 75.5) IMR90 Cells were fixed with paraformaldehyde, extracted with Triton X-100, and then visualized via immuno-fluorescence on a Spinning Disk Confocal Nikon Eclipse Ti-U microscope. Cells were stained with α*hRap1*, α*Trf2*, and 4',6-diamidino-2-phenylindole (*DAPI*).

Supplementary Figure 6-1

A.

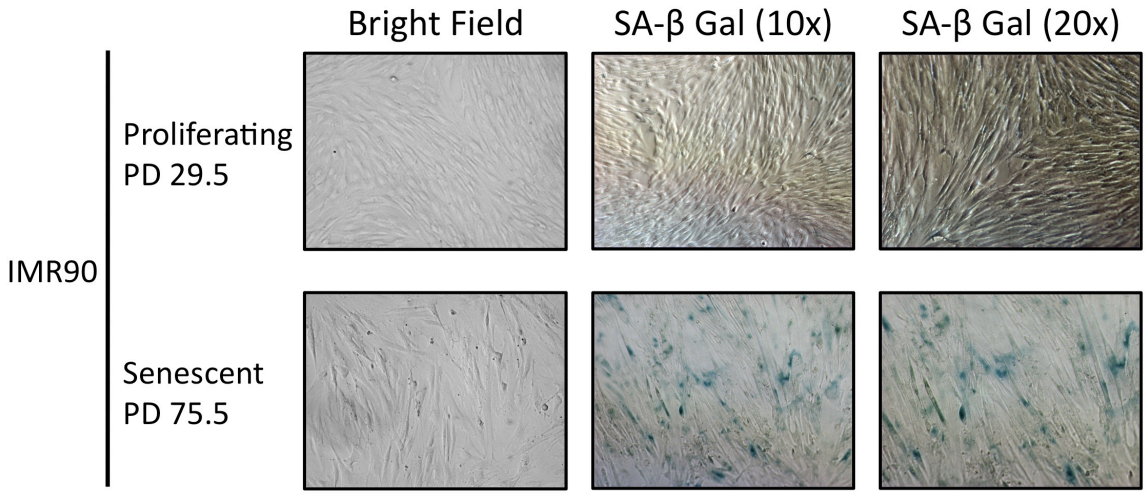

B.

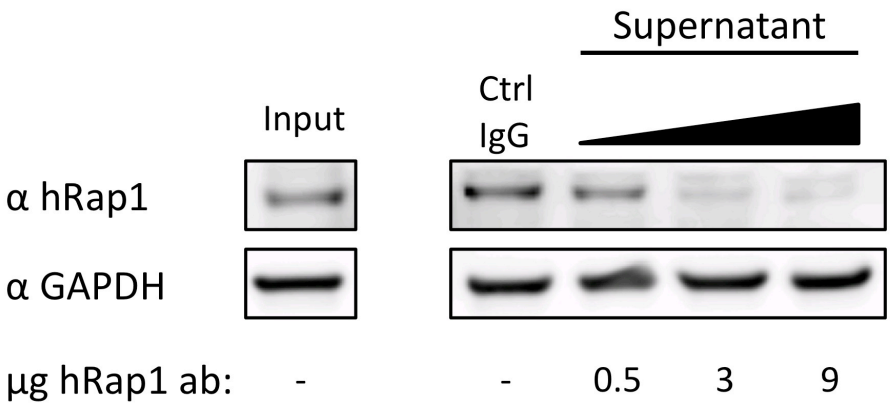

Supplementary Figure 6-1.

(A) At senescence, 60-70% of IMR90 cells were SA-β Gal positive (cells senesced at PD 75.5). In contrast, no proliferating cells (PD 29.5) were SA-β Gal positive. Cells were imaged on a Nikon Eclipse Ti-U microscope. (B) Immuno-depletion of hRap1. We immuno-depleted hRap1 from ~500μg of protein lysate with 3μg of hRap1 antibody (*ab*). GAPDH was used as a loading control (ie. a protein that should not be immuno-depleted from the lysate).

ChIP RT-PCR Primers

Name	Sequence
negative.chr2-F	CCAGGACTTGGCTTGAGCTT
negative.chr2-R	CAGGATTCAAGTCAGGAAGATTTAGG
subtel.chr1-F	GCTGTATTGCAGGGTTCAACTG
subtel.chr1-R	GGGTGTCATGTGTGCATTAGGA
subtel.OPRL1-F	TGTGGACTTGGAAGCCTTTTG
subtle.OPRL1-R	CCTACAGTTGCCAGAGGTTTCTG
SCARF1-F	GCAGTGAAGCTCAGGTGCAA
SCARF1-R	TCTGTCACCTGCTGGATTTGG
PAK2-F	TGGGCTGCACTCTGCTAGAA
PAK2-R	CAGCACTAAATGGCACCATAAGC
SSU_rRNA_5(chr21)-F	CACGGCCGGTACAGTGAAA
SSU_rRNA_5(chr21)-R	CGACCAAAGGAACCATAACTGAT
KIAA0020-F	TCACAGTGAGACCAGACAGATCCT
KIAA0020-R	CTGTTTGCTAGACTCTGCATTTGAG
AL162458.5-F	CGCCTAACTCTACCCGAAGCT
AL162458.5-R	TGCCGGAGTCAGAGAGGAA
AC114291.1-F	ACCTCGGCCCTCTTTGCT
AC114291.1-R	TGAACAGTAGATGGGAGATCAGATG
AC013473.1-F	CACTTGAGGGCACTGCTCTGT
AC013473.1-R	AGGTGAGCCCTCAGACAAACA
not define.chr11-F	ACCTCCAGGCACCATGGA
not define.chr11-R	TGGAGAGGGCAGGTTTTCAG
not define.chr2-F	GCAGTGGCTCAGGCCTGTAA
not define.chr2-R	CATGATCCGCCCACTTCAG

Supplementary Figure 6-2.

ChIP RTPCR primer that were used.

CHAPTER 7: Conclusions and future directions

SUMMARY

Cellular senescence is an active response to many stresses that promote cancer including telomeric dysfunction, oncogenic signaling, and ionizing radiation. Senescence prevents neoplastic transformation in a cell-autonomous fashion and is increasingly appreciated to promote cancer and age-associated pathologies in a non cell-autonomous fashion. Senescent cells are characterized by persistent cell cycle arrest mediated by DNA damage checkpoint factors and also display profound changes in gene expression, chromatin organization, metabolism, and secretory behavior. The mechanisms underlying these changes are not well understood, but such knowledge promises to enhance our understanding of cancer and other age-related diseases.

We considered an older untested hypothesis that as telomeres shorten as cells approach senescence a factor that binds to telomeres and subtelomeres relocalizes to internal genomic loci and changes gene expression (Campisi 1997). To test this hypothesis, we used a yeast model of senescence that is driven by telomeric dysfunction in part because there is a wonderful candidate transcription factor, Rap1 (repressor activator protein 1); it binds every 18 base pairs at yeast telomeres, acts as a transcriptional activator or repressor at other sites throughout

the genome, and relocalizes to new target genes under various stresses (Buck and Lieb 2006; Tomar et al. 2008; Gilson et al. 1993). At senescence, we see that Rap1 leaves subtelomeres and targets around 500 NRTS genes (new Rap1 targets at senescence), binding the upstream promoter regions of these genes. Rap1 and Bre1, an E3 ubiquitin ligase that ubiquitylates H2BK123, upregulate the expression of many NRTS genes at senescence. This redistribution of Rap1 depends on the Mec1 DDR kinase and plays direct roles in senescence-related gene expression. Remarkably, the genes encoding the core histones are among the new targets of Rap1, and Rap1 contributes to a global decline in histone levels and also decreases nucleosome occupancy selectively at the promoters of genes that are up-regulated at senescence. Moreover, this Rap1–histone interplay impacts not only gene expression, but apparently also the pace of senescence.

DISCUSSION and FUTURE DIRECTIONS

Characterization of transcription factor re-localization to and from subtelomeres at senescence

We have shown that cellular senescence is associated with Rap1 leaving subtelomeres and targeting the NRTS genes. Though we known Rap1 relocalization depends on the checkpoint kinase *MEC1* and is associated with post-translationally modified Rap1 species, precisely how Rap1 leaves subtelomeres is not clear. This

process likely depends on changes to either Rap1 and its cofactors or subtelomeric chromatin at senescence. Though we have classified the potential changes into two neat categories, because they are not mutually exclusive, they both might be actively participating in Rap1 relocalization at senescence. To address how Rap1 leaves subtelomeres at senescence, both biochemical and genetic approaches will likely improve our understanding of the process.

First we should further characterize the slow-mobility Rap1 species that are present at senescence. Currently, we know that some of the species depend on *MEC1*, *SIZ2*, and *UBI4*, and that similar Rap1 species, which affect Rap1 activity, are seen under other stress conditions (Hang et al. 2011; Lescasse et al. 2013). However, it is still not clear if these senescence-associated Rap1 species either cause Rap1 relocalization or are just a 'bio-marker' of senescence and do not affect this process. First, we should map the senescence-associated post-translational modifications to Rap1 with IP-mass spec and then determine how they affect Rap1 relocalization with Rap1 point mutants that block these modifications. Nonetheless, it is also possible that the changes we see at senescence are a result of modifications to the Rap1 complex. We should purify the normal and senescent Rap1 protein complexes and characterize how it changes at senescence.

It is also possible that changes in subtelomeric chromatin drive Rap1 relocalization at senescence. Subtelomeric chromatin changes at senescence (Kozak

et al. 2010) and some of these histone modifications have been shown to affect Rap1/Sir2/3/4 complex stability (Emre et al. 2005; Sperling and Grunstein 2009), in particular H4K16Ac. One possibility is that at senescence H2BUb levels go up at subtelomeres, which destabilizes the Rap1 complex. This mechanism should be further analyzed by characterizing Rap1 and H2BUb localization at senescence with ChIP-RTPCR and then determining how H2BK123R, *bre1Δ*, and *lge1Δ* affect this process. However, it is also possible that other histone modifications in addition to (or instead of) H2BUb promote Rap1 relocalization at senescence. We should screen how all histone modifications change at subtelomeres at senescence with ChIP-seq and then use point mutants to assess how these modifications affect Rap1 localization and the rate of senescence.

Our data are also consistent with an idea that has been gaining some traction in recent years that subtelomeres are depots that factors relocalize *to* and *from* under various stresses. Yeast subtelomeres contain many stress-response genes, ion-transport genes, and genes involved in alternate carbon metabolism (i.e. non-glucose) and they are preferentially upregulated at senescence (and other stress conditions) (Mak et al. 2009; Nautiyal et al. 2002). Ideker and colleagues performed a meta-analysis and determined that many transcription factor relocalize *to* and *from* subtelomeres under various stress conditions (Harbison et al. 2004; Mak et al. 2009). However, how the stress of senescence affects transcription factor localization was not assessed. Because Rap1 only explains the gene expression of at

most 100 genes, it is likely that other transcription factors are either leaving or targeting subtelomeres at senescence (for example *AFT2*, *GZF3*, *XBP1*, etc. based on work from Ideker and colleagues). We should screen all yeast transcription factors and determine how their localization changes at senescence using ChIP-seq. Because the DNA damage response and the stress-response are two of the most important sets of gene expression changes seen at senescence, transcriptions factors involved in these pathways will be prioritized.

Because yeast constitutively express telomerase and thus should never senesce in the 'wild' the question remains: why is Rap1 relocalization hardwired into the cell? Most likely the Rap1 relocalization pathway is an individual module of a larger DNA damage response pathway that is co-opted during senescence. Because Rap1 has been shown to target new genes in the presence of MMS and low glucose (Buck and Lieb 2006; Tomar et al. 2008), it will be interesting to determine if Rap1 leaves subtelomeres under other stresses with Rap1 ChIP-RTPCR or ChIP-seq.

Characterization of Rap1 post-translational modification at senescence

At senescence, post-translationally modified Rap1 species accumulate, which depends on many factors including – *MEC1*, *SIZ2*, and *UBI4*. Our findings are consistent with previous reports, which show that Rap1 is post-translationally

modified under various stress conditions, and that some post-translational modifications affect Rap1 function (Lescasse et al. 2013; Hang et al. 2011; Smolka et al. 2007).

We need to identify the Rap1 modifications at senescence and how they affect Rap1 function (or are they just a bio-marker of senescence)? As an extension of our focused screen, we will perform Rap1 and SUMO (Smt3) IP mass-spectrometry experiments in wild type and senescent yeast. We will investigate the function of these modifications at senescence with point mutants that block the PTMs and analyzing how they affect the rate of senescence, NRTS gene expression, and Rap1 protein complex formation.

Finely mapping the Rap1 RNA binding domain and characterizing its effects *in vivo*

Even though Rap1 is one of the most highly characterized yeast proteins, we are first group to show that Rap1 binds RNA. This is one of our most interesting findings. However, we need to characterize: **1.** Which residues of Rap1 are necessary to bind RNA? **2.** What is the RNA binding motif of Rap1? **3.** Which RNA species does it bind *in vivo*? **4.** What is the function of Rap1 binding RNA in the cell? The first set of experiments should establish if Rap1 specifically binds RNA (using various cold oligonucleotide competitors – ssRNA, dsRNA, RNA:DNA dimers, ssDNA,

dsDNA) and which sequences it prefers *in vitro* (using systematic evolution of ligands by exponential enrichment (SELEX)). Ultimately, we should perform Rap1 cross-linking immunoprecipitation (CLIP)-Seq and carefully map and characterize the function of the Rap1 RNA binding domain *in vivo*.

Though our finding is extremely preliminary, Rap1 RNA binding is the most parsimonious explanation of Choder and colleagues finding that Rap1 upstream activating sequences (UAS) that are not transcribed negatively affect the stability of its transcripts (Bregman et al. 2011). These transcripts, many of which had high G-quadruplex forming potential (QFP; the chimeric transcripts have a poly-guanine tract in their 3'-UTR), were degraded in an exosome dependent manner (Bregman et al. 2011). Choder and colleagues speculated that another factor recruited the transcripts to the exosome. However, not only does Rap1 have strong genetic interactions with both *XRN1*, one of the two cellular 5'-3' RNA exonucleases, and *SKI3*, a member of 3'-5' RNA exosome, but also we find that Rap1 binds RNA species with high QFP. It is possible that Rap1 participates in the hand off of its transcripts to the RNA degradation machinery.

Further mapping the Rap1 G-quadruplex binding domain and characterizing its effects *in vivo*

In hopes of understanding the biological role of Rap1's G4DNA-binding activity and how it affects Rap1 function, we tried to map Rap1's G-quadruplex binding domain. Previous work had shown that Rap1's minimal DNA binding domain (DBD) was not sufficient to G-quadruplex DNA, as a result we assessed if either the N- or C-terminus was necessary to bind to these structures. Even though the N-terminus of Rap1 has been ascribed few functions (including DNA bending and interacting with Gcr1 and Gcr2 via yeast two hybrid (Mizuno et al. 2004; Muller et al. 1994)), we found that it was important for G-quadruplex binding and was sufficient to weakly bind G-quadruplex DNA. However, more work needs to be done to better define the G-quadruplex binding domain of Rap1. Ultimately, we will use phage display to engineer a Rap construct that cannot bind G-quadruplexes but still binds duplex DNA. We will use these alleles in a battery of experiments to understand the role of Rap1's G-quadruplex binding activity – in particular telomere capping, telomere length maintenance, the rate of senescence, and transcriptional activation/repression.

REFERENCES

Bregman A, Avraham-Kelbert M, Barkai O, Duek L, Guterman A, Choder M. 2011. Promoter Elements Regulate Cytoplasmic mRNA Decay. *Cell* **147**: 1473–1483.

Buck MJ, Lieb JD. 2006. A chromatin-mediated mechanism for specification of conditional transcription factor targets. *Nat Genet* **38**: 1446–1451.

Campisi J. 1997. The biology of replicative senescence. *European Journal of Cancer* **33**: 703–709.

Emre NCT, Ingvarsdottir K, Wyce A, Wood A, Krogan NJ, Henry KW, Li K, Marmorstein R, Greenblatt JF, Shilatifard A, et al. 2005. Maintenance of low histone ubiquitylation by Ubp10 correlates with telomere-proximal Sir2 association and gene silencing. *Mol Cell* **17**: 585–594.

Gilson E, Roberge M, Giraldo R, Rhodes D, Gasser SM. 1993. Distortion of the DNA double helix by RAP1 at silencers and multiple telomeric binding sites. *Journal of Molecular Biology* **231**: 293–310.

Giraldo R, Rhodes D. 1994. The yeast telomere-binding protein RAP1 binds to and promotes the formation of DNA quadruplexes in telomeric DNA. *EMBO J* **13**: 2411–2420.

Giraldo R, Suzuki M, Chapman L, Rhodes D. 1994. Promotion of parallel DNA

quadruplexes by a yeast telomere binding protein: a circular dichroism study. *Proc Natl Acad Sci USA* **91**: 7658–7662.

Hang LE, Liu X, Cheung I, Yang Y, Zhao X. 2011. SUMOylation regulates telomere length homeostasis by targeting Cdc13. *Nat Struct Mol Biol* **18**: 920–926.

Harbison CT, Gordon DB, Lee TI, Rinaldi NJ, Macisaac KD, Danford TW, Hannett NM, Tagne J-B, Reynolds DB, Yoo J, et al. 2004. Transcriptional regulatory code of a eukaryotic genome. *Nature* **431**: 99–104.

Kozak ML, Chavez A, Dang W, Berger SL, Ashok A, Guo X, Johnson FB. 2010. Inactivation of the Sas2 histone acetyltransferase delays senescence driven by telomere dysfunction. *EMBO J* **29**: 158–170.

Lescasse R, Pobiega S, Callebaut I, Marcand S. 2013. End-joining inhibition at telomeres requires the translocase and polySUMO-dependent ubiquitin ligase Uls1. *EMBO J* **32**: 805–815.

Mak HC, Pillus L, Ideker T. 2009. Dynamic reprogramming of transcription factors to and from the subtelomere. *Genome Research* **19**: 1014–1025.

Nautiyal S, DeRisi JL, Blackburn EH. 2002. The genome-wide expression response to telomerase deletion in Saccharomyces cerevisiae. *Proc Natl Acad Sci USA* **99**: 9316–9321.

Smolka MB, Albuquerque CP, Chen S-H, Zhou H. 2007. Proteome-wide identification of in vivo targets of DNA damage checkpoint kinases. *Proc Natl Acad Sci USA* **104**: 10364–10369.

Sperling AS, Grunstein M. 2009. Histone H3 N-terminus regulates higher order structure of yeast heterochromatin. *Proceedings of the National Academy of Sciences* **106**: 13153–13159.

Tomar RS, Zheng S, Brunke-Reese D, Wolcott HN, Reese JC. 2008. Yeast Rap1 contributes to genomic integrity by activating DNA damage repair genes. *EMBO J* **27**: 1575–1584.